

STUDY ON HEAVY METAL ADSORPTION BY CHITOSAN BIOPOLYMER

Janitha Madusanka Unagolla

(128008A)



University of Moratuwa, Sri Lanka.
Electronic Theses & Dissertations
www.lib.mrt.ac.lk

Thesis submitted in partial fulfillment of the requirements for the degree
Master of Science in Materials Science and Engineering

Department of Materials Science and Engineering

University of Moratuwa
Sri Lanka

August 2015

Declaration

I declare that this is my own work and this thesis with the title “**Study on Heavy metal Adsorption by Chitosan Biopolymer**” does not incorporate without acknowledgement any material previously submitted for a Degree or Diploma in any other University or Institute of higher learning and to the best of my knowledge and belief it does not contain any material previously published or written or orally communicated by another person except where due reference is made in the text.

Also, I hereby grant to University of Moratuwa the non-exclusive right to reproduce and distribute my thesis, in whole or in part in print, electronic or other medium. I retain the right to use this content in whole or part in future works (such as articles or books).

Signature of the candidate:

.....
Date:



University of Moratuwa, Sri Lanka.
Electronic Theses & Dissertations
www.lib.mrt.ac.lk

The above candidate has carried out research for the Masters thesis under my supervision.

Signature of the supervisor:

.....
Date:

Dr. S.U. Adikary

Abstract

Heavy metal pollution is a serious problem to aquatic ecosystems because some of these metals are potentially toxic even at very low concentrations. Chitosan, a biopolymer produced from crustacean shells, has applications in various areas, particularly in drinking water and wastewater treatment due to its ability to remove metallic ions from solutions. The purpose of this research work was to study the adsorption of cadmium and lead ions into chitosan, produced from shrimp shells at the laboratory level. Shrimp type “penaeus monodon” (giant tiger prawn) was used to synthesize the chitosan. The main characteristic properties such as degree of deacetylation (DD); the amount of amine groups in chitosan, viscosity, crystallinity and thermal analysis were done by using Fourier transform infrared spectroscopy, Brookfield viscometer, X-ray spectroscopy, thermo gravimetric analysis (TGA) and differential thermal analysis (DTA). Chitosan, with a degree of deacetylation between 80%- 95% was used in the experimental part and the flake sizes were smaller than 0.25mm. Experimental work involved the determination of the adsorption isotherms and kinetic studies for each metallic ion in a batch system.

Effect of Degree of deacetylation (DD) of the chitosan, effect of initial pH of the metal ion solution, effect of particle size, effect of initial heavy metal concentration, and effect of chitosan dosage were studied. The results showed that the adsorption capacity depends strongly on pH of the solution, DD of chitosan and slightly depends on the particle size. According to the results, pH values at 6.5 for cadmium and pH values at 4.5 for lead show higher adsorption capacity. High DD chitosan showed higher adsorption capacity mainly due to the higher number of active amino groups in high DD sample.

Simplified kinetic models such as pseudo-first-order, pseudo-second-order, Elovich model and intra-particle diffusion model were used to determine the rate limiting step. Both linear and non-linear According to the kinetic models pseudo second order model best described the adsorption process. Both linear and non-linear models and Elovich model best described the adsorption process. Multilinearity in the intraparticle diffusion model suggested that the adsorption of heavy metal consists of two major steps, due to the different pore sizes of chitosan.

Equilibrium experimental data were analyzed by using two different isotherm models namely, Langmuir and Freundlich. According to the results, adsorption process of cadmium and lead heavy metals is heterogeneous and multilayer adsorption as it best fit with the Freundlich isotherm model. According to the thermodynamic experiments, adsorption process is favorable and physical adsorption was predominant in the adsorption process. Desorption of the heavy metals was possible by using different regeneration solutions.

Key words : Chitosan, Heavy metals, Isotherm, Kinetics, Adsorption

Acknowledgment

My foremost sincere gratitude is expressed to my supervisor, Dr. S.U. Adikary who gave me the opportunity to carry out this research work and for the immense help and guidance given throughout the project work.

I would also like to thank Dr. P.G. Rathnasiri, progress review committee chair, and Dr. N.M.V.K. Liyanage, M.Sc coordinator of the department, for providing correct guidance through the project work. I also like to express my sincere gratitude to Dr. D.A.S. Amarasinghe, who provided valuable instructions during my research work.

I also like to express my sincere gratitude to senate research committee (SRC) grant of University of Moratuwa, for providing financial assistantship to this research work (Grant No. SRC/LT/2012/12).

In addition to that, I like to express my thanks to all the academic staff members of the Department of Materials Science and Engineering, University of Moratuwa for their assistance and contribution to my research work.

I would like to express my sincere gratitude to Mr. D.M.R.K. Dissanayake, PhD student at Department of Chemistry, University of Colombo for his excellent support and contribution during my research work.

I also like to thank Mr. K.G.N Thilawala, Mrs. K.A.D. Rathnayake, Mr. H.V.H.H. Senavirathne for their support during my research work.

I am grateful to Mr. S.D. Karunaratna and Mr. Abeyarathne and other nonacademic staff members of the Department of Materials Engineering, for their assistance and contribution to my research work.

In conclusion, I would like to express my pardon if I have inadvertently omitted the name of those to whom thanks is due.

J.M. Unagolla

Table of Contents

Declaration	i
Abstract	ii
Acknowledgment	iii
Table of Contents	iv
List of Figures	vii
List of Tables.....	xi
List of terms, abbreviations and symbols.....	xiii
1 Introduction	1
2 Literature review	5
2.1 Chitin and chitosan.....	5
2.2 Characteristics of Chitosan.....	7
2.2.1 Determination of degree of deacetylation (DD).....	8
2.2.1.1 Elemental analysis.....	8
2.2.1.2 Titration methods	8
2.2.1.3 Hydrolytic methods.....	9
2.2.1.4 Spectroscopic methods.....	9
2.2.2 Solubility.....	12
2.2.3 Scanning Electron Micrograph (SEM) of chitosan.....	13
2.2.4 Complex formation with metals.....	14
2.3 Applications of chitosan.....	14
2.3.1 Agricultural applications.....	14
2.3.2 Biomedical and Pharmaceutical applications.....	14
2.3.3 Cosmetic applications	15
2.3.4 Food, Paper and Textile applications	16
2.3.5 Environmental Applications.....	16
2.4 Effect of Heavy Metals.....	17
2.4.1 Effect of Cadmium on the environment and human health	18
2.4.2 Effect of lead on the environment and human health	19
2.5 Interaction Mechanisms of Heavy metals in chitosan.....	20

2.5.1	Complexation (Chelation).....	21
2.5.2	Electrostatic Attraction/ Ion exchange	22
2.5.3	Uptake by formation of ternary complexes.....	23
2.6	Adsorption	23
2.6.1	Adsorption Kinetics	24
2.6.1.1	Pseudo-first order model.....	26
2.6.1.2	Pseudo-second order model	27
2.6.1.3	Elovich model	29
2.6.1.4	Intraparticle diffusion model.....	29
2.6.2	Adsorption Isotherm	30
2.6.2.1	Freundlich isotherm	30
2.6.2.2	Langmuir isotherm.....	31
2.6.3	Thermodynamic parameters of adsorption.....	32
2.7	Previous studies on chitosan as an adsorbent.....	34
3	Materials and Methods	38
3.1	Adsorbent material – Chitosan.....	38
3.1.1	Extraction of chitosan.....	38
3.1.2	Characterization of Chitosan.....	39
3.1.2.1	Fourier Transform Infrared (FTIR) spectroscopic analysis	39
3.1.2.2	Viscosity	39
3.1.2.3	Thermo gravimetric analysis (TGA) and differential thermal analysis (DTA)	40
3.1.2.4	Degree of Deacetylation.....	40
3.2	Adsorbates	40
3.3	Adsorption experiments	41
3.3.1	Kinetics experiments.....	41
3.3.2	Isotherm experiments	43
3.3.3	Thermodynamic experiments.....	43
3.3.4	Desorption experiments	44
3.4	Evaluation of Experimental Data	45
3.5	Analysis of adsorption kinetics and isotherms	46

4	Results and Discussion.....	47
4.1	Characteristics of Chitosan.....	47
4.1.1	Degree of Deacetylation (DD)	47
4.1.2	Viscosity.....	49
4.1.3	Thermal analysis	49
4.2	Adsorption of Cadmium and Lead by chitosan.....	50
4.2.1	Effect of contact time	51
4.2.2	Effect of degree of deacetylation (DD).....	52
4.2.3	Effect of solution pH.....	53
4.2.4	Effect of particle size	56
4.2.5	Effect of initial metal ion concentration.....	58
4.2.6	Effect of chitosan dosage	60
4.3	Analysis of Adsorption Kinetics	61
4.3.1	Adsorption kinetics models for different DD.....	62
4.3.2	Adsorption kinetics model for different pH.....	72
4.3.3	Intra-particle diffusion model	81
4.4	Modeling of adsorption isotherms.....	86
4.5	Thermodynamic Studies.....	92
4.5.1	Effect of Temperature	92
4.5.2	Thermodynamics of adsorption.....	93
4.6	Desorption Studies	95
5	Conclusions	96
6	Suggestions for Future Works.....	97
7	References	99
	<i>[Appendix - I: Determination of Degree of deacetylation]</i>	107
	<i>[Appendix - II: FTIR Characterization of heavy metal adsorbed chitosan]</i>	109
	<i>[Appendix - III: Adsorption test results]</i>	114
	<i>[Appendix – IV: Publications]</i>	121

List of Figures

Figure 2.1 Structure of chitin	5
Figure 2.2 Orientation of a) α -chitin b) β -chitin c) γ -chitin.....	6
Figure 2.3 Identification of α -chitin and β -chitin using FTIR spectroscopy a) α -chitin b) β -chitin.....	6
Figure 2.4 Structure of chitosan.....	7
Figure 2.5 ^1H NMR spectrum of chitosan.....	9
Figure 2.6 FTIR spectroscopy and the two baseline systems used in determination of DD.....	12
Figure 2.7 SEM micrograph of chitosan (a) $\times 50$ (b) $\times 150$ magnification	13
Figure 2.8 Heavy metal cycle	18
Figure 2.9 Chitosan metal complexes; left- Bridge model, right- pendant model.....	21
Figure 2.10 Formation of ternary complexes; Source: Benavent, 2008.....	23
Figure 2.11 Schematic illustration of adsorption steps	25
Figure 2.12 Isotherm classification.....	30
Figure 3.1 Process flow chart of chitosan extraction	38
Figure 3.2 GBC 932 PLUS atomic adsorption spectrophotometer (AAS).....	41
Figure 3.3 Process flow chart for kinetic experiments.....	42
Figure 3.4 Experimental steps for adsorption isotherm studies	43
Figure 3.5 Experimental steps for thermodynamics study.....	44
Figure 3.6 Experimental steps for desorption studies	44
Figure 4.1 Characteristic absorption bands of chitin	47

Figure 4.2 Comparison of characteristics bands of high DD and low DD FTIR spectroscopy a) Low DD b) High DD	48
Figure 4.3 Thermo gravimetric (TGA) and differential thermal (DTA) analysis of Chitosan	50
Figure 4.4 Adsorption capacity with contact time at room temperature ($28\pm 2^{\circ}\text{C}$) and high pH (for Cd- 6.5 & for Pb- 4.5)	51
Figure 4.5 Effect of DD on % removal of cadmium and lead at room temperature ($28\pm 2^{\circ}\text{C}$) and high pH (for Cd-6.5 & for Pb-4.5).....	52
Figure 4.6 Effect of pH on % removal of cadmium from chitosan.....	54
Figure 4.7 Chemical speciation of Cadmium (100mg/L) in water as a function of pH	54
Figure 4.8 Effect of pH on % removal of lead from chitosan.....	55
Figure 4.9 Chemical speciation of Cadmium (100mg/L) in water as a function of pH	55
Figure 4.10 Effect of particle size on the % removal of cadmium at room temperature ($28\pm 2^{\circ}\text{C}$) and high pH (6.5)	57
Figure 4.11 Effect of particle size to the % removal of lead at room temperature ($28\pm 2^{\circ}\text{C}$) and high pH (4.5).....	58
Figure 4.12 Effect of initial metal ion concentration on the % adsorption of cadmium at room temperature ($28\pm 2^{\circ}\text{C}$) and high pH (6.5)	59
Figure 4.13 Effect of initial metal ion concentration on the % adsorption of lead	59
Figure 4.14 Effect of chitosan dosage on the % adsorption of cadmium	60
Figure 4.15 Non-linear pseudo first order model of Cadmium with effect of DD	62



Figure 4.16 Non-linear pseudo first order model of Cadmium with effect of DD @ pH-5.5	63
Figure 4.17 Non-linear Elovich model of Cadmium with effect of DD @pH- 5.5 ...	63
Figure 4.18 Linear Pseudo first order model of Cadmium with effect of DD @ pH- 5.5.....	65
Figure 4.19 Linear pseudo second order model of cadmium with effect of DD @pH- 5.5.....	65
Figure 4.20 Linear Elovich model of Cadmium with effect of DD @ pH – 5.5	66
Figure 4.21 Non-linear pseudo first order model of Lead with effect of DD @ pH- 3	68
Figure 4.22 Non-linear pseudo second order model of Lead with effect of DD @ pH - 3	68
Figure 4.23 Non-linear Elovich model for lead with effect of DD @ pH-3	69
Figure 4.24 Linear pseudo first order model for lead with effect of DD @ pH -3	70
Figure 4.25 Linear pseudo second order model for lead with effect of DD @ pH-3	70
Figure 4.26 Linear Elovich model for lead with effect of DD @ pH-3.....	71
Figure 4.27 Non-linear pseudo first order model for Cadmium with effect of pH....	72
Figure 4.28 Non-linear pseudo second order model for Cadmium with effect of pH	73
Figure 4.29 Non-linear Elovich model for Cadmium with effect of pH.....	73
Figure 4.30 Linear pseudo first order model for Cadmium with effect of pH.....	74
Figure 4.31 Linear pseudo second order model for Cadmium with effect of pH	75
Figure 4.32 Linear Elovich model for Cadmium with effect of pH.....	75
Figure 4.33 Non-linear pseudo first order model for Lead with effect of pH.....	76
Figure 4.34 Non-linear pseudo second order model for Lead with effect of pH.....	77



Figure 4.35 Non-linear Elovich model for lead with effect of pH.....	77
Figure 4.36 Linear pseudo first order model for Lead with effect of pH.....	78
Figure 4.37 Linear pseudo second order model for Lead with effect of pH.....	79
Figure 4.38 Linear Elovich model for Lead with effect of pH	79
Figure 4.39 Intra-particle diffusion model of cadmium adsorption at different DD .	82
Figure 4.40 Intra-particle diffusion model of lead adsorption at different DD.....	82
Figure 4.41 Intra-particle diffusion model of cadmium adsorption at different pH of metal ion solution.....	83
Figure 4.42 Intra-particle diffusion model of cadmium adsorption at different pH of metal ion solution.....	83
Figure 4.43 Linearized Langmuir isotherm model of C_e/q_e Vs. C_e (linear 1) @ 28 ± 2 $^{\circ}\text{C}$	87
Figure 4.44 Linearized Langmuir isotherm model of $1/q_e$ Vs. $1/C_e$ (linear 2) @ 28 ± 2 $^{\circ}\text{C}$	87
Figure 4.45 Linearized Langmuir isotherm model of q_e/C_e Vs. q_e (linear 3) @ 28 ± 2 $^{\circ}\text{C}$	88
Figure 4.46 Nonlinear Langmuir isotherm model @ 28 ± 2 $^{\circ}\text{C}$	88
Figure 4.47 Linearized Freundlich isotherm model @ 28 ± 2 $^{\circ}\text{C}$	89
Figure 4.48 Nonlinear Freundlich isotherm model @ 28 ± 2 $^{\circ}\text{C}$	90
Figure 4.49 Effect of temperature on the adsorption capacity for Cadmium and Lead: C-50ppm, 0.1 g of chitosan dosage, contact time 3 hr.....	92
Figure 4.50 Thermodynamic estimations for cadmium and lead.....	93
Figure 4.51 Desorption percentages of metal ions for three regeneration solution ...	95



List of Tables

Table 2.1 Characteristic peaks and the respective wave numbers in FTIR spectroscopy.....	10
Table 2.2 Distinguish features between physisorption and chemisorption.....	24
Table 4.1 Viscosity of two chitosan samples.....	49
Table 4.2 Non-linear regression kinetic parameter estimates for cadmium with effect of DD.....	64
Table 4.3 Linear regression kinetic parameter estimates for cadmium with effect of DD.....	66
Table 4.4 Non-linear regression kinetic parameter estimates for lead with effect of DD.....	69
Table 4.5 Linear regression kinetic parameter estimates for lead with effect of DD	71
Table 4.6 Non-linear regression kinetic parameter estimates for cadmium with effect of pH of initial metal ion solution.....	74
Table 4.7 Linear regression kinetic parameter estimates for cadmium with effect of pH of initial metal ion solution.....	76
Table 4.8 Non-linear regression kinetic parameter estimates for lead with effect of pH of the initial metal ion solution.....	78
Table 4.9 Linear regression kinetic parameter estimates for lead with effect of pH of the initial metal ion solution.....	80
Table 4.10 Intra-particle diffusion model parameter estimates for different DD values of chitosan.....	85
Table 4.11 Intra-particle diffusion model parameter estimates for different initial pH of the metal ion solution.....	85

Table 4.12 Linear and nonlinear forms of Langmuir and Freundlich isotherms	86
Table 4.13 Langmuir isotherm model parameters for cadmium and lead adsorption	89
Table 4.14 Freundlich isotherm model parameters for cadmium and lead adsorption	90
Table 4.15 Effect of separation factor on shape of isotherm	91
Table 4.16 Calculated values of separation factor R_L for different plot types.....	91
Table 4.17 Thermodynamic parameter estimations of cadmium and lead adsorption	94



University of Moratuwa, Sri Lanka.
 Electronic Theses & Dissertations
www.lib.mrt.ac.lk

List of terms, abbreviations and symbols

DA	Degree of acetylation
DD	Degree of deacetylation
DTA	Differential Thermal Analysis
FTIR	Fourier Transform Infrared Spectroscopy
NMR	Nuclear Magnetic Resonance
PFO	Pseudo first order
PSO	Pseudo second order
TGA	Thermogravimetry Analysis
C_e	liquid phase adsorbate concentration in equilibrium (mg/L)
C_0	Initial metal ion concentration of the solution (mg/L)
C_t	Metal ion concentration of the solution at time t (mg/L)
C_f	Final metal ion concentration of the solution (mg/L)
K_1	Pseudo first order rate constant (min^{-1})
K_2	Pseudo second order rate constant (g/mg.min)
K_d	Distribution ratio (L/g)
K_F	Freundlich constant
K_i	Intra-particle diffusion rate constant ($\text{mg/gmin}^{0.5}$)
K_L	Langmuir constant
m	Mass of the adsorbent (g)
q_e	Adsorption capacity at equilibrium (mg/g)

q_t	Adsorption capacity at time t (mg/g)
q_m	Monolayer adsorption capacity (mg/g)
R_L	Langmuir separation factor
R	Universal gas constant (8.314 J/mol.K)
T	Absolute solution temperature (K)
V	Volume of the aqueous metal ion solution (L)
ΔG^0	Standard state Gibbs free energy change
ΔH^0	Standard state Enthalpy change
ΔS^0	Standard state Entropy change
α, β	Elovich constants

$1/n$ heterogeneity factor

 University of Moratuwa, Sri Lanka.
 Electronic Theses & Dissertations
www.lib.mrt.ac.lk

Chapter 1

1 Introduction

The humongous increase in the use of heavy metal over the past decades has ensued in an increased level of metallic substances in aquatic environment. Even at very low concentrations, some of those heavy metals are potentially toxic and those metals are not biodegradable and tend to accumulate in living organisms (Senarathne & Pathiratne, 2007). These factors can generate stern problems to both human and aquatic life.

In Sri Lanka, industrial development and uncontrolled agricultural practices have resulted in severe environmental problems. Most of the water resources in country have been polluted and therefore reduced the quality of water and ensuing health related problems. Proliferation of agricultural chemicals and uncontrolled and excessive use of fertilizers play a major role in heavy metal pollution in North central province and most of the water reservoirs in those areas are contaminated with excessive level of cadmium and arsenic heavy metals which leads to the chronic kidney disease spread across that area (Wanigasuriya, 2012). In Sri Lanka, garment/textile industry has rapidly developed in past years. It plays an important role in the economy of the country as it is one of the major foreign exchange earners. More than two thousand types of chemicals and seven thousand types of dyes, mainly consists of heavy metals lead, chromium, cadmium and copper, main elements that are used for the production of color pigments, exaggerate the pollution of heavy metal by surpassing the accepted maximum heavy metals concentrations in water resources in the industrialized areas (Syuhadah, Muslim, & Rohasliney, 2015).

Recent research works carried out in different part of the country also shows that the heavy metal concentration of the water exceeded the maximum contamination level set by the World Health Organization (WHO). In western province of Sri Lanka, recent studies reveal that Werasingha Ganga, Bolgoda Lake and Lunawa lagoon are contaminated with excess heavy metal concentrations. In these

water bodies, zinc, copper, lead, cadmium and chromium levels above the maximum safety level of the country. Most importantly, fish in the Weras Ganga and Bolgoda Lake contain high level of cadmium and lead due to the bioaccumulation of those metals and creates a serious threat to the people who consume those fish (Senarathne & Pathiratne, 2007). The reservoirs and ground water in the north central province were contaminated with heavy metals and exceed the WHO limit of 0.01ppm for arsenic and 0.003ppm for cadmium (Noble & Amerasinghe, 2014).

Since it is imperative to jettison or moderate the level of heavy metals in the aquatic ecosystems, various approaches and technologies are commonly applied to the wastewater effluents before they are discharged to the environment. These methods include chemical precipitation, coagulation-flocculation, ion exchange, reverse osmosis membrane, ultrafiltration and electrodialysis (Pérez-Marín et al., 2007). Nevertheless, due to inefficiency and economic constraints, some of these techniques may be impractical in real world situations. Further, some of these techniques generate hazardous products (Azouaou, Sadaoui, Djaafri, & Mokaddem, 2010; Ng, Cheung, & McKay, 2003).

Activated carbon is the most widely used adsorbent material in waste water treatment but, high cost of that restrained the commercial use of it in wide scale. To overcome from those problems most researchers are focusing in to the synthesis of low cost adsorbent from agricultural residues or industrial by products like palm kernel husk, corn cobs, rice shell, litter of poplar forest wool, chitosan, apple residue, olive mill products, banana husks, pine bark, sawdust, algae, etc. (Azouaou et al., 2010; Doyurum & Çelik, 2006; SenthilKumar, Ramalingam, Sathyaselvabala, Kirupha, & Sivanesan, 2011) In this study, chitosan was synthesized by using shrimp waste from local shrimp processing factories.

Chitosan is the soluble derivative of chitin and chitin is the second most abundant natural polysaccharide on the earth after the cellulose. Chitin can be mainly found in the cell walls of fungi, exoskeleton of arthropods such as crustaceans (crabs, lobster and shrimps) and insects (Rinaudo, 2006). Chitin

percentage depends on the chitin source and the living environment of the species. The crustaceans waste is the most important chitin source when considering the availability and high percentage of chitin in their shells. Chitin and Chitosan demonstrate wide range of properties like bio-degradability, bio-compatibility, antioxidant, adsorption enhancer and analgesic etc. Due to these broad characteristic properties, chitin and chitosan have been used in diverse areas such as biotechnology, medicine, dentistry, agriculture, food processing, environment protection and textile production (Mahmoud Abbas, 2010; Rinaudo, 2006).

Availability of high proportion of free amino sites explains the strong affinity for metal ions in chitosan. Furthermore, the metal adsorption capacity also varies with degree of deacetylation (DD) which relates to amino group content, affinity for water and crystallinity (Benavente, 2008; Chu, 2002).

Currently, Sri Lanka produces nearly 30,000 metric tons of shrimp per year and the waste shell, the raw material for chitin, constitute about 15-20% of the production volume. Most of the fishery factories are located in near to the western coast of Sri Lanka and the production of large volume of shrimp shell waste now only use as an animal food and majority of the waste doesn't use for any financially viable process. After the thirty years of civil war, fast growing fishery industries in Northern and Eastern provinces may provide favorable environment for local shrimp industry and that will creates more shrimp waste in near future. This atmosphere greatly influence the production of chitosan biopolymer from shrimp waste in Sri Lanka and that chitosan can be used as a low cost adsorbent material for industrial waste water effluents.

The design of chitosan filter for removal of heavy metal ions from industrial waste water effluent requires equilibrium and kinetics data for the system. According to the various kinetics studies, adsorption rate of metallic ions onto chitosan depends on the raw material type (shrimp, crab or lobster shells), preparation method, particle size of the chitosan, chemical modifications and physical modifications. The adsorption rate also depends on the characteristics of the aqueous solutions, such as pH, temperature, metallic ion concentration of the

aqueous solution, pE and type of the metal ion species present in the solution (ex: Cr(III) or Cr(VI) / As(III) or As(V))(Evans, Davids, MacRae, & Amirbahman, 2002).

The objectives of this research work were to synthesize chitosan from locally available shrimp type and characterize the properties of chitosan. Further, chitosan as an adsorbent, investigate the adsorption characteristics of lead and cadmium and study equilibrium and kinetics models to find optimum process parameters. For identification of the rate controlling step, simplified kinetic models like pseudo first order model, pseudo second order model, Elovich model and intra-particle diffusion models were used. To find the nature and the favorability of adsorption process, Langmuir isotherm model and Freundlich isotherm model were used. Furthermore, desorption experiments were also carried out with different regeneration solutions.



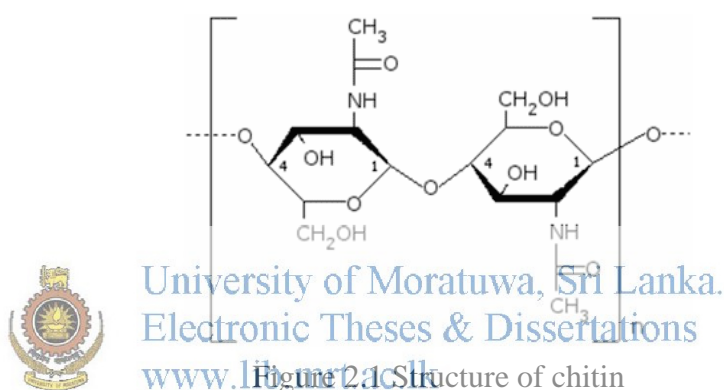
University of Moratuwa, Sri Lanka.
Electronic Theses & Dissertations
www.lib.mrt.ac.lk

Chapter 2

2 Literature review

2.1 Chitin and chitosan

Chitin, the second most abundant natural polysaccharide in earth after the cellulose, was first identified in 1884 with a molecular structure of poly(β -(1 \rightarrow 4)-N-acetyl-D-glucosamine); occurring in nature as ordered crystalline microfibrils. Therefore, the exoskeleton of arthropods, which is mainly found in seafood crustaceans such as shrimps, prawn, crab and lobster shells and cell walls of fungi and yeast are consist of ordered crystalline microfibrils (Rinaudo, 2006).



Depending on the source, chitin has three allomorphs (Figure 2.2), namely the α chitin, β chitin and γ chitin which can be distinguished by infrared and solid-state NMR spectroscopy together with X-ray diffraction (Rinaudo, 2006). α -Chitin is the most abundant allomorph, mainly found in fungal and yeast cell walls, in crab, in krill and in lobster tendons and shells, and in shrimp shells. It is also found in insect cuticle, the harpoons of cone snails, the filament ejected by the seaweed *Phaeocytis* and the oral grasping spine of *Sagitta*. β -Chitin, the rarer form of chitin is found in squid pens and in the tubes produced by vestimetiferan and pogonophoran worms (Rinaudo, 2006; Van de Velde & Kiekens, 2004). γ -Chitin mainly presents in the stomach of *Loligo* and cocoon fibers of the *Ptinus* beetle. However, after a detailed analysis, Rinaudo, M. (2006) suggested that γ -chitin was a variant of the α -chitin family. The adsorption capacity of chitosan depends of the origin of polysaccharide (chitin) (Miretzky & Cirelli, 2009).

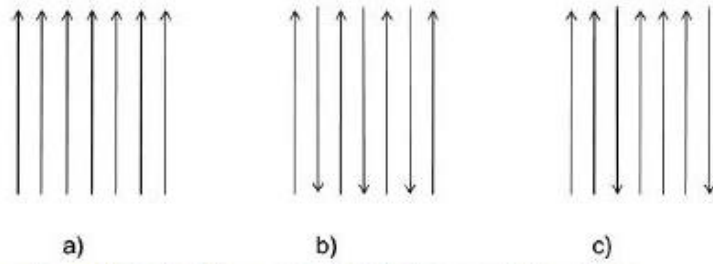


Figure 2.2 Orientation of a) α -chitin b) β -chitin c) γ -chitin

From the infrared (IR) spectroscopy of chitin, α -chitin and β -chitin can be identified separately. Due to the high crystallinity of the chitin, IR spectroscopy displays very sharp adsorption bands. Figure 2.3 shows the difference between α -chitin and β -chitin with respect to the C=O stretching of amide bond between 1600 cm^{-1} and 1500 cm^{-1} . For α -chitin, due to splitting of amide I band, at 1656 cm^{-1} and 1621 cm^{-1} two sharp adsorption band can be identified. In contrast, for β -chitin, one single sharp adsorption band at 1626 cm^{-1} can be identified by providing unique characteristic property (Rinaudo, 2006).

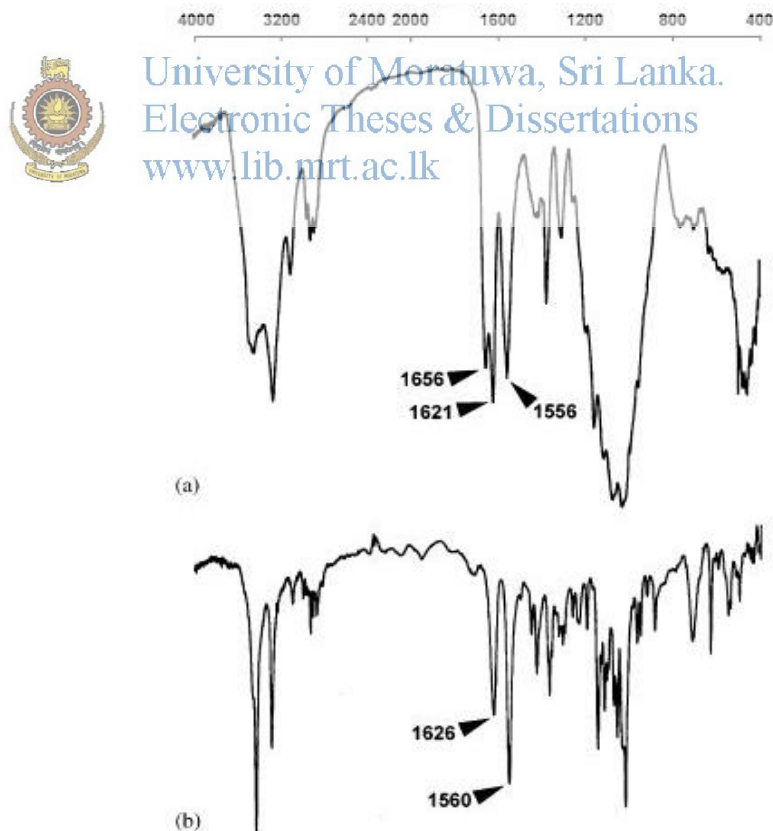


Figure 2.3 Identification of α -chitin and β -chitin using FTIR spectroscopy
a) α -chitin b) β -chitin

Chitosan, obtained by deacetylation of chitin is the most important derivative of chitin. Normally, when the degree of deacetylation of chitin reaches 60% or above, it is called as chitosan and becomes soluble in aqueous acidic media (Trung, Thein-Han, Qui, Ng, & Stevens, 2006; Van de Velde & Kiekens, 2004). The solubility in the aqueous media is due to the protonation of the $-NH_2$ functional group on the C-2 position of the D-glucosamine repeat unit. Chitosan is a semicrystalline polymer with orthorhombic unit cell which can be observed from electron diffraction diagram (Rinaudo, 2006). The free amino groups present in chitosan provide greater importance compare with chitin.

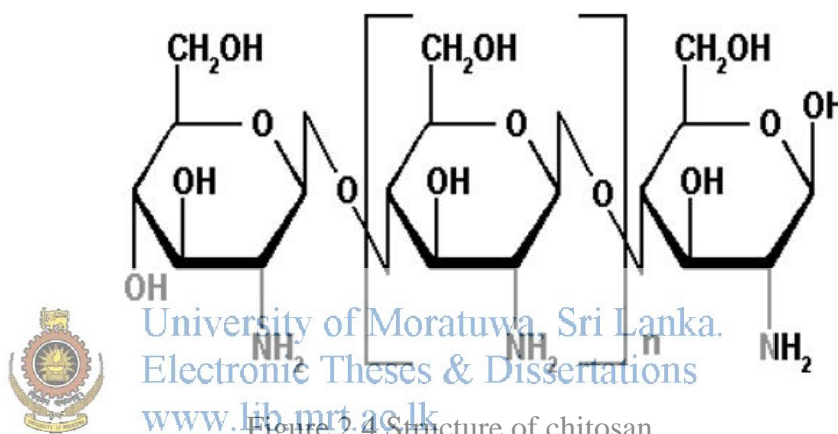


Figure 2.4 Structure of chitosan

2.2 Characteristics of Chitosan

Chitosan exhibits innumerable field of applications such as food biotechnology, agriculture, tissue engineering, textile, packaging, cosmetics, pharmaceuticals and medicinal etc. The main characteristic property of the chitosan is degree of deacetylation (DD), which is the measurement of the amount of amino groups present in the polysaccharide. Other main characteristic properties are crystallinity, molecular weight and viscosity. These main characteristic properties affect its conformation in solution, and its physio-chemical and biological properties including biodegradability, biocompatibility, acid base and electrostatic characteristics, non-antigenic, self-aggregation, sorption properties, non-toxic, and the ability to chelate metal ions (Rinaudo, 2006).

2.2.1 Determination of degree of deacetylation (DD)

Since the degree of deacetylation (DD) is an extremely important structural property of the chitosan, many methods are available to determine DD; such as,

2.2.1.1 Elemental analysis

A known weight of chitosan is heated up to 600°C for 1 hour, and the remaining residue, the quantity of inorganic material, is weighed. The deacetylation degree is calculated according to the Equation 2.1 and Equation 2.2 (Alvarenga, 2011).


$$\%DA = \frac{(8.695 - \%N)}{8.695 - 6.896} \times 100 \quad (2.1)$$

$$DD = 100 - DA \quad (2.2)$$

Where;

8.695–Percentage of nitrogen in fully deacetylated chitosan(100% DD)

6.896-Percentage of nitrogen in fully acetylated chitin (100% DA)

 University of Moratuwa, Sri Lanka.
Electronic Theses & Dissertations
www.lib.mrt.ac.lk

This method is not accurate due to the relatively small variation in percentage of nitrogen in sample with varying DD. This technique is more accurate when the nitrogen content of chitosan more than 7% and nitrogen content of chitin less than 7% (Dos Santos, Caroni, Pereira, da Silva, & Fonseca, 2009).

2.2.1.2 Titration methods

Several titration method were used to calculate DD including, acid-base titration, potentiometric titration, colloid titration and conductometric titration. DD values calculated from these methods show discrepancies, when the solubility of the chitosan in aqueous acidic medium is little. Since the solubility is directly proportional to the DD of the chitosan, chitosan with lower DD values not appropriate for titration method (Alvarenga, 2011).



University of Moratuwa, Sri Lanka.
Electronic Theses & Dissertations
www.lib.mrt.ac.lk

The DD was calculated from the Equation 2.3,

$$\%DA = \left(\frac{2 \times A_{CH_3}}{A_{H_2-H_6}} \right) \times 100 \quad (2.3)$$

This is the most reliable NMR technique available nowadays and the results obtained by this method are more reliable and reproducible (Alvarenga, 2011). Solid-state ^{13}C NMR method (Van de Velde & Kiekens, 2004) and solid-state ^{15}N NMR method (Alvarenga, 2011) are also available, but high cost restrained the availability of those techniques.

2. Infrared spectroscopy

Infrared absorption spectroscopy is a widely used technique for determination of DD. This method gives quantitative analyses of the compound. Characteristic peaks present in the IR spectroscopy were used to determine the structure of the chitosan and using those characteristic bands, DD of the sample can be calculated.

Table 2.1 shows the characteristic bands and their wave number (Kasaai, 2008).

Table 2.1 Characteristic peaks and the respective wave numbers in FTIR spectroscopy

Adsorption band	Wave number (cm^{-1})
OH Stretching	3450
N-H Stretching	3270
C-H Stretching	2870-2880
C=O Stretching	1655
C-N Stretching of amide I	1625
C-O-C Stretching	1030 or 1070
-CH ₂ Bending	1420
-NH bending of NH ₂	1620-1630
Anti-symmetric stretching of the C-O-C bridge	1160
Amide III	1315-1320

Since the spectrum of chitosan changes as a function of the degree of deacetylation (DD), no unique reference band is defined. Therefore, for different DD ranges, different reference bands are used. The most common reference bands are the OH stretching at 3450 cm^{-1} and C=O stretching at 1655 cm^{-1} (Kasaai, 2008; Van de Velde & Kiekens, 2004). Two equations were developed to determine DD from this two reference bands with respect to acetylation degree (DA).

The Equation 2.4 was proposed by Moore and Roberts (1978) for determination of DA (Kasaai, 2008; Khan, Peh, & Ch'ng, 2002):

$$DA = \left(A_{1655} / A_{3450} \right) \times 100 / 1.33 \quad (2.4)$$

Baxter et al (1992) proposed following equation to determine the DD of chitosan (Kasaai, 2008).

$$DA = \left(A_{1655} / A_{3450} \right) \times 115 \quad (2.5)$$



University of Moratuwa, Sri Lanka.
Electronic Theses & Dissertations
www.lib.mrt.ac.lk

$$DD = 100 - DA \quad (2.6)$$

(A_{1655}/A_{3450}) is the most widely used adsorption ratio in determination of DD of chitosan. Equation 2.4 and Equation 2.5 are given more accurate readings when the DD of the chitosan between 75 and 90 (Alvarenga, 2011). Figure 2.6 shows the two base line systems which are used to determine DD of chitosan.

The intensity of the O-H stretching band does not change with the DD of the chitosan, but this band also can experience some interference with other bands due to the various reasons. Since chitosan is a hygroscopic material, one reason is the humidity or moisture of the sample. Increase in the water content of the sample can be observed as increase in intensity of the OH band and increase in the width (broadening) of the OH band. This error can be minimized by drying the sample (Kasaai, 2008). In addition, the intensity of the N-H stretching band, appeared around 3270 cm^{-1} , varied with DD and due to the water effect, O-H and N-H band are overlapped. Therefore the peaks appeared around 3450 cm^{-1} is broad and not

sharp. This method is valid only for chitosan with DD between 90 and 75, but the results obtained from this method have large margin of errors. Due to the low cost and low analysis time, this method is widely used for the qualitative analysis (Alvarenga, 2011).

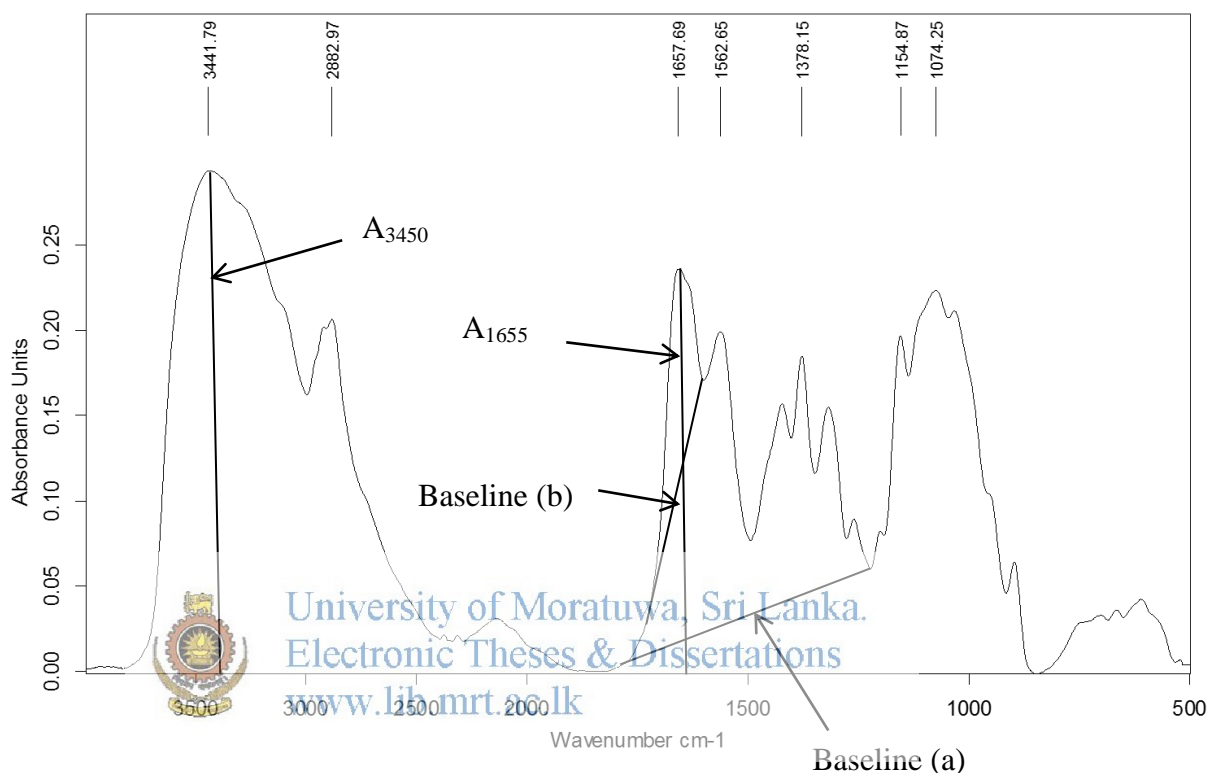


Figure 2.6 FTIR spectroscopy and the two baseline systems used in determination of DD

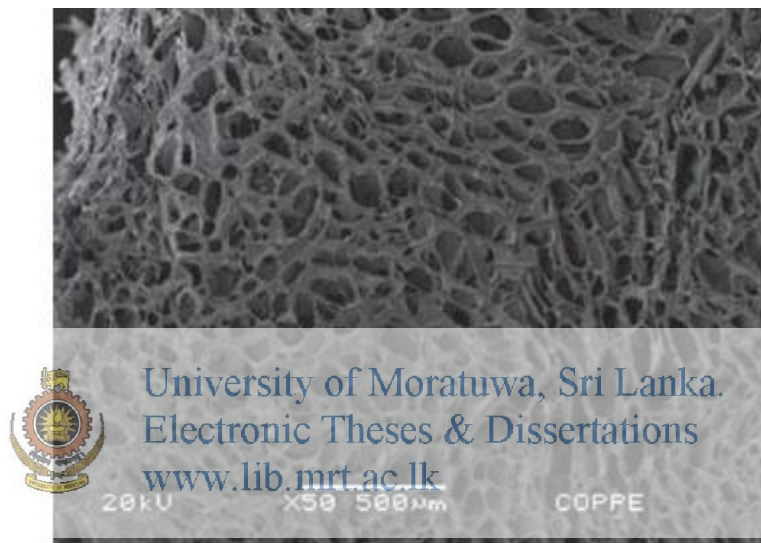
2.2.2 Solubility

Solubility of the chitosan depends on the molecular weight, degree of acetylation, total acid present in the solution and the temperature. In addition to the molecular weight of the chitosan, distribution of the acetyl groups along the main chain has major influence on the solubility. Both chitin and chitosan are not dissolved in neutral water and chitin is semi crystalline polymers which has extensive intra and inter molecular H – bonds. Therefore it is difficult to dissolve in dilute acid or organic solvent under mild condition (Aranaz et al., 2009).

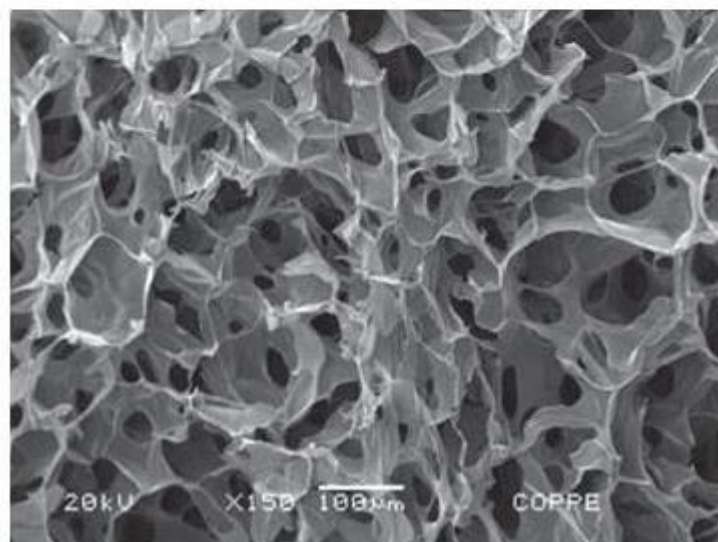
The deacetylation of the chitin gives an irregular structure due to the semi crystalline character of the initial polymer and this irregular structure is depend on

the degree of acetylation. The solubilization of the chitosan is occurred by protonation of the $-NH_2$ function on the C-2 position of the D-glucosamine repeat unit (Rinaudo, 2006). Degree of protonation of the chitosan in hydrochloric acid depends on the pH and the pK of the acid. So if degree of acetylation of chitosan is greater than 60%, it promotes the insolubility in acidic media. In addition, solubility at neutral pH has also claimed for chitosan with DA around 50% (Aranaz et al., 2009).

2.2.3 Scanning Electron Micrograph (SEM) of chitosan



(a)



(b)

Figure 2.7 SEM micrograph of chitosan (a) $\times 50$ (b) $\times 150$ magnification

Chitosan has a porous homogeneous structure as shown in the above SEM micrographs. Due to this porous structure of the chitosan, adsorption capacity increases as it increases surface area of the adsorbent. This porosity can be further increased by physical modification of chitosan such as preparation of chitosan beads and preparation of chitosan porous membranes.

2.2.4 Complex formation with metals

Chitosan shows good complexing ability with metals as a result of $-NH_2$ groups on the chain, which are involved in specific interaction with metals. Therefore this interaction with metals is used to recover heavy metals from various waste water effluents. This complexing ability depends on the physical state of chitosan such as powder, gel, film and fiber forms. Better chelation can be obtained for high degrees of deacetylation of chitosan. In the process of complexing with heavy metals, apart from the number of $-NH_2$ groups, distribution of the $-NH_2$ groups on the polymer chain is also important (Aranaz et al., 2009; Rinaudo, 2006).

2.3 Applications of chitosan

2.3.1 Agricultural Applications

Chitosan and chitin have potential in controlling plant diseases due to its toxicity and inhibition of fungal growth. Chitosan and its derivatives were shown resistant against viruses, bacteria and other pests and therefore those can be successfully used in agricultural systems to reduce the negative effects of diseases on quality and yield of the crops (El Hadrami, Adam, El Hadrami, & Daayf, 2010). Further, in seeds, chitosan used as a coating material to prevent microbial infections. For pesticides, herbicides, fertilizers, and nematocides, chitosan is used as a coating material to control the releasing process of nutrients to soil.

2.3.2 Biomedical and Pharmaceutical applications

Due to its high biocompatibility, biodegradability, and bioactivity, chitosan has been employed in implantable and injectable systems such as periodontal and orthopedic composites, drug delivery systems, scaffold for tissue regeneration and wound healing management (Aranaz et al., 2009).

Since chitosan activates immunocytes and inflammatory cells such as PMN, fibroblasts, macrophage, and angioendothelial cells, it can be used in wound healing management. These effects depend on the DD of the chitosan; high DD facilitates this property. The drug delivery systems such as hydrogels, microspheres, nanoparticles, films, and tablets use chitosan due to its cationic character. Chitosan is the only pseudo natural cationic polymer and therefore, it can be able to react with polyanions giving rise to polyelectrolyte complexes. Molecular weight, purity and DD are the three main characteristics properties of chitosan which should be considered during synthesis of drug delivery system. Chitosan has the ability to interact with negative molecules such as DNA, due to its positive charge. In 1995, this property was used for the first time to prepare a non-viral vector for gene delivery system by Mumper (Rinaudo, 2006).

Tissue Engineering; a process in which the tissue are repaired or improved by using various combinations of cells, biochemical factors, materials, and technologies, is a major field which used chitosan as a main part of artificial scaffolds or extracellular matrices. Those matrices facilitate formation of tissues by acting as a support system or framework to body cells. As the cells of tissue began to undergo proliferation, scaffolds degrade and materials are absorbed by the body. Chitosan scaffolds are promising material for tissue engineering, due to the controlled biodegradability, low immunogenic activity and porous structure (Aranaz et al., 2009; Rinaudo, 2006).

2.3.3 Cosmetic applications

Chitosan and its derivatives are used in cosmetic industry as a constituent of different cosmetics, hair care products, toothpaste, and body and hand creams. Chitosan was also identified as a material which is suitable for sensitive skin because of the moisturizing effect. This moisturizing effect on the skin is dependent on degree of deacetylation (DD) and molecular weight of the chitosan. Further, that moisturizing property offer protection from mechanical hair damage and exhibits antielectrostatic effect on hair. High molecular weight chitosan increase the water resistance of emulsions protecting against sun

irradiation and consequently enhances its film forming ability (Synowiecki & Al-Khateeb, 2003).

2.3.4 Food, Paper and Textile applications

Chitosan plays a significant role in food industry and it offers wide range of applications, including formation of biodegradable films, preservation of foods from microbial deterioration, and recovery of materials from food processing discards. Moreover it can act as a dietary fiber and as a functional food ingredient. Chitosan have been identified as versatile biopolymers of natural origin for food preservation due to their antimicrobial action against food spoilage microorganisms and antioxidant properties. The pH- dependent solubility allows them to be formed into various shapes (membranes, films, and beads) using aqueous processing (Aranaz et al., 2009).

Chitosan use as a processing additive for surface treatment applications in paper industry (Ashori, Raverty, & Harun, 2005). Further, it is also used in carbonless copy paper and photographic papers (Struszczyk, 2002). Chitin and chitosan can be used in the textile industry for the production of manmade fibers and as textile fiber finishes, coatings, and textile auxiliaries. The fibers are prepared by a spinning process involving the extrusion of chitosan, or chitin formate and acetate bath into coagulation bath. Chitin and its derivatives are used only as a coating material for nylon, wool, and cotton fibers. The use of such modified fibers includes the production of wound dressing, medical textiles, sanitary absorbents and not allergenic, deodorizing, and antimicrobial underwear, sportswear, and socks (Synowiecki & Al-Khateeb, 2003).

2.3.5 Environmental Applications

Due to the chelating ability and high porosity of chitosan, it is widely used as a flocculating and chelating agent for the removal of heavy metals such as chromium, cadmium, copper, lead, mercury, and arsenic etc., from the wastewater effluents (Rinaudo, 2006). Apart from the heavy metals, it is also used to remove synthetic polymers such as dyes, oil and reduce the odors in water. Chitosan has better sorption capacity and selectivity than zeolites, activated carbon, or organic

sorbents traditionally used for the reduction of the contamination of surface water or waste water from industrial effluents tank.

2.4 Effect of Heavy Metals

There is no clear definition for the heavy metals but the density is regarded as a defining factor. Heavy metals are thus commonly defined as those having specific density of more than 5g/cm^{-3} . Heavy metals are natural constituents of Earth's crust, but as a result of industrial activities, mining, and geochemical processes, concentration of heavy metals in aquatic environments have increased. Heavy metals are widely used in industrial applications such as manufacture of batteries, pesticides, mining operations, alloys, textile dyes, metal plating facilities, tanneries, etc. (Benavente, 2008). In Sri Lanka, main source of heavy metal contamination in aquatic system is uncontrolled agricultural practices.

Trace amount of heavy metals are required by the living organisms to maintain the metabolism of the human body, e.g., copper, iron, and zinc. Since these heavy metals cannot be degraded or destroyed, higher concentration of these metals may lead to poisoning (Crini, 2005). When the heavy metals are not metabolized by the body, they tend to accumulate in the body, especially in the soft tissues and as a result of this the heavy metal concentration in the body is higher than the actual heavy metal concentration in the environment (Benavente, 2008). This phenomenon is called as bioaccumulation. So, fish in water resources, which polluted with heavy metals, have more high concentration of heavy metal than water and when human consume those fish, heavy metals enter to the human body. Heavy metals can enter to the human body via the drinking water, food chain, air or adsorption through the skin. Typical heavy metal cycle is shown in Figure 2.8.

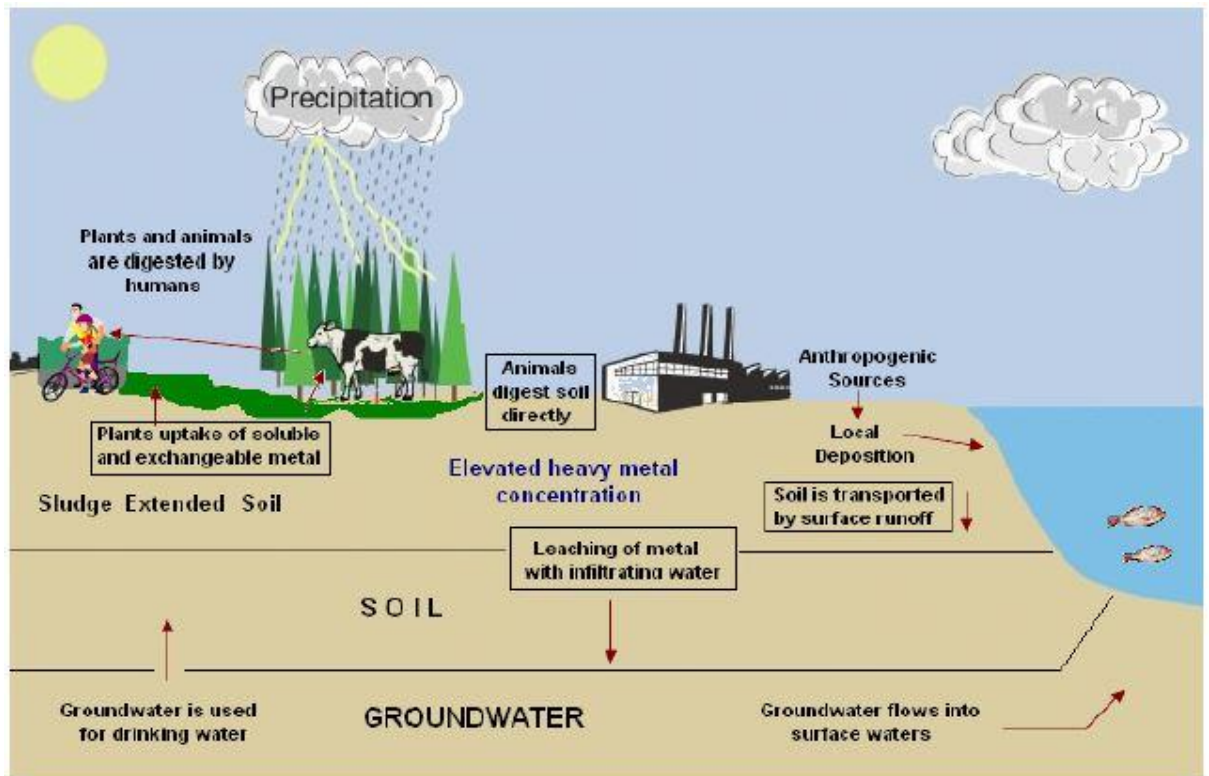


Figure 2.8 Heavy metal cycle

2.4.1 Effect of Cadmium on the environment and human health

University of Moratuwa, Sri Lanka.
 Electronic Theses & Dissertations
 www.lib.mrt.ac.lk

Cadmium is a silver white, ductile, lustrous, very malleable metal. Cadmium is mainly used in Ni-Cd batteries (nearly three-fourth), and also used as pigments for coating and plating and as stabilizers for plastics. Cadmium is mainly found in earth's crust with a combination with zinc. Naturally, nearly 25000 tons a year of cadmium is released into the environment. Half of this amount is released into rivers through weathering of rocks, and also released into air through forest fires and volcanoes. Other half of cadmium is directly released through human activities (Lenntech BV, 2014a).

Uptake of cadmium into the human body mainly takes place through food such as mushrooms, shellfish, fish, mussels, cocoa powder, and dried seafood. Exposure to higher cadmium levels also can occur when people smoke. People reside near hazardous waste sites or factories and people who work in the metal refining industry are exposed to high cadmium levels due to the polluted air with cadmium. After entering to the body, cadmium is first transported to the liver

through blood. In the liver, cadmium forms complexes with protein and those complexes are transported to the kidneys. After accumulation of cadmium into liver, it damages filtering mechanism of kidney (WHO, 2010).

Health effect that can be caused by cadmium (Benavente, 2008; Lenntech BV, 2014a);

1. Diarrhea, stomach pains and severe vomiting
2. Reproductive failure and possibility for infertility
3. Bone fracture
4. Damage to the immune system
5. Damage to the central nervous system
6. Psychological disorders
7. DNA damage or cancer development

2.4.2 Effect of lead on the environment and human health

Lead is a bluish-white lustrous, very soft, ductile and highly malleable metal. Lead, a rare metal in nature, is mainly found in ore with zinc, silver, and copper. Lead is the main constituent of the lead-acid battery and it is further used as a coloring element in ceramic glazes, traditional base metal for organ pipes, electrodes in the process of electrolysis, and as a glass of computer and television screens which protects the viewers from radiation. Paints and pesticides also contain significant amount of lead (Lenntech BV, 2014b).

Main reason for the increase in lead concentration in the environment is the lead in gasoline. When lead is burned in the engine, lead salts (bromines, chlorines, oxides) will generate, and those salts enter to the environment. The larger particles will pollute soil and surface water by immediately drop into ground, while smaller particles will travel long distances through air and remain in atmosphere. Part of this lead will fall back to earth as a rain. Lead can enter to the human body through uptake of food (65%), water (20%), and air (15%). Food such as fruit, vegetables, meats, grains, seafood, and soft drinks may contain significant amount of lead according to the origin of those. Cigarette smoke also contain small amount of lead. Due to the corrosion of pipes lead can enter to the water.

Health effects that can be caused by cadmium (Abadin et al., 2007; Lenntech BV, 2014b);

1. Kidney damage
2. Disruption of nervous system
3. Disruption of the biosynthesis of hemoglobin and anemia
4. Miscarriages and subtle abortions
5. A rise in blood pressure
6. Declined fertility of men through sperm damage
7. Brain damage
8. Behavioral disruptions of children, such as aggression, impulsive behavior and hyperactivity
9. Diminished learning abilities of children

2.5 Interaction Mechanisms of Heavy metals in chitosan

It is widely accepted that the metal binding takes place essentially on amine groups. According to some studies, hydroxyl groups also contribute to this binding process, but now it is considered that the hydroxyl groups only stabilize the metal binding on amine groups. The main reactive group $-NH_2$, can bind metal ions through three different mechanisms (Benavente, 2008; Holfetz, 2012);

- i. Complexation on N, in amine groups (chelation)
- ii. Formation of ternary complexes
- iii. Ion exchange/ electrostatic attraction

The metal ion affinity of chitosan shows the selectivity in following order(Rinaudo, 2006):





University of Moratuwa, Sri Lanka.
Electronic Theses & Dissertations
www.lib.mrt.ac.lk

2.5.2 Electrostatic Attraction/ Ion exchange

Chitosan is a weak base. Complexation can occur through the ion association mechanism, when the amine groups of chitosan are protonated. The pK_a of the chitosan determined the protonation of amine group, which in turn depend on DD and charge density.

The dissociation of chitosan is described by,



Dissociation constant, K_a of chitosan,

$$K_a = \frac{[-\text{NH}_2][\text{H}_3\text{O}^+]}{[-\text{NH}_3^+]} \quad (2.8)$$

From the above Equation 2.8, following relationship was derived

$$pK_a = \text{pH} + \log \left(\frac{1 - \alpha}{\alpha} \right) \quad (2.9)$$



University of Moratuwa, Sri Lanka.
Electronic Theses & Dissertations

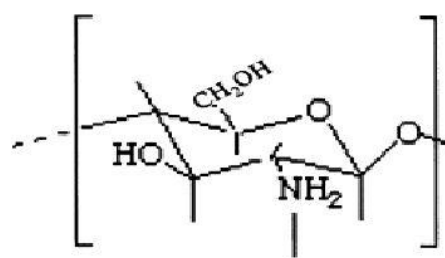
$$\alpha = \frac{[\text{H}^+]}{[\text{NH}_2]} \quad (2.10)$$

Where, α' is the experimental neutralization degree and $[\text{NH}_2]$ is the concentration of amine group, which varies with DD (Holfetz, 2012).

According to Solier, Denuziere, Viton, & Dormard, (2001), The pK_a of chitosan for complete dissociation (when $\alpha = 1$, $pK_a = \text{pH}$) is between 6.3 and 7.2. At acidic pH, most of the amine groups will be protonated and positively charge and therefore it is more likely to form ion associates with anions. So, at acidic pH, sorption of metallic anions and anionic dyes are increased and optimum pH level was found around 2-4. When pH increases, number of protonated amine groups decreases, and hence, the amino groups are available for the uptake of metallic cations (Benavente, 2008; Holfetz, 2012).

2.5.3 Uptake by formation of ternary complexes

It is widely accepted that adsorption of alkaline and alkaline earth metals into chitosan is not effective. However, Piron & Domard, 1997 found that adsorption of metal cations like Sr^{2+} and Ba^{2+} by chitosan in carbonate media was also possible due to the formation of ternary complexes. According to them, the interactions between chitosan, Sr^{2+} , and CO_3^{2-} were not due to the electrostatic attraction because the $\text{Sr}^{2+}\text{-CO}_3^{2-}$ ion pair was first formed, and that ion pair was then formed complex with amine groups of chitosan. The proposed model is shown in Figure 2.9.



University of Moratuwa, Sri Lanka.
Electronic Theses & Dissertations

Figure 2.10 Formation of ternary complexes;
Source: Benavente, 2008
www.lib.mru.ac.lk

2.6 Adsorption

“An increase in the concentration of a dissolved substance at the interface of a condensed and a liquid phase due to the operation of surface forces” - Adsorption can also occur at the interface of a condensed and a gaseous phase. – IUPAC definition

Adsorption can be further classified as a process through which a substance, originally present in one phase, is removed from that phase by accumulation at the interface between that phase and a separate (solid) phase. Temperatures, concentration of the liquid and specific surface area of the adsorbent are the major factors which effect to the adsorption process.

The adsorption process is generally classified in to two processes.

1. Physisorption (Physical adsorption)
2. Chemisorption (Chemical adsorption)

Some specific features which are useful in identifying chemisorption and physisorption are given in Table 2.2.

Table 2.2 Distinguish features between physisorption and chemisorption

Physisorption	Chemisorption
Low enthalpy of adsorption (5-50 Kj/mol)	High enthalpy of adsorption (200-400 Kj/mol)
This process is reversible	This process is irreversible
Intermolecular forces of attraction are van der waals forces, hydrogen bonds, etc..	Valence forces of attraction are chemical bond forces.
Multi-molecular layers may be formed	Generally, monomolecular layer is formed
This process is observed under conditions of low temperature	This process is taken place at high temperature
It is not specific	It is highly specific

Physisorption is also called as physical adsorption, consists the adsorption mechanism and adsorption of precipitates. Chemisorption may occur due the certain functional groups present in the chitin or chitosan chain; such as amino groups and acetylamide groups. Therefore adsorption of heavy metal into chitosan biopolymer can be categorized as a combination of both physisorption and chemisorption. A better understanding about the adsorption process and design of adsorption equipment needs knowledge of equilibrium isotherms and adsorption kinetics of Chitosan heavy metal adsorption.

2.6.1 Adsorption Kinetics

A study of the kinetics of adsorption in a system is important as it determines the rate limiting step(s) of adsorption and the kinetic parameters. These

parameters are important to design large scale adsorption system, to determine maximum adsorption capacity and to determine optimal contact time. Further, knowledge of the kinetic model and also the rate limiting step(s) of adsorption can give deep insight to the nature of the adsorption mechanism (Gupta & Babu, 2009; Holfetz, 2012).

Normally, the adsorption process consists of four steps (Holfetz, 2012).

1. Transport of the solute from the bulk solution to the adsorbent boundary film (bulk diffusion)
2. Diffusion of the solute from the boundary film to the adsorbent surface (film diffusion)
3. Diffusion of the solute from the adsorbent site to intraparticle spaces/pores of the adsorbent (intraparticle diffusion)
4. Adsorption (or desorption) of the solute at active sites on the surface and pores of the adsorbent.

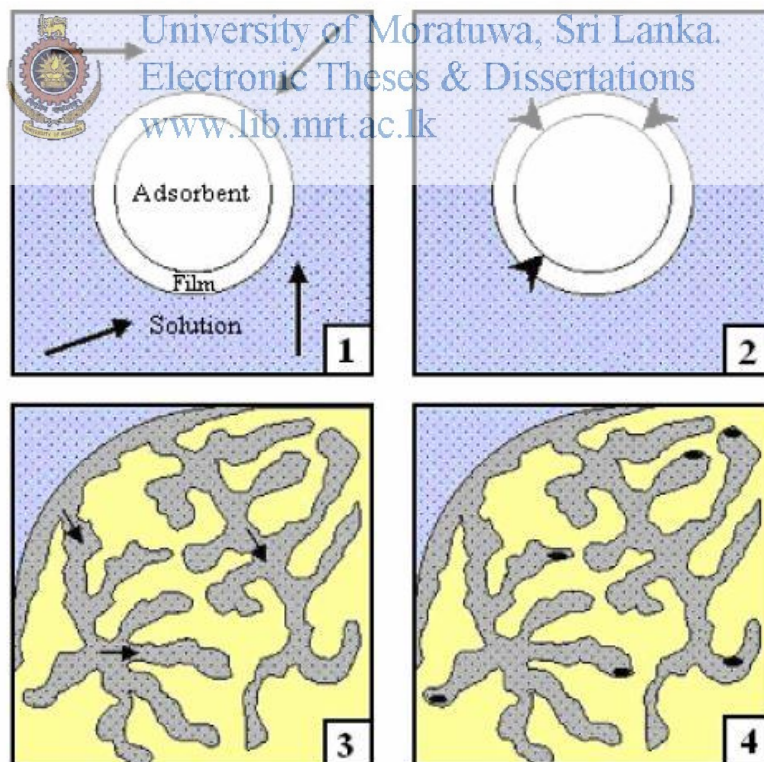


Figure 2.11 Schematic illustration of adsorption steps

Figure 2.11 shows the schematic illustration of above four adsorption steps. The complete adsorption process depends on those four steps. Therefore any changes to a step affect the whole adsorption process and these steps are susceptible to many experimental conditions such as, particle size, pH and agitation rate. Initial two steps can be eliminated by using vigorous agitation from being rate controlling step. So, most of the kinetic models consider step 3 and step 4 as rate limiting steps (Holfetz, 2012).

To find the rate limiting step of an adsorption process, various kinetic models have been developed. In an adsorption process, it can be observed either only one or more than one rate limiting steps. Even in some systems, rate limiting step changes with the contact time. Most of the commonly used kinetic models assume only one rate limiting step. Pseudo-first order (Lagergren) and pseudo-second order kinetic equations are the most commonly used kinetic models, which assumes step 4 is rate limiting. The diffusion models assume step 3; diffusion step, as a rate limiting step. Intraparticle diffusion model (Weber-Morris model) is the most widely used diffusion model (Ahmad, Sumathi, & Hameed, 2005; Holfetz, 2012; Pérez-Marin et al., 2007).



University of Moratuwa, Sri Lanka.
Electronic Theses & Dissertations
www.lib.mrt.ac.lk

2.6.1.1 Pseudo-first order model

This model was introduced by Lagergren to empirically describe the adsorption of acid into charcoal, and this is considered as one of the first kinetic equation, which is used to determine adsorption rates for liquids onto solids. It is summarized as follows (Lagergren, 1898):

$$\frac{dx}{dt} = k(X - x) \quad (2.11)$$

Where X and x (mg/g) are the adsorption capacities at equilibrium and time t (min), respectively, and k is the rate constant of the first order adsorption (1/min). Equation 2.11 was integrated with the boundary conditions of t=0 to t=t and x=0 to x=x to and following Equation 2.12 was obtained,

$$\ln\left(\frac{X}{X-x}\right) = kt \quad (2.12)$$

This equation can be further rewritten by taking $X=q_e$ and $x=q_t$ as follows:

$$q_t = q_e(1 - e^{-K_1 t}) \quad (2.13)$$

Above Equation 2.13 is the non-linear form of pseudo first order model. In order to identify the kinetic equations based on solution concentration and adsorbent solids, Lagergren's first order equation has been called pseudo first order equation (Yuh Shan Ho, 2006).

From the above Equation 2.13, two linear forms of pseudo first order (PFO) models can be obtained.

$$\log(q_e - q_t) = \log q_e - \left(\frac{K_1}{2.303}\right) t \quad (2.14)$$

$$\ln(q_e - q_t) = \ln q_e - K_1 t \quad (2.15)$$

Where, $q(t)$ is the adsorption capacity (mg/g) at time t , and q_e is the adsorption capacity at equilibrium, and K_1 is the pseudo first order rate constant, respectively. Above Equation 2.15 can be simplified into the following Equation 2.16.

$$\frac{\ln q_e}{\ln(q_e - q_t)} = K_1 \cdot t \quad (2.16)$$

2.6.1.2 Pseudo-second order model

This model was first proposed by the Blanchard in 1984 to remove heavy metals from waste water using zeolite (Blanchard, Maunaye, & Martin, 1984). That second order rate kinetic model proposed by Blanchard further developed by Ho in 1995 and pseudo second order (PSO) kinetic model was obtained (Y. S. Ho, 1995).

According to Ho, the driving force, $(q_e - q_t)$ was proportional to the available fraction of active sites. Then the kinetic rate equation can be written as follows;

$$\frac{dq_t}{dt} = K_2(q_e - q_t)^2 \quad (2.17)$$

Where, q_t is the adsorption capacity (mg/g) at time t , q_e is adsorption capacity at equilibrium, and K_2 is the pseudo-second order rate constant ($\text{mg.g}^{-1}.\text{t}^{-1}$) respectively. We can obtain following Equation 2.18 by solving the Equation 2.13 using the boundary conditions $t=0$ to $t=t$ and $q_t=0$ to $q_t=q_t$;

$$q_t = \frac{K_2 q_e^2 t}{1 + K_2 q_e t} \quad (2.18)$$

The linear form of PSO model can be obtained as follows;

$$\frac{t}{q_t} = \frac{1}{K_2 q_e^2} + \frac{1}{q_e} t \quad (2.19)$$

$$h = K_2 q_e^2 \quad (2.20)$$

Finally following Equation () can be taken;

$$\frac{t}{q_t} = \frac{1}{h} + \frac{1}{q_e} t \quad (2.21)$$

Pseudo-second order equation was theoretically derived by Azizian in 2004 (Azizian, 2004). One of the main advantages of this model is that it can be used to determine the equilibrium adsorption capacity, q_e , due to less sensitivity to the experimental errors than other models.

Apart from the above mentioned linear PSO model, known as PSO 1, another four linear models were mentioned in the literature (Lin & Wang, 2009) Those models are given below;

$$\text{PSO 2; } \frac{1}{q_e - q_t} = \frac{1}{q_e} + K_2 t \quad (2.22)$$

$$\text{PSO 3; } \frac{1}{q_t} = \frac{1}{q_e} + \frac{1}{K_2 q_e^2} \cdot \frac{1}{t} \quad (2.23)$$

$$\text{PSO 4; } q_t = q_e - \frac{1}{K_2 q_e} \cdot \frac{q_t}{t} \quad (2.24)$$

$$\text{PSO 5; } \frac{q_t}{t} = K_2 q_e^2 - K_2 q_e q_t \quad (2.25)$$

PSO 1 is the most widely used linear form of pseudo second order model and most of the situations it is best fitted with the experimental data.

2.6.1.3 Elovich model


Zeldowitsch introduced the Elovich equation, the kinetic law of chemisorption in 1934 to describe the adsorption kinetics of carbon monoxide on manganese dioxide (Zeldowitsch, 1934). The equation is given by;

$$\frac{dq_t}{dt} = \alpha e^{-\beta q_t} \quad (2.26)$$

Non-linear form of Elovich model can be obtained by integrating the above Equation 2.26 using boundary conditions of $q_t = 0$ at $t=0$ and $q_t=q_t$ at $t=t$;

$$q_t = \frac{1}{\beta} \ln(1 + \alpha\beta t) \quad (2.27)$$

From the above Equation 2.26, linear form of Elovich model can be derived by applying boundary conditions as given above.



$$q_t = \frac{1}{\beta} \ln(\alpha\beta) + \frac{1}{\beta} \ln t \quad (2.28)$$

Where, α ($\text{mg.g}^{-1}.\text{t}^{-1}$) and β (g/mg) are the Elovich constants. When, $t \rightarrow \infty$, the model results in non-physical behavior; therefore the model is more suitable to describe the initial stage of adsorption. When considering the theoretical interpretation of the Elovich model, it assumes heterogeneity of the adsorbent surface (Pérez-Marín et al., 2007).

2.6.1.4 Intraparticle diffusion model

The adsorption capacity (q_t) vary linearly with square root of contact time, when intraparticle diffusion is the rate limiting step.

$$q_t = K_i \sqrt{t} + C \quad (2.29)$$

Where, K_i is the intraparticle diffusion rate constant ($\text{mg.g}^{-1}.\text{t}^{-0.5}$) and C is a constant which gives the information about the boundary layer thickness around the adsorbent particles. It is also possible to observe multilinearity in the model, due to

variation of the pore sizes of the adsorbent (Cheung, Szeto, & McKay, 2007; Holfetz, 2012; Yu, Wu, Ma, & Zhang, 2013).

2.6.2 Adsorption Isotherm

Adsorption isotherms usually describe the retention of an adsorbate under different adsorbate concentrations. For a given concentration of adsorbate, C , and the concentration of adsorbate retained on the adsorbent, q , the function of f then can be written as $q=f(C)$. This type of function is normally known as an adsorption isotherm. Empirical determination of adsorption isotherm requires data of an adsorption system at equilibrium with varying only adsorbate concentration under identical conditions; such as constant temperature throughout the process, constant pH, and ionic strength etc (Holfetz, 2012).

Brunauer et al classified five isotherm shapes for physical adsorption by van der Waals forces (see Figure 2.12). Type I represents the typical Langmuir adsorption isotherm, especially observe for microporous adsorbents. Adsorbents which have very wide range of pore sizes exhibit the type II and III isotherms. Type IV isotherm facilitate formation of two surface layers (multilayer adsorption –BET isotherm). If the intermolecular attraction effects are significant, type V isotherm can be observed (Benavente, 2008).

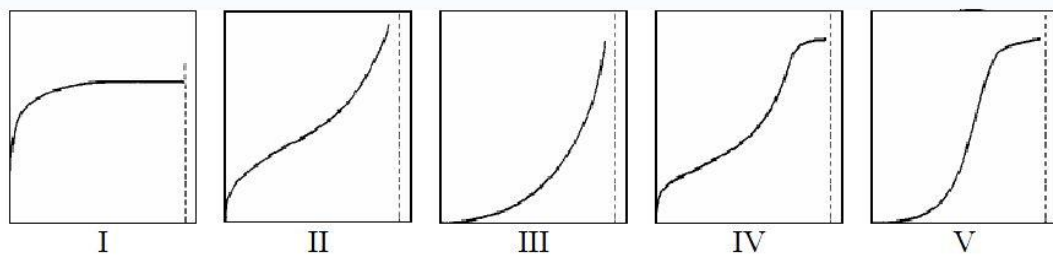


Figure 2.12 Isotherm classification

2.6.2.1 Freundlich isotherm

This isotherm model was the one of the earliest empirical model used to describe adsorption system. This isotherm model is widely used for non-ideal adsorption on heterogeneous surfaces and also for multilayer adsorption (Ng et al.,

2003; Ngah & Fatinathan, 2008; Tseng & Wu, 2009; Unlü & Ersoz, 2006). The nonlinear equation is given in Equation 2.30;

$$q_e = K_F C_e^{1/n} \quad (2.30)$$

Where, q_e is solid phase adsorbate concentration in equilibrium (g/g), C_e is liquid phase adsorbate concentration in equilibrium (g/l), K_f is Freundlich constant and $1/n$ is the heterogeneity factor. Mathematically, for all K_f and n , q_e does not reach a limit as $C_e \rightarrow \infty$, therefore the isotherm never reach to a plateau. The linear form of Freundlich isotherm can be written by taking the logarithm of Equation 2.30 (Agrawal & Sahu, 2006; Liang, Guo, Feng, & Tian, 2010; Paulino et al., 2007).

$$\log q_e = \log K_f + (1/n) \log C_e \quad (2.31)$$

From a linearized plot $\log q_e$ vs. $\log C_e$, constant K_f and exponent $1/n$ can be determined. The magnitude of the heterogeneity factor $1/n$ gives an indication of the favorability of adsorption. Where, $n > 1$ represents favorable adsorption (Khan et al., 2002).



University of Moratuwa, Sri Lanka.
Electronic Theses & Dissertations
www.lib.mrt.ac.lk

2.6.2.2 Langmuir isotherm

Irving Langmuir in 1918 proposed the Langmuir isotherm. Although six different cases were considered by the Langmuir, only first case (simple adsorption) is widely used in practical situations. This first case assumes all adsorption sites are identical and only one molecule is adsorbed by those sites. Further, the adsorbed molecules don't interact with each other and at the maximum adsorption, only a monolayer is formed. Based on the above, Langmuir derived the following relationship (Ahmed & Theydan, 2012; Holfetz, 2012; Ng et al., 2003).

$$q_e = \frac{q_m K_L C_e}{1 + K_L C_e} \quad (2.32)$$

Where, q_e (mg/g) is the adsorption capacity and C_e is the concentration at equilibrium. The equation parameters are K_L and q_m ; K_L (L/mg) is the Langmuir constant, which defines the strength of interaction between the adsorbate and

adsorbent. When $C_e \rightarrow \infty$, q_e approaches the maximum value of the parameter, q_m , which results a plateau in graph.

The most common linear form of Langmuir model can be rewritten as follows;

$$C_e/q_e = (1/q_m)C_e + (1/K_L q_m) \quad (2.33)$$

2.6.3 Thermodynamic parameters of adsorption

When designing the adsorption system, changes during the adsorption process and the speed of the reaction should be known by the designer. The speed of the reaction can be determined from the kinetic studies, but to find the expected changes during the reaction process requires brief idea of the thermodynamic parameters. Since the energy cannot be increased or decreased in an isolated system, entropy change is the driving force. Enthalpy of adsorption (ΔH), entropy change (ΔS), and free energy change (ΔG) are the main parameters must be known to analyze the process. For a closed thermodynamic system at constant temperature and concentration of pressure the following relationship can be obtained.



University of Moratuwa, Sri Lanka.
Electronic Theses & Dissertations
www.lib.mrt.ac.lk

$$\Delta G = \Delta H - T\Delta S \quad (2.34)$$

Since most of thermodynamic quantities depend on temperature and concentration or pressure, all thermodynamic parameters expressed as thermodynamic standard state. The above Equation 2.34 can be rewritten as follows;

$$\Delta G^\circ = \Delta H^\circ - T\Delta S^\circ \quad (2.35)$$

However, non-standard state ΔG can be found by introducing the concept of chemical potential. Chemical potential can be expressed as follows;

$$\mu_i^\alpha = \left(\frac{\partial G}{\partial n_i} \right)_{T, P \text{ or } C, n_{j \neq i}} \quad (2.36)$$

Where μ_i^α is the chemical of species in phase α and $(\partial G/\partial n_i)_{T,P,n_{j \neq i}}$ expresses how much Gibbs free energy of the system changes for an infinitesimal increase in the quantity of species i .

Chemical potential is related to concentration through activity a_i ;

$$\mu_i = \mu_i^0 + RT \ln a_i \quad (2.37)$$

Where μ_i^0 is the reference chemical potential of species at standard state condition and a_i is the activity of species i .

From Equation 2.36 and 2.37, changes in the Gibbs free energy for a system of I chemical species can be calculated by;

$$dG = \sum_i \mu_i dn_i = \sum_i (\mu_i^0 + RT \ln a_i) dn_i \quad (2.38)$$

Consider an arbitrary chemical reaction placed on a molar basis for species A in the form;



University of Moratuwa, Sri Lanka.
Electronic Theses & Dissertations
www.lib.mrt.ac.lk

(2.39)

Where A and B are reactants, M and N are products, and 1, b , m , and n represent the number of moles of A, B, M, and N, respectively. On a molar basis for species A, ΔG for this reaction can be calculated from the following Equation 2.40;

$$\Delta G = (m\mu_M^0 + n\mu_N^0) - (\mu_A^0 + \mu_B^0) + RT \ln \frac{a_M^m a_N^n}{a_A^1 a_B^b} \quad (2.40)$$

Recognizing that the lumped standard-state chemical potential terms represent the standard-state molar free-energy change for reaction, ΔG^0 , the equation can be simplified to a final form;

$$\Delta G = \Delta G^0 + RT \ln \frac{a_M^m a_N^n}{a_A^1 a_B^b} \quad (2.41)$$

$$\Delta G = \Delta G^0 + RT \ln Q \quad (2.42)$$

This Equation 2.42 called the van't Hoff isotherm. Q ia the reaction quotient.

When system is at equilibrium, $\Delta G = 0$, Q becomes K_d and it is known as distribution coefficient. The distribution coefficient, K_d can be calculated from the following Equation

$$K_d = \frac{q_e}{C_e} \quad (2.43)$$

Where; q_e and C_e are adsorption capacity and equilibrium concentration of solute in solution respectively.

The standard state free energy change, ΔG^0 , can be calculated from the following equation;

$$\Delta G^0 = -RT \ln K_d \quad (2.44)$$

By substituting ΔG^0 from Equation 2.44 to the Equation 2.35, following Equation 2.45 can be obtained;

$$\ln K_d = \frac{\Delta S^0}{R} - \frac{\Delta H^0}{RT} \quad (2.45)$$

Where, R is the universal gas constant (8.314 J/mol.K), T is absolute temperature (K) and K_d is the distribution coefficient. From the plot of $\ln K_d$ versus $1/T$, the values of ΔH^0 and ΔS^0 can be calculated.

The positive value of ΔH^0 indicates the endothermic process and negative value of ΔH^0 indicates exothermic process. The parameter ΔS^0 gives an indication about the spontaneity of the process (Vadivelan & Kumar, 2005).

2.7 Previous studies on chitosan as an adsorbent

Evans et al. (2002) investigated the kinetics of cadmium uptake using chitosan based crab shells. According to that study, porous chitosan showed highest average equilibrium uptake of 105mg/g for 10mg/L initial concentration which was greater than porous alumina and hydrous ferric oxide. Particle size of the chitosan was not a significant factor for adsorption of cadmium as it indicates that

adsorption takes place on the surface of the chitosan microporous matrix. However, solution pH has a significant effect on the adsorption of cadmium onto chitosan. In this study, chitosan showed significant removal of heavy metal between pH 5 and 9. Below pH 5, there was no adsorption due to the protonation of the amino groups and above pH 9, $\text{Cd}(\text{OH})_2$ was precipitated. Further, the rate of cadmium adsorption by chitosan synthesized from crab shells was controlled by intraparticle diffusion. The authors suggested that an increase in the agitation rate reduced boundary layer thickness of the particles and hence increase the uptake rate.

According to the Ng et al., 2003, particle size significantly effect to the adsorption of lead onto chitosan. This phenomenon not valid for the chitosan particles which are perfectly spheres and it is for chitosan flakes with different particle sizes. Experiments were carried out at two different solution pH values (3.5 and 4.5) and it was observed that slight increase in adsorption at higher pH. Langmuir isotherm model, Redlich-Peterson isotherm model and Freundlich isotherm model were used to analyze the experimental data. Lead adsorption onto chitosan more likely to be governed by the Freundlich isotherm. However, authors suggested that the comparatively high correlation coefficients of Langmuir and Redlich-Peterson isotherms indicates more than one mechanism of adsorption.

Chu, 2002 investigated adsorption equilibrium and kinetics of copper adsorption onto chitosan in prawn shell. Prawn type “*penaeus monodon*” was used as chitin source for this investigation and exterior surface of the prawn shell was converted to chitosan. Due to this partial conversion, the time and the amount of reagents required for deacetylation process significantly reduced. According to Chu, 2002, copper adsorption greatly depend on the pH of the solution. At lower pH (pH 3.0), due to the protonation of amino groups, metal adsorption capability of chitosan was significantly reduced. Experimental results were fitted well with the Langmuir isotherm model and authors developed new extended version of Lagmuir-Freudlich model which was better fitted with experimental data.

According to Wu, Tseng, & Juang, (2009), adsorption capacity depends on the type of chitin source because the surface area decreases for different sources as

in the order of; crab > lobster > shrimp. Both flake type chitosan and bead type chitosan were used for adsorption experiment and it was reported that bead type chitosan has higher adsorption capacity compare to flake type one. This behavior was explained by the pore- blockage mechanism. This mechanism suggested that the distribution of the solutes adsorbed can be determined by intraparticle diffusion rate of the solutes (heavy metal or dye) into the porous matrix, which is governed by the concentration gradient of solutes and adsorbent particle porosity. At low initial metal ion concentration, the initial flux through the porous material is low and metal ion binds with amino sites near to the exterior surface of the particle. So, the adsorbed metal ions clog the pores near the exterior surface and that prevents the further diffusion of metal ions into active sites deep in the interior surface. In contrast, at high concentration flux is high and therefore heavy metal ions shoot deep into the interior matrix until pores are clogged. Since flake chitosan has a more restricted pore structure, this behavior is more likely occurred. According to the kinetic studies, pseudo first order model, pseudo second order model and intraparticle diffusion model couldn't be successfully confirmed the mechanism of adsorption.



University of Moratuwa, Sri Lanka.
Electronic Theses & Dissertations

www.lib.mrt.ac.lk

Apart from the heavy metal adsorption, Ahmad et al., (2005) investigated the adsorption of residue oil from palm oil mill effluent using powder and flake chitosan. Even at a lower dosage, chitosan powder almost adsorbed all the residue oil in palm oil mill effluent. Ahmad et al., (2005) also reported that chitosan in powder form had a higher adsorption capacity for residue oil compared to the flake form and this was mainly due to the effect of surface area. It was also observed that the adsorption capacity greatly depends on pH of the solution. Experimental data best fitted with the Freundlich isotherm model and both chitosan types showed favorable adsorption characteristics. Adsorption kinetics of residue oil onto chitosan powder and flake was better described by pseudo second order model.

Pitakpoolsil & Hunsom, 2014, studied the adsorption of biodiesel onto commercial chitosan flakes. According to that study, the optimum conditions for the adsorption process were set as an initial wastewater pH of 4.0, chitosan flake dose of 3.5g/L and contact time for 3 hours at 300rpm. According to the authors,

the adsorption of pollutants onto the chitosan can be divided into parts; (a) the transport of the pollutant from bulk solution to the chitosan surface and (b) the adsorption of pollutants onto chitosan surface. The pollutants were attached to the protonated amino groups ($-\text{NH}_3^+$). Therefore authors suggested that the adsorption process was diffusion controlled. Kinetic studies revealed that the initial 1.5 hours of adsorption process was best fitted with the pseudo first order model and from 2 hours to 5 hours it was controlled by the pseudo second order model. Reusability of the chitosan flakes was also studied by using NaOH as regenerative solution. Studies suggested that only 40% of the adsorbed pollutants were removed from the chitosan.



University of Moratuwa, Sri Lanka.
Electronic Theses & Dissertations
www.lib.mrt.ac.lk

Chapter 3

3 Materials and Methods

3.1 Adsorbent material – Chitosan

Chitosan was synthesized from the locally available shrimp type “penaeus monodon”; which gives highest percentage of chitin percentage and hence the chitosan yield. Shrimp shells were collected from the local shrimp processing factories located in the Western province of Sri Lanka.

3.1.1 Extraction of chitosan

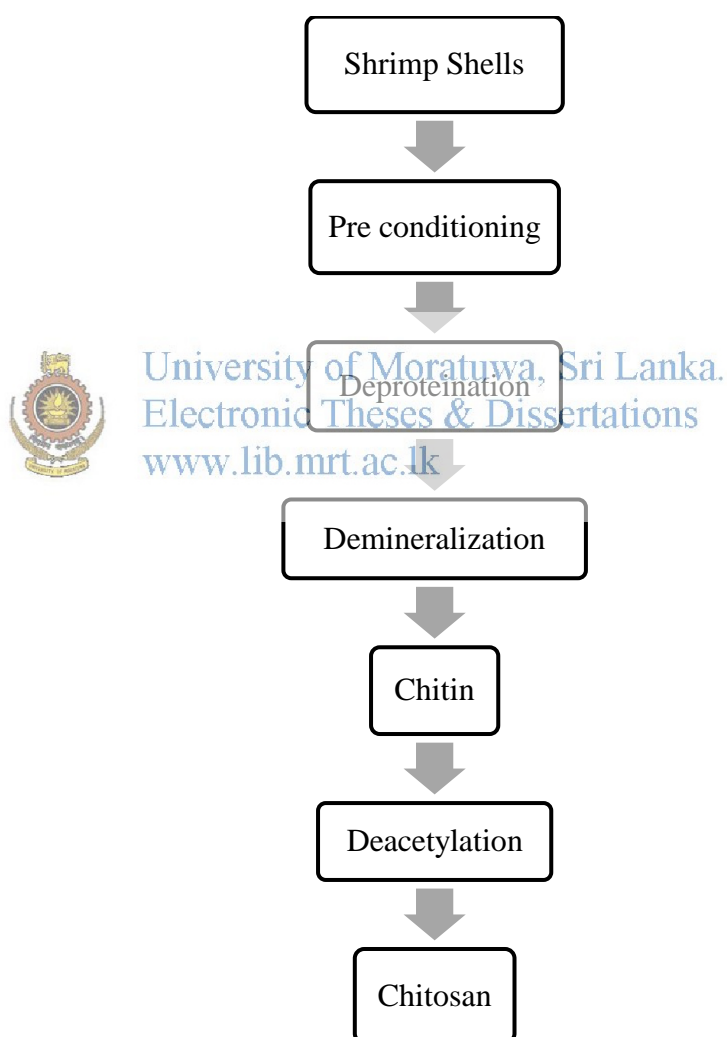


Figure 3.1 Process flow chart of chitosan extraction

During transportation of waste shrimp shells, it is necessary to keep the temperature close to the 0°C and avoid direct exposure to sunlight. Obtained shrimp shells were stored at -18°C in the storage facility until needed (Khanafari & Marandi, 2008). Then shrimp shells are allowed to decay naturally at the ambient temperature for 24-48 hours before subjecting the material to chitin extraction. After the 24-48 hours, shrimp shell produced putrescent compounds and released bad smell. The next step was pre conditioning; shrimp shells were soaked in 0.02molL⁻¹ acidic acid solution for 8hr at 28-32°C to remove the unbound protein in shells.

Preconditioned shrimp shells were demineralized with 1 mol/dm³ (M) HCl (1:10 w/v) at ambient temperature (30°C) for 6 hours. The residue was washed to maintain neutralized pH value. It was then dewatered and deproteinized with 1 M NaOH solution (1:10 w/v) at ambient temperature (30°C) for 16 hours. The residue was washed with distilled water to maintain neutralized pH value and then it was dewatered. Synthesized chitin was ground and sieved with 250, 106 and 75 mesh sizes and three particle sizes were obtained. The chitin, synthesized from the above process was deacetylated in NaOH (1:10 w/v). After deacetylation, the chitosan was washed with distilled water until neutralize the pH (6.5 -7.5).

3.1.2 Characterization of Chitosan

3.1.2.1 Fourier Transform Infrared (FTIR) spectroscopic analysis

Chitosan samples were prepared in the form of film using potassium bromide (KBr). Approximately 20-40mg of chitosan powder and 120mg of KBr was blended and film was prepared using mold and hand compressing equipment. Then it was heated up to 105°C for nearly 2-3 hours to remove moisture. The spectra of chitosan samples were obtained using a Bruker FTIR instrument with a frequency range of 4000-600 cm⁻¹. Characteristic spectrum of chitosan consists of the peaks at specific wave numbers as given in the Table 2.1 in chapter 2.

3.1.2.2 Viscosity

Viscosity of chitosan was determined with a Brookfield viscometer. Chitosan solution was prepared in 1% acetic acid at a 1% concentration on a dry

basis (1g in 100ml). Measurement was made in duplicate using a No.2 spindle at 50rpm on solutions at 25°C with values reported in centipoise (cps) units.

3.1.2.3 Thermo gravimetric analysis (TGA) and differential thermal analysis (DTA)

These tests were carried out using Rigaku thermoflex TG8110 instrument. 8-12 mg of chitosan was measured and then it was placed on the balance system equipment. The temperature was raised from 25 to 600 °C at a heating rate of 10 °C per minute. The mass of the sample pan was continuously recorded as a function of the temperature.

3.1.2.4 Degree of Deacetylation

Degree of deacetylation is an amount of chitosan (amino groups) formed during the deacetylation process. DD of the chitosan samples were calculated using Fourier transform infrared spectroscopic (FTIR) method using KBr film method. DD was calculated from the Equation 3.1,

$$DD = 100 \left[\frac{A_{1655}}{A_{3450}} \times \frac{1.33}{1.33} \right] \quad (3.1)$$

Where A_{1655} and A_{3450} are the absorbance at wave length 1655cm of the amide –I band as a measure of the N- acetyl group content and wave length 3450 cm of the hydroxyl band (Trung et al., 2006).

3.2 Adsorbates

Stock solutions (1000mg/L) of cadmium (Cd^{2+}) and lead (Pb^{2+}) ions were prepared by dissolving required amount of analytical grade $CdSO_4$ and $Pb(NO_3)_2$ in deionized water. Those stock solutions were diluted with deionized water to obtain desired concentration of heavy metal ions ranging from 5 to 1000 mg/L. pH of the metal ion solutions were adjusted using 0.1M NaOH and 0.1M HCl.



University of Moratuwa, Sri Lanka.
Electronic Theses & Dissertations
www.lib.mrt.ac.lk

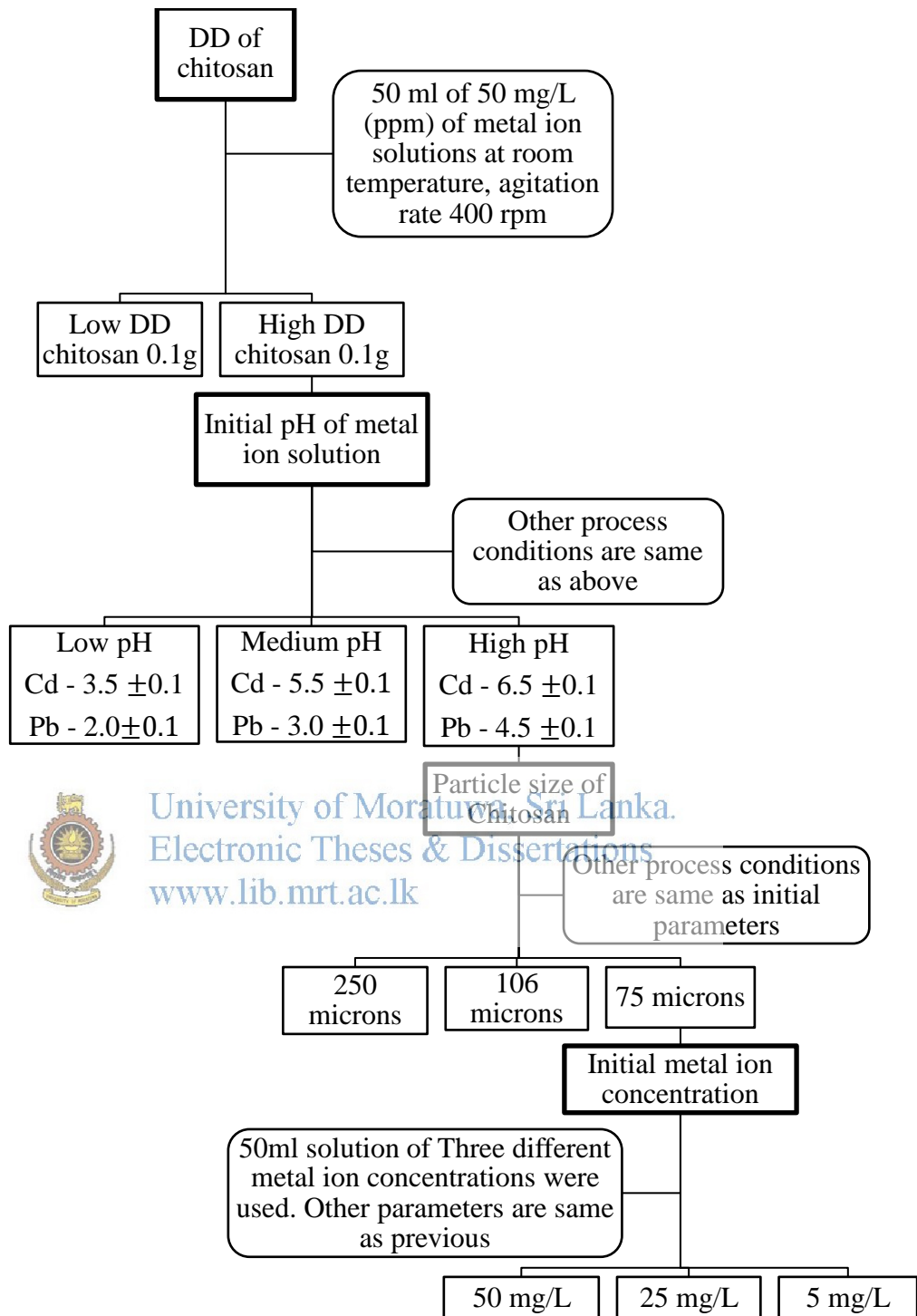


Figure 3.3 Process flow chart for kinetic experiments

3.3.2 Isotherm experiments

Isotherm experiments were conducted for varying initial metal ion concentration of metal ion solution and all other process parameters were fixed. The concentration of the metal ion solution was varied from 5 mg/L (ppm) to 1000 mg/L (ppm).

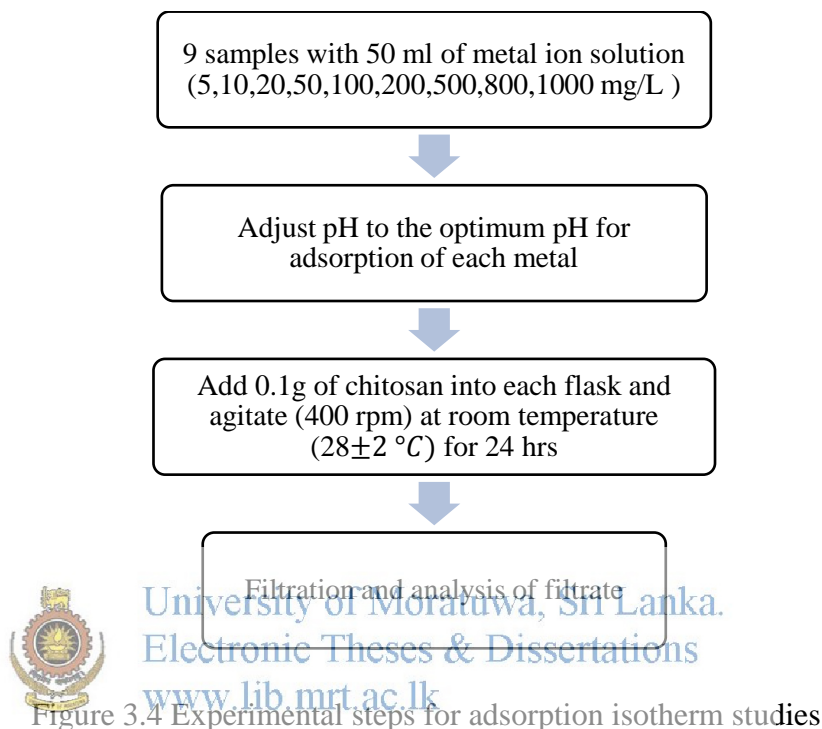


Figure 3.4 Experimental steps for adsorption isotherm studies

Experimental results were analyzed by using Langmuir and Freundlich isotherm models and adsorption parameters were determined.

3.3.3 Thermodynamic experiments

To find the thermodynamic parameter and effect of temperature on heavy metal adsorption, adsorption experiments were conducted at four different temperatures (30, 40, 50, 60 °C).

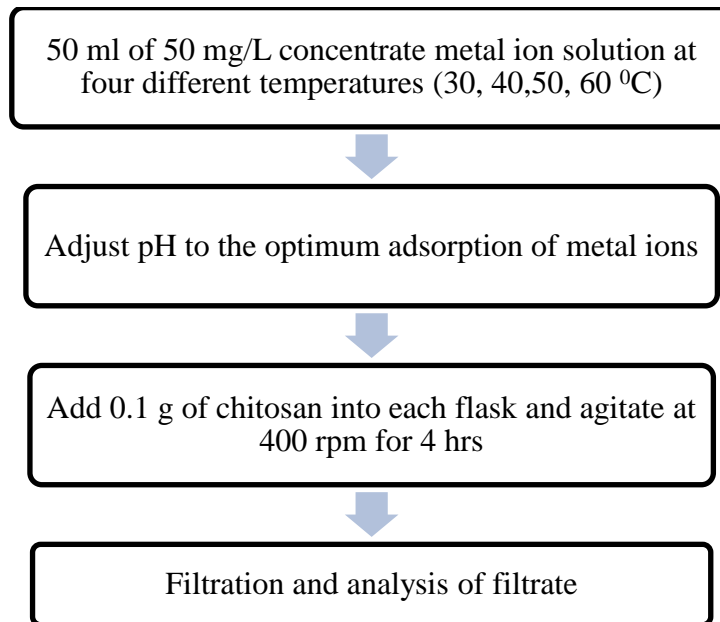


Figure 3.5 Experimental steps for thermodynamics study

3.3.4 Desorption experiments

The desorption experiments were conducted for known amount of heavy metal adsorbed chitosan to heavy metals in different regenerating solutions. Deionized water and NaOH were used as regenerating solutions.

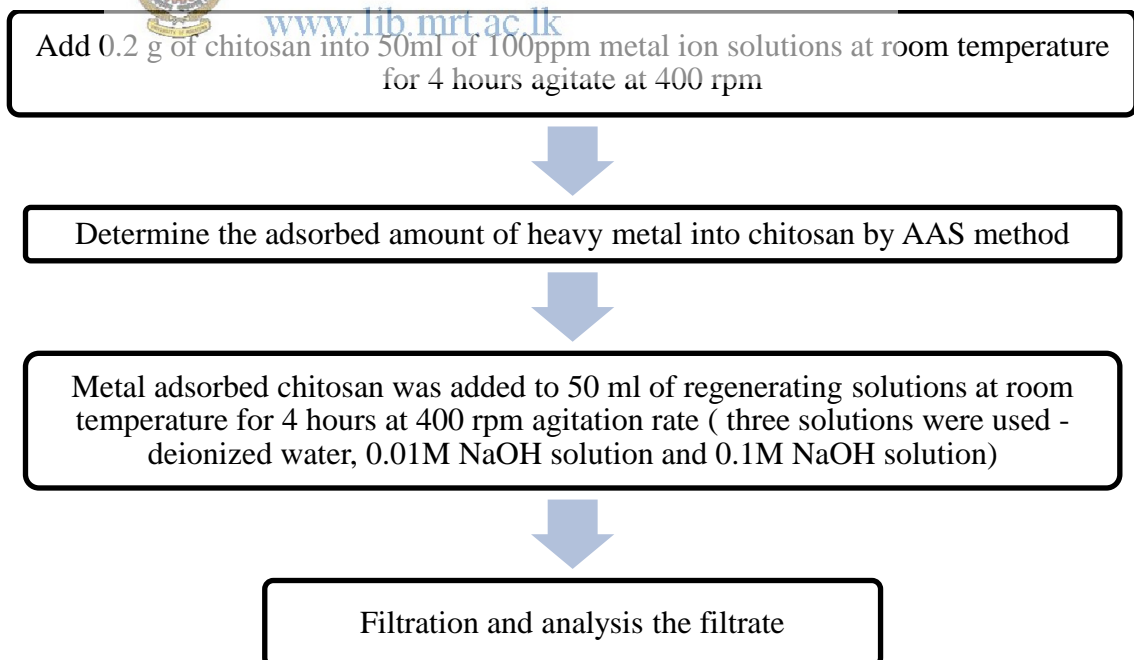


Figure 3.6 Experimental steps for desorption studies

3.4 Evaluation of Experimental Data

Adsorption capacity (q_t), the uptake % and distribution ratio (K_d) of chitosan adsorbents were determined by the mass balance equation. The adsorption capacity, q_t (mg/g), was calculated at time t as following Equation 3.2 (Ng et al., 2003; Ngah & Fatinathan, 2008).

$$q_t = (C_0 - C_t) \frac{V}{m} \quad (3.2)$$

Where, C_0 is the initial metal ion concentration of the solution (mg/L), C_t is the metal ion concentration in solution at time t , and m and V are mass of the adsorbent (g) and volume of aqueous metal solution (L) respectively. The percentage of adsorption of heavy metal was calculated according to the following Equation 3.4 (Holfetz, 2012; Semerjian, 2010).

$$\text{Adsorption (\%)} = \frac{C_0 - C_f}{C_0} \times 100 \quad (3.4)$$

Where, C_0 is the initial metal ion concentration and the C_f is the final metal ion concentration of the solution. The distribution ratio K_d , was found by according to the Equation 2.43 and it can be rewritten as follows by expanding the q_e (Holfetz, 2012).

$$K_d = \left(\frac{C_0 - C_f}{C_f} \right) \times \frac{V}{m} \quad (3.5)$$

Where, C_0 is the initial metal ion concentration, C_f is the final metal ion concentration of the solution, and m and V are mass of the adsorbent (g) and volume of aqueous metal solution (L).

3.5 Analysis of adsorption kinetics and isotherms

Modeling of adsorption kinetics and isotherms was done by using statistical analysis software.

To find the rate limiting step of the process, four kinetic models were used. Pseudo first order model, pseudo second order model Elovich model and intra-particle model were used as kinetic models. Non-linear regression method was done as given in the chapter 2 and kinetic parameters and R^2 values were calculated using statistical analysis software.

Freundlich and Langmuir isotherm models were used to analyze the adsorption process and favorability. Both linear and non-linear methods were used to analyze the results.



University of Moratuwa, Sri Lanka.
Electronic Theses & Dissertations
www.lib.mrt.ac.lk

Chapter 4

4 Results and Discussion

4.1 Characteristics of Chitosan

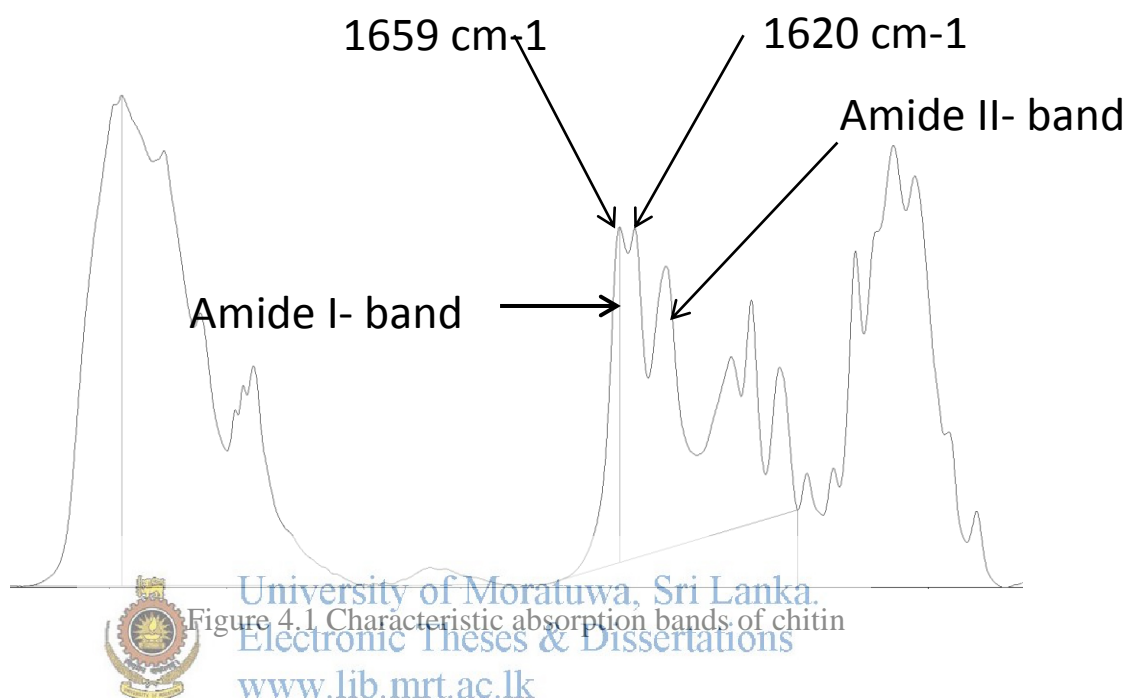


Figure 4.1 Characteristic absorption bands of chitin
University of Moratuwa, Sri Lanka.
Electronic Theses & Dissertations
www.lib.mrt.ac.lk

According to the FTIR spectrum of chitin shown in Figure 4.1, it can be clearly observed that the amide I band is split into two at 1659 cm⁻¹ and 1620 cm⁻¹, which further gives an indicator of the type of allomorphs of chitin. According to Rinaudo, 2006, it revealed that the shrimp type, *penaeus monodon*, which used to synthesize chitosan contain α -chitin, due to the splitting of amide I band, whereas it's specific to α -chitin. Since most of the physio-chemical characteristics of chitosan depend on the type of chitin, it is important to identify the allomorphs of chitin in the natural chitin source.

4.1.1 Degree of Deacetylation (DD)

DD obtained from FTIR method is varied according to the selected base line system. It was identified that back titration method is a reliable method to calculate DD. DD depends on the processing parameters of the process, such as

concentration of NaOH, temperature, reflux time and number of times of deacetylation (Van Toan, Ng, Aye, Trang, & Stevens, 2006).

Apart from the processing parameters, DD depends on the structural variation of the chitosan. Therefore chitosan can be chemically modified by changing the process parameters, especially increasing the severity of process parameters. That structural variation can be clearly observed in the following FTIR graphs shown in Figure 4.2. According to the Figure 4.2, the characteristic peak for the C=O stretching, found in 1650 cm^{-1} , shows significant reduction in high DD sample implying more C=O bonds converted into NH_2 and resulted in low

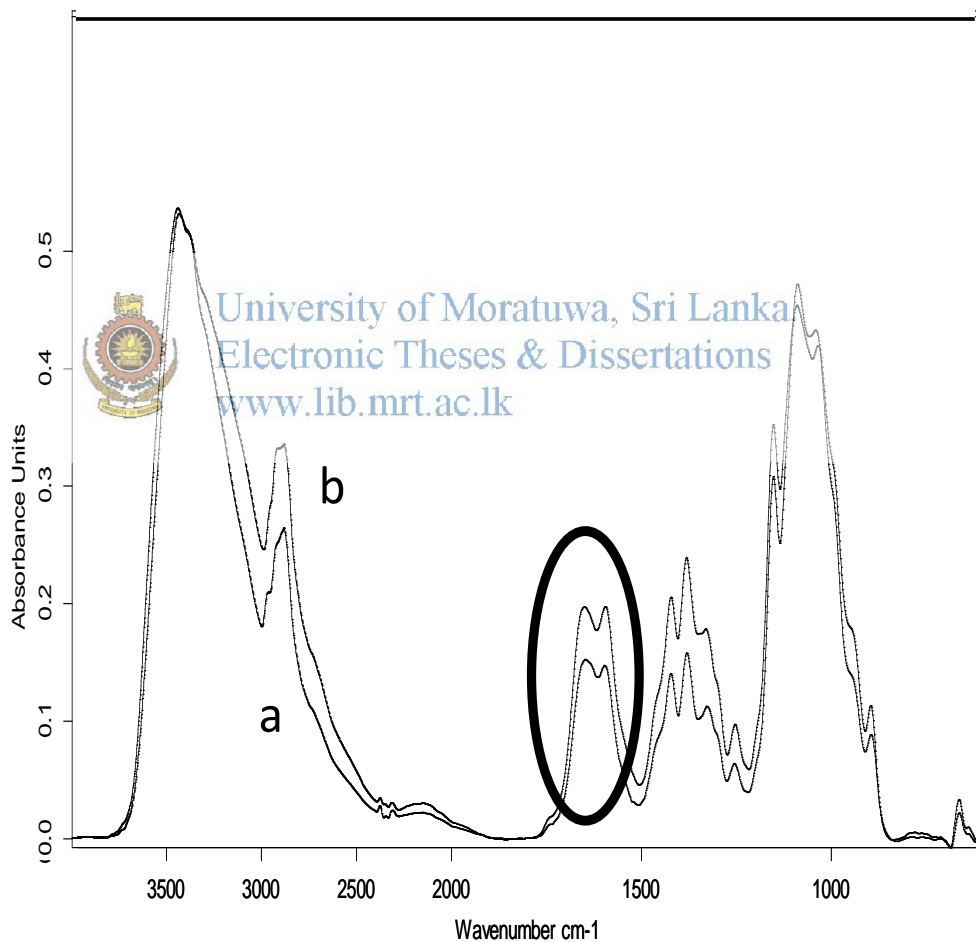


Figure 4.2 Comparison of characteristics bands of high DD and low DD FTIR spectroscopy a) Low DD b) High DD

4.1.2 Viscosity

According to the severity of the deacetylation treatment (alkaline concentration, process temperature and reflux time), chitin chain is more susceptible of the hydrolysis, resulting cleavage of the main chain. Because of the cleavage of the main chain, molecular weight and viscosity of the chitosan solution is reduced.

The viscosity of the chitosan solution, at the molecular level, is a direct measurement of the hydrodynamic volume of the chitosan molecules which in turn is governed by molecular size or the chain length and hence the molecular weight (Rinaudo, 2006). As mentioned in the methodology, viscosity of the chitosan solution was measured by using Brookfield viscometer. Results are shown in the Table 4.1. It can be clearly seen that with increasing DD, viscosity of the chitosan was reduced and it was further implied that molecular weight reduced with increasing DD.



University of Moratuwa, Sri Lanka.
Table 4.1 Viscosity of two chitosan samples
Electronic Theses & Dissertations

Sample	Viscosity (cps)
Sample 1(low DD)	208.4
Sample 2(high DD)	168.6

4.1.3 Thermal analysis

According to the Figure 4.3, chitosan exhibits a broad endothermic peak centered at about 89⁰C and the peak is attributed to the loss water associated with hydrophilic groups (free -NH₂ groups). The exothermic peak, which appears at the temperature about 328⁰ C, corresponds to the decomposition of the polymer and thermal degradation of chitosan was started at about 175⁰ C. Therefore chitosan undergo thermal decomposition at 212⁰ C prior to melting.

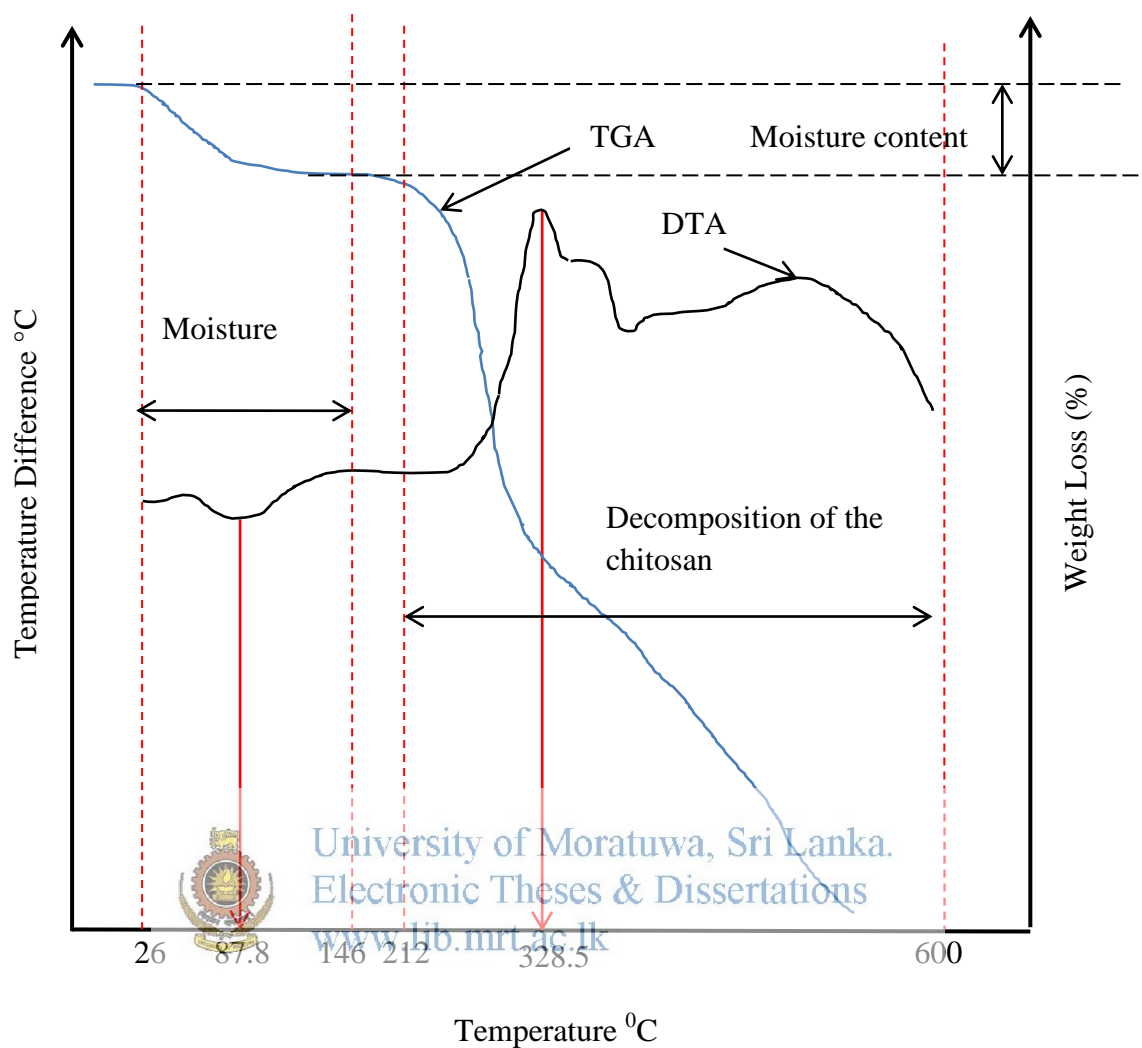


Figure 4.3 Thermo gravimetric (TGA) and differential thermal (DTA) analysis of Chitosan

4.2 Adsorption of Cadmium and Lead by chitosan

Adsorption of cations by chitosan was found to be dependent on contact time, pH of the metal ion solution, initial metal ion concentration of the solution, chitosan dosage, and particle size of the chitosan powder. These are discussed on the section below.

4.2.1 Effect of contact time

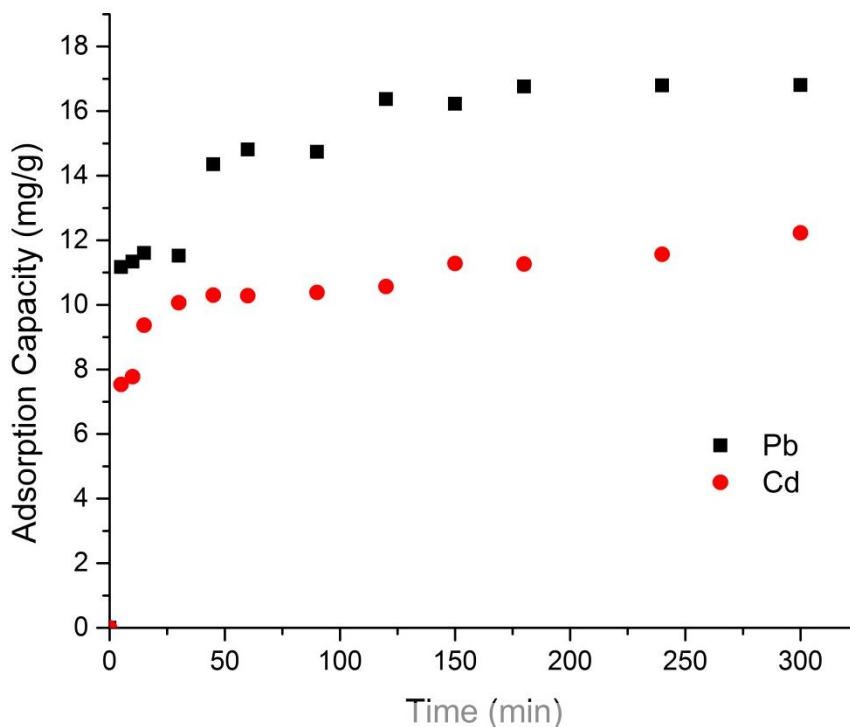


Figure 4.4 Adsorption capacity with contact time at room temperature ($28 \pm 2^\circ\text{C}$) and high pH (for Cd- 6.5 & for Pb- 4.5)

Figure 4.4 shows rapid initial uptake of both cadmium and lead at the beginning until 60 minutes and, thereafter reduce the adsorption rate up to 150 minutes and adsorption process became equilibrium. The initial cadmium and lead concentration was fixed in to 50 mg/L, the agitation rate 600 rpm, particle size less than 250microns, and at ambient temperature ($28 \pm 2^\circ\text{C}$). Lead shows higher adsorption rate compare to the cadmium due to its high affinity to chitosan. According to Figure 4.4, around 12 mg/g of cadmium and around 17 mg/g of lead were adsorbed into chitosan. Initial high adsorption rate was due to the availability of large number of vacant sites in chitosan surface and high solution concentration. Consequently, with increasing contact time, the metal uptake by the chitosan slowing down due to competition for the availability of active sites for intensified metal ions remaining in the solution. Contact time is an important parameter because this factor determines the adsorption kinetics of an adsorbate at a given

initial concentration of the adsorbate. Lead shows higher adsorption capabilities compare with cadmium (Unlü & Ersoz, 2006)

4.2.2 Effect of degree of deacetylation (DD)

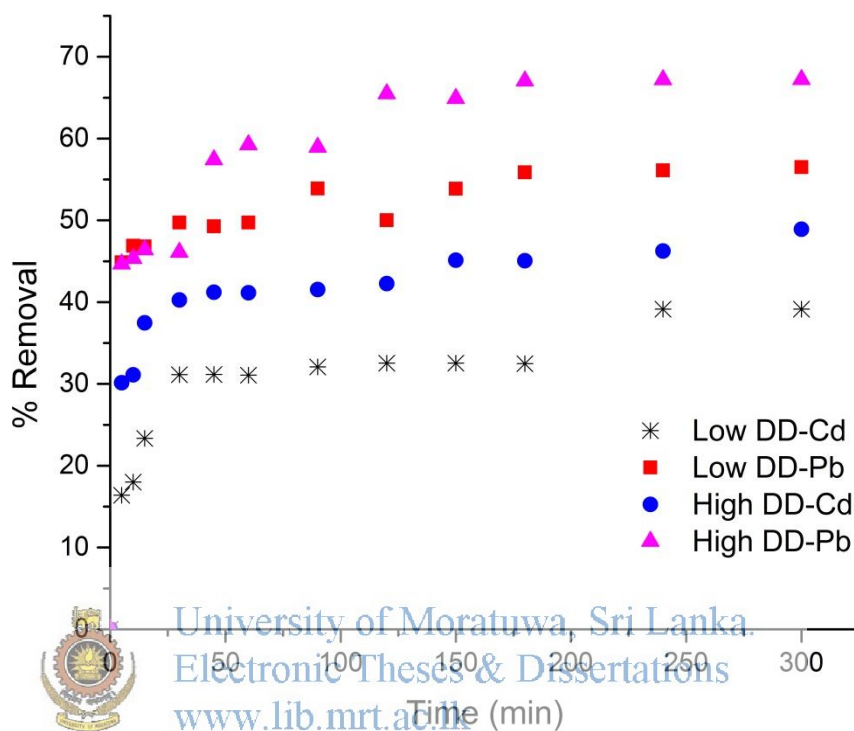


Figure 4.5 Effect of DD on % removal of cadmium and lead at room temperature (28 ± 2 °C) and high pH (for Cd-6.5 & for Pb-4.5)

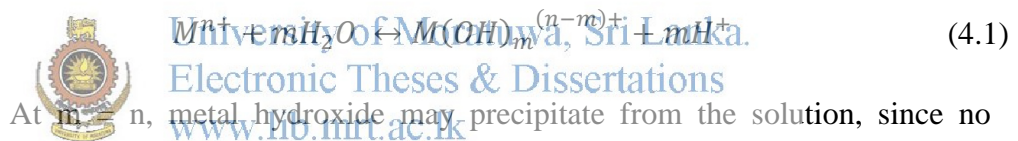
As indicated in the figure 4.5, since DD is directly related to the number of amino groups available in the chitosan, adsorption of heavy metal significantly dependent on the DD. High DD represents high number of amino groups, increase the number of active sites for adsorption and hence increase the adsorption of metal cations. At high DD, nearly 46% of cadmium and 67% of lead was adsorbed in to chitosan while in low DD 35% of cadmium and 56% of lead was adsorbed. This is a chemical modification of the chitosan. The different DD values can be obtained by changing the process parameters of the chitosan synthesis process. By increasing the severity of deacetylation process, high DD chitosan can be synthesized (NaOH concentration and temperature). To observe other process conditions, high DD chitosan was used.

4.2.3 Effect of solution pH

The protonation of amine groups in chitosan and speciation of heavy metals depend on the pH of the solution. Both of these factors are significant to the adsorption process, and therefore it is important to examine the effect of pH as it influence the adsorption efficiency in order to optimize a real world adsorption system.

The amine group of chitosan becomes protonated in acidic solutions (at low pH). Due to this protonation of amine groups, it facilitates ion association interaction with anions. Contrastly, high protonation of the amine groups reduce the available sites for complexation with metal cations via other appliances, like formation of coordination complexes.

In the solution, most of the cations undergo hydrolysis, which results the formation of metal hydroxide. The hydrolysis of M^{n+} metal ion is given in Equation 4.1;



At $m = n$, metal hydroxide may precipitate from the solution, since no charge in metal species. There is a possibility for formation of polynuclear species, like $M_l(OH)_n^{(lm-n)+}$. Due to the precipitation of metal hydroxide, the calculated value of metal adsorbed by the chitosan may be erroneous, as it assumes all other metal ions not remaining in the solution are adsorbed by the chitosan according to the mass balance equation (Holfetz, 2012).

According to the Figure 4.6, the pH of the solution greatly affects the adsorption of cadmium into chitosan; adsorption capacity is increased with increasing pH. The range of pH was selected from 3.5 (low) to 6.5 (high) (medium – 5.5) according to the speciation diagram of cadmium. At the pH values greater than 6.5 Cd^{2+} ions are not dominant in the solution as shown in the Figure 4.6 and hence the pH values less than 6.5 was used. As shown in Figure 4.7, when pH greater than 7, Cd^{2+} is not dominant and there are other species form in the solution. Especially, due to formation of $Cd(OH)_2$; a white color precipitate, pH values

greater than 7 was avoided in this experiment (Kelesglu, 2007). Around 51% of cadmium was adsorbed at high pH solution and around 19% of cadmium was adsorbed at low pH solution. So, the pH of the solution is a critical factor in heavy metal adsorption into chitosan.

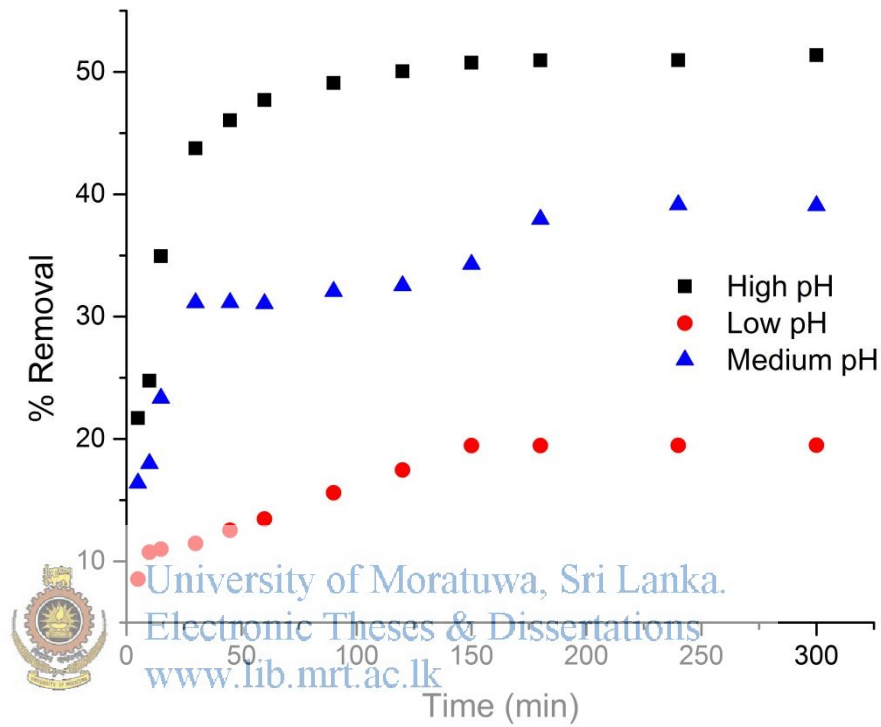


Figure 4.6 Effect of pH on % removal of cadmium from chitosan

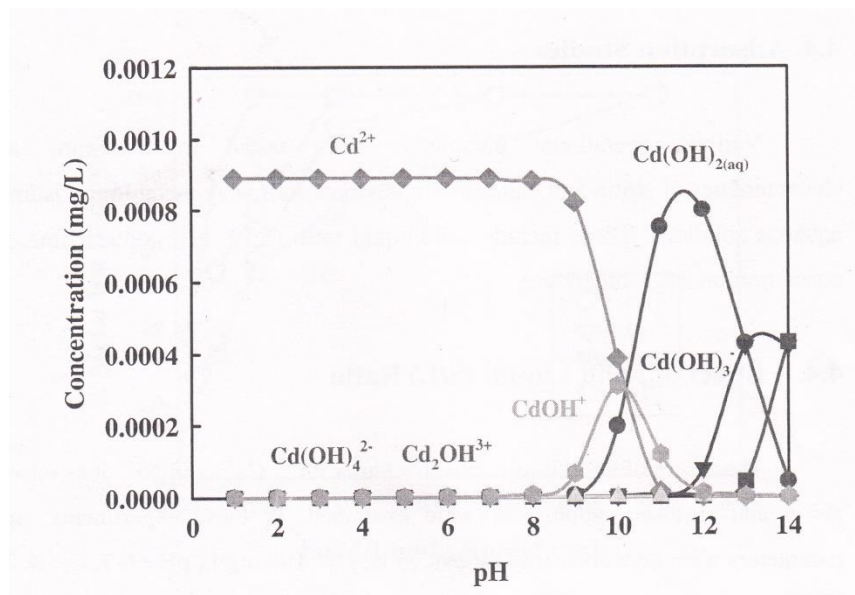


Figure 4.7 Chemical speciation of Cadmium (100mg/L) in water as a function of pH

Source:(Kelesglu, 2007)

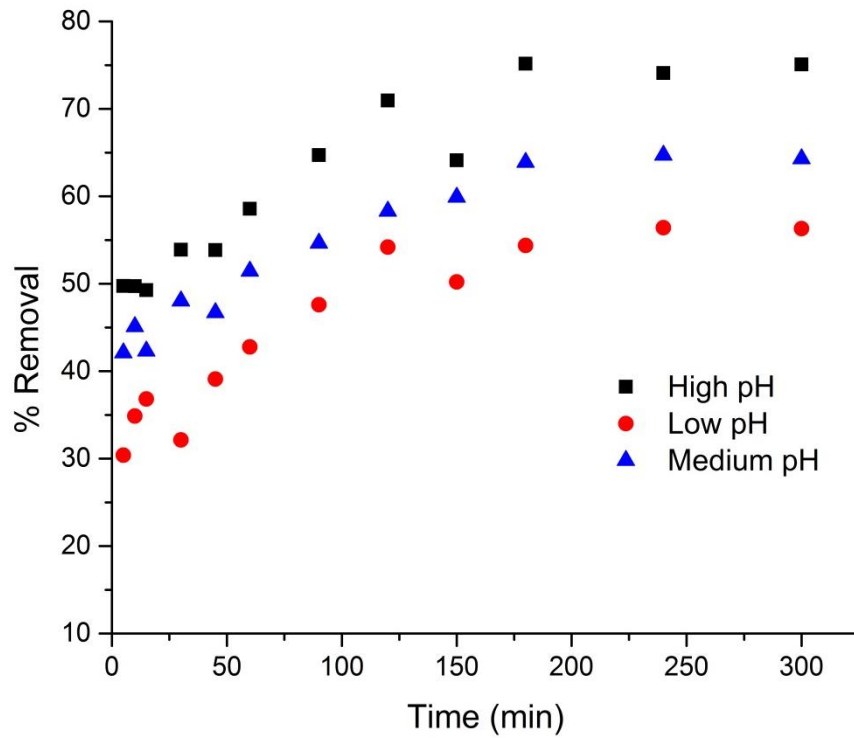


Figure 4.8 Effect of pH on % removal of lead from chitosan



University of Moratuwa, Sri Lanka.
Electronic Theses & Dissertations

www.lib.mrt.ac.lk

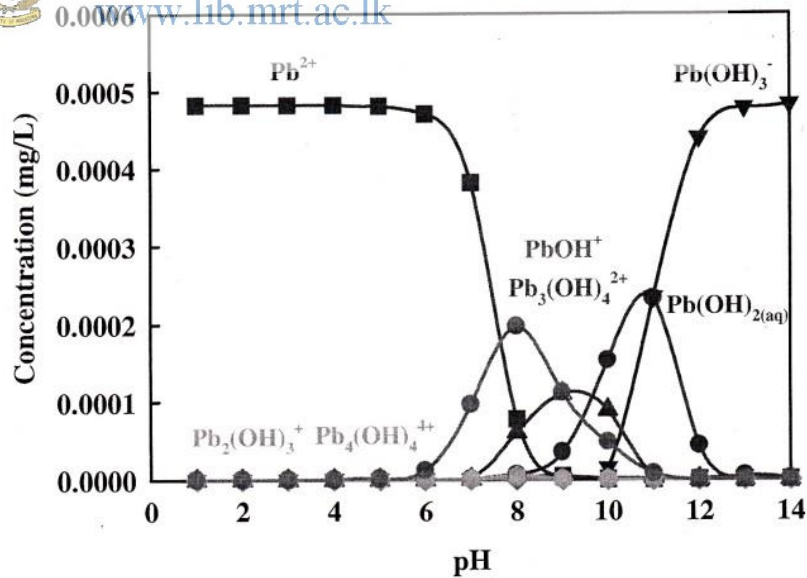
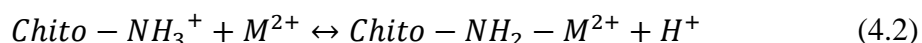


Figure 4.9 Chemical speciation of Cadmium (100mg/L) in water as a function of pH

Source : Kelesglu, 2007

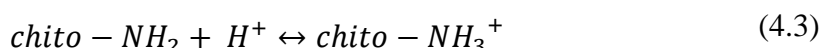
According to the Figure 4.8, as same as in the cadmium, pH of the solution greatly affects to the adsorption of lead. The pH range was selected from 2 to 4.5 according to the speciation diagram of lead. 2, 3, and 4.5 were the pH values used in this experiment. As shown in Figure 4.9, after pH 5, Cd^{2+} is not the dominant species, so pH values greater than 5 was avoided due to precipitation of $Pb(OH)_2$ (Kelesglu, 2007). Around 75% and 54% of lead was adsorbed at high pH and low pH solutions respectively.

The low adsorption capacity in acidic solution can be explained by the competition between protons and metallic ions for available amino adsorption sites, and by electrostatic repulsion. The following reaction shows the influence of pH on the uptake of metallic ions (Benavente, 2008);



At low pH, the equilibrium of this reaction is shifted to the left reducing the number of binding sites for metallic ions. In addition, due to the protonation of electrostatic repulsion of metal cations, available number of binding sites for metal cations is reduced. On the other hand, at higher pH, there is a decreased in H^+ ions and that shifted to the reaction right and both competition for binding sites and electrostatic repulsion are reduced. Therefore adsorption performance is improved.

It was observed that after some time, solution pH was raised. This behavior can be explained using the following Equation 4.3;



Chitosan act as a weak acid. At high H^+ concentration, amine groups of chitosan takes the protons available in the solution as according to the Equation 4.3. Therefore H^+ concentration of the solution reduces and increases the pH of the solution. Mizera, Mizerová, Machovic, & Borecká, 2007 also reports this effect.

4.2.4 Effect of particle size

Several authors found that the effect of particle size in adsorption of heavy metal into chitosan was significant (Benavente, 2008; Holfetz, 2012). Maximum

adsorption depends on the specific surface area of adsorbent and therefore maximum adsorption can be seen in small particle size chitosan flakes, as smaller particles have large surface area per unit weight. In some situations, compare with the smaller particles, large particles show higher removal efficiency if particles are in spherical shapes. In general, higher external mass transfer can be observed in larger particles in spherical shape than smaller particles (Aderonke et al., 2014). Benavente, 2008 found that copper uptake in chitosan significantly depends on the particle size. However, that effect only exhibits at high metal concentrations and not for the low metal concentration, as it suggest that, resistance against diffusion not the mechanism which influence the process. According to Azouaou et al., 2010, cadmium adsorption into coffee grounds not depends on the particle size.

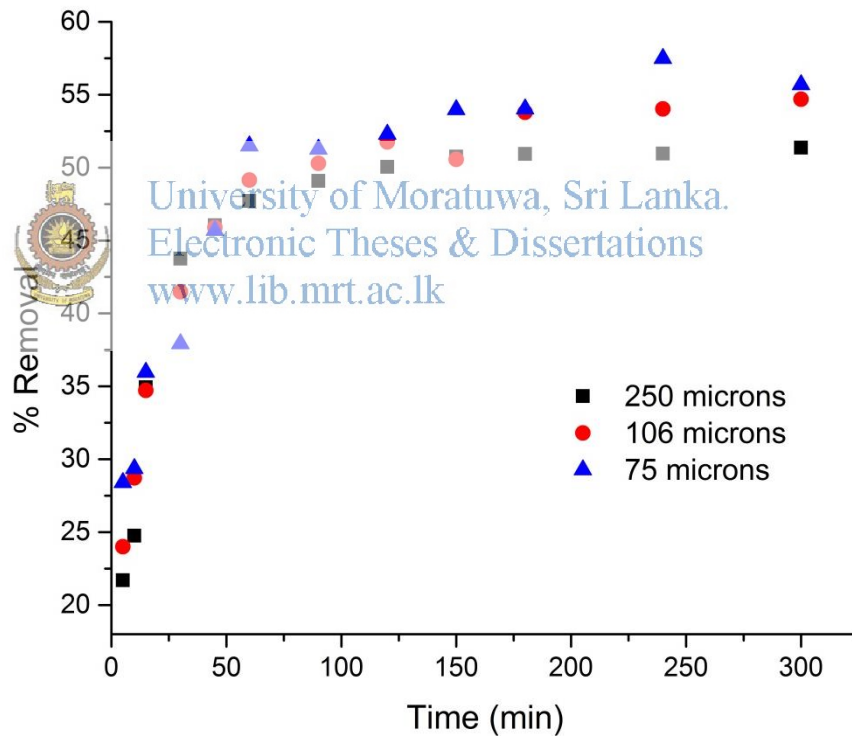
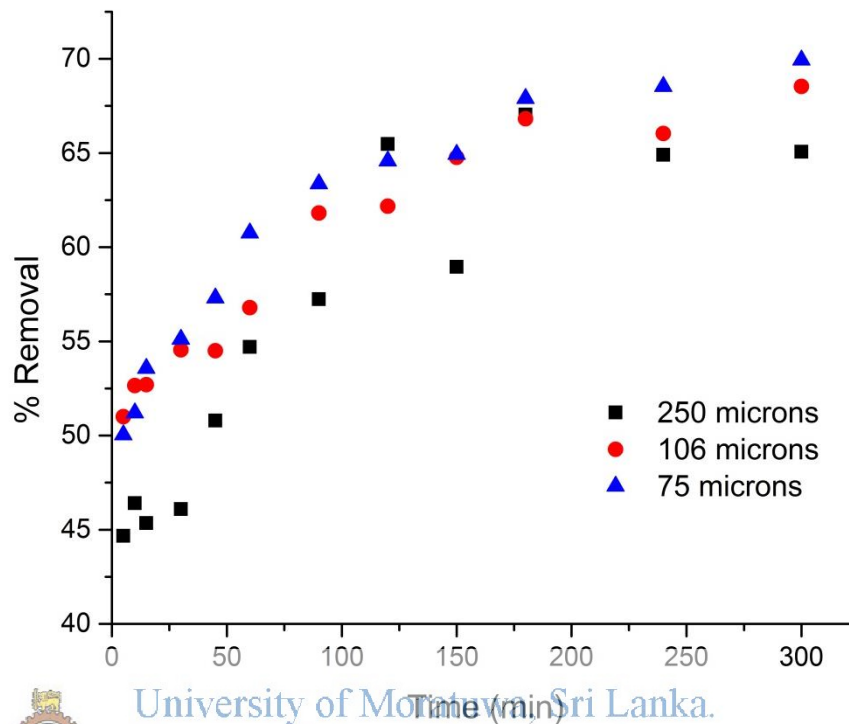


Figure 4.10 Effect of particle size on the % removal of cadmium at room temperature ($28\pm 2^{\circ}\text{C}$) and high pH (6.5)

According to the Figure 4.10 and Figure 4.11, adsorption efficiency depends on particle size for both cadmium and lead heavy metals. The effect is not

significant as it for pH of the solution and DD. This was supported by the Dzul Erosa, Saucedo Medina, Navarro Mendoza, Avila Rodriguez, & Guibal, 2001.



University of Moratuwa Sri Lanka.
Electronic Theses & Dissertations
www.lib.mrt.ac.lk

Figure 4.11 Effect of particle size to the % removal of lead at room temperature (28±2 °C) and high pH (4.5)

4.2.5 Effect of initial metal ion concentration

According to the Figure 4.12 and Figure 4.13, initial metal ion concentration of solution significantly effect to the removal of cadmium and lead. At 5 mg/L concentration solution, over 90% of cadmium and almost 99% of lead were adsorbed by the chitosan. This can be explained by the competition to the available active sites in chitosan surface. At high concentration, ratio of initial number of moles of metal ions to the available adsorption sites are high and those available sites saturated quickly with metal ions as it leads to low adsorption (Pérez-Marín et al., 2007). But at low concentration, competition for available active sites of the adsorbent is less and therefore, more percentage of metal ions are adsorbed into chitosan, as it leads to high percentage removal of both cadmium and lead.

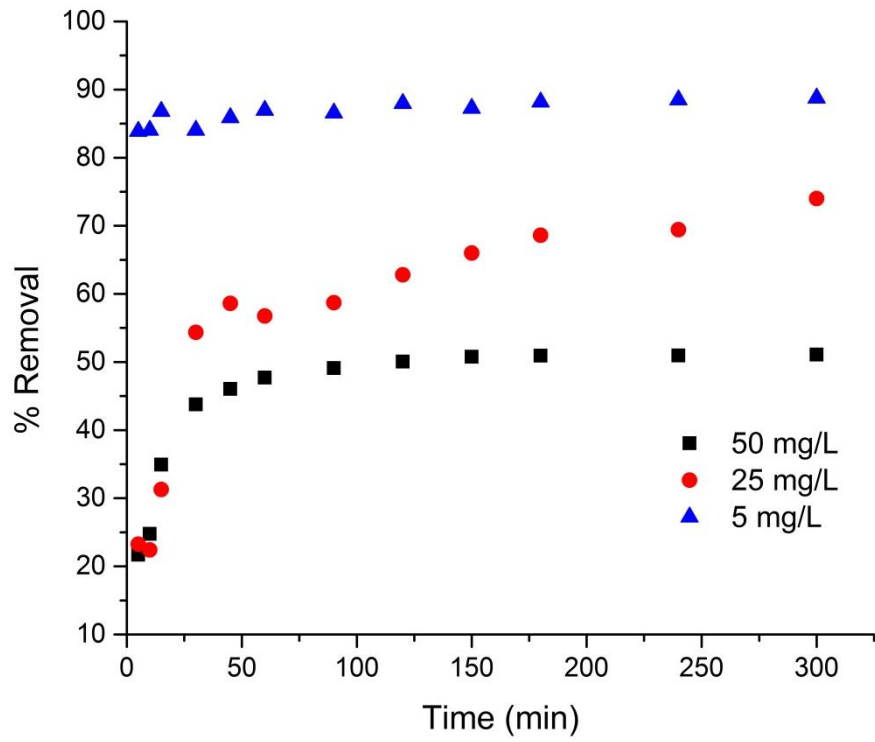


Figure 4.12 Effect of initial metal ion concentration on the % adsorption of cadmium at room temperature ($28 \pm 2^{\circ}\text{C}$) and high pH (6.5)

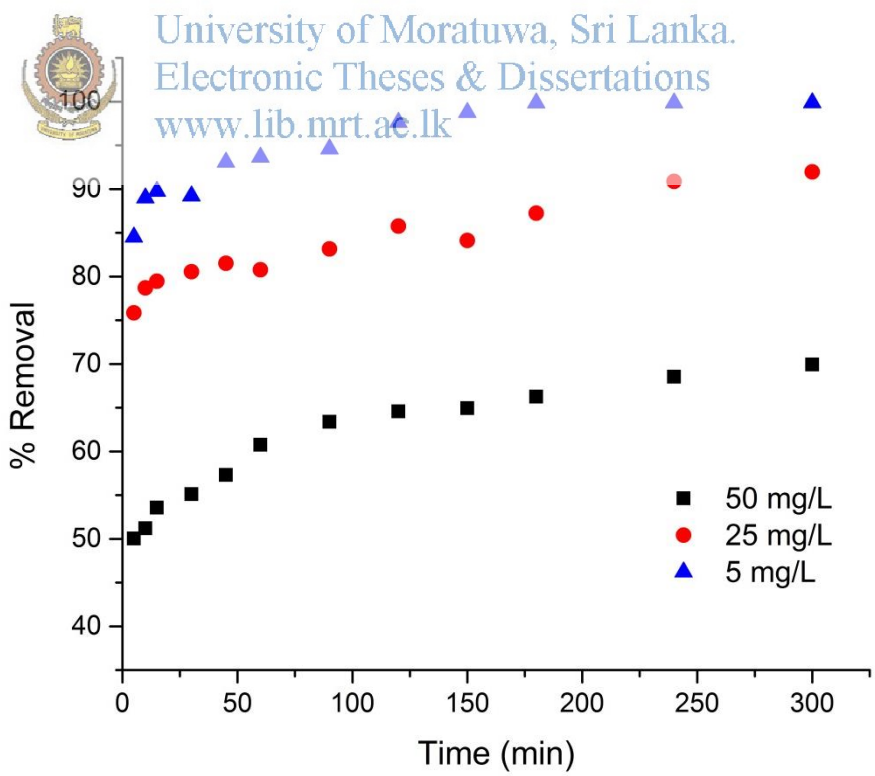


Figure 4.13 Effect of initial metal ion concentration on the % adsorption of lead

4.2.6 Effect of chitosan dosage

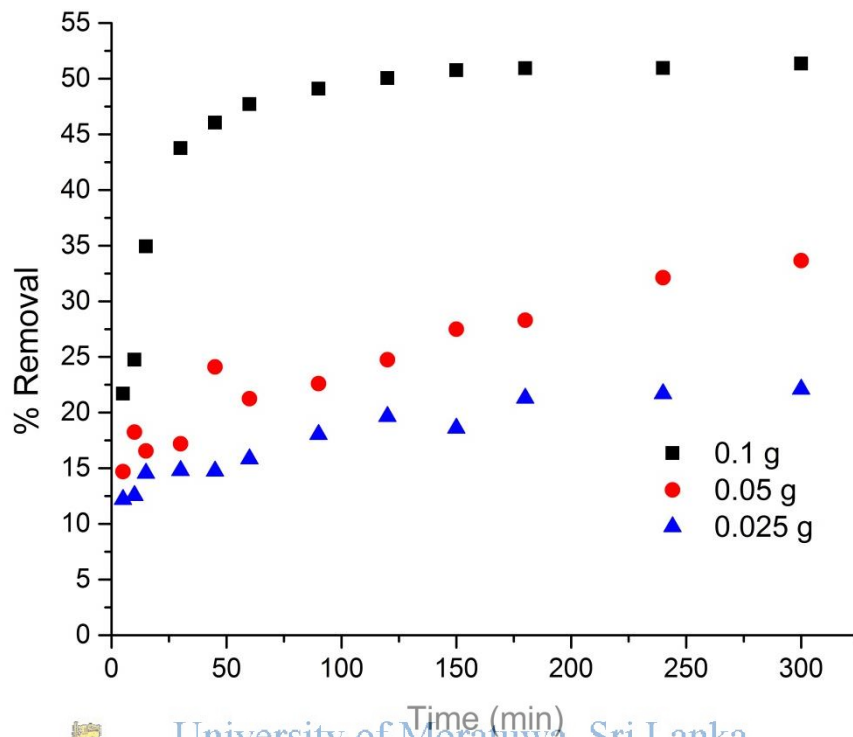


Figure 4.14 Effect of chitosan dosage on the % adsorption of cadmium

According to the Figure 4.14, The adsorbent dosage is also a significant factor for adsorption of heavy metals. This has similar effect in initial metal ion concentration. When chitosan dosage is increased, the number of active sites for adsorption also increased, so this leads to a higher percentage removal of heavy metals. These results are in agreement with most of the previous researches, reported on literature (Gupta & Babu, 2009; Kannamba, Reddy, & AppaRao, 2010; Pitakpoolsil & Hunsom, 2014). Since this effect similar to the above initial metal concentration behavior, this experiment was only carried out for cadmium. For this experiment, 50 ml of 50 mg/L concentrate cadmium solution was used under the optimal process parameters (high DD and high pH).

4.3 Analysis of Adsorption Kinetics

A study of the adsorption kinetics is important to find the rate limiting step of adsorption process and to find the kinetic parameters. When designing a real world large scale adsorption system, those parameters are very important to further implementations of the process (Ahmed & Theydan, 2012). In this study, kinetic parameters were determined by fitting the data to kinetic models. Pseudo first order model, pseudo second order model, Elovich model, and intraparticle diffusion model were used to identify the rate limiting step. Nonlinear models were fitted to data by using statistical software except for intraparticle diffusion model, which was fitted using linear regression method.

The kinetic equations stated in the chapter 2 and chapter 3, were used for the analysis part. Summary of the equations are given below;

Pseudo first order (PFO) kinetics

Non-linear model;


$$q_t = q_e(1 - e^{-K_1 t}) \quad (4.4)$$

Linear model; www.lib.mrt.ac.lk

$$\ln \frac{q_e}{q_e - q_t} = K_1 \cdot t \quad (4.5)$$

Pseudo second order (PSO) kinetics

Non-linear model;

$$q_t = \frac{K_2 q_e^2 t}{1 + K_2 q_e t} \quad (4.6)$$

Linear model;

$$\frac{t}{q_t} = \frac{1}{K_2 q_e^2} + \frac{1}{q_e} t \quad (4.7)$$

Elovich model

Non-Linear model;

$$q_t = \frac{1}{\beta} \ln(1 + \alpha\beta t) \quad (4.8)$$

Linear model;

$$q_t = \frac{1}{\beta} \ln(\alpha\beta) + \frac{1}{\beta} \ln t \quad (4.9)$$

Intraparticle diffusion model

$$q_t = K_d \sqrt{t} + C \quad (4.10)$$

Further, in this section, comparison between linear and non-linear kinetic models was done.

4.3.1 Adsorption kinetics models for different DD

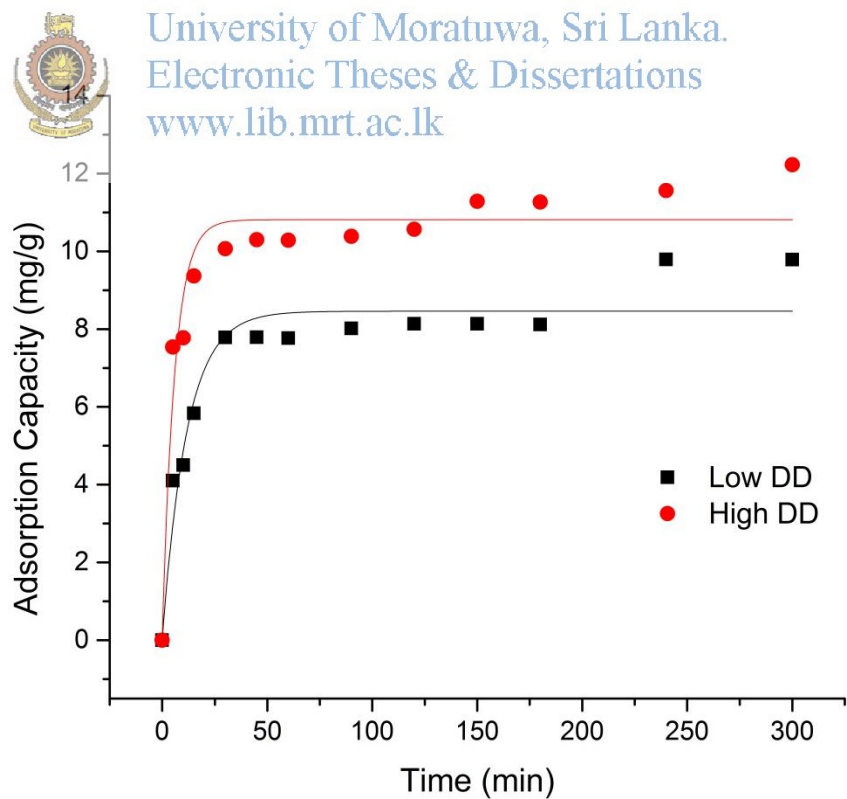


Figure 4.15 Non-linear pseudo first order model of Cadmium with effect of DD

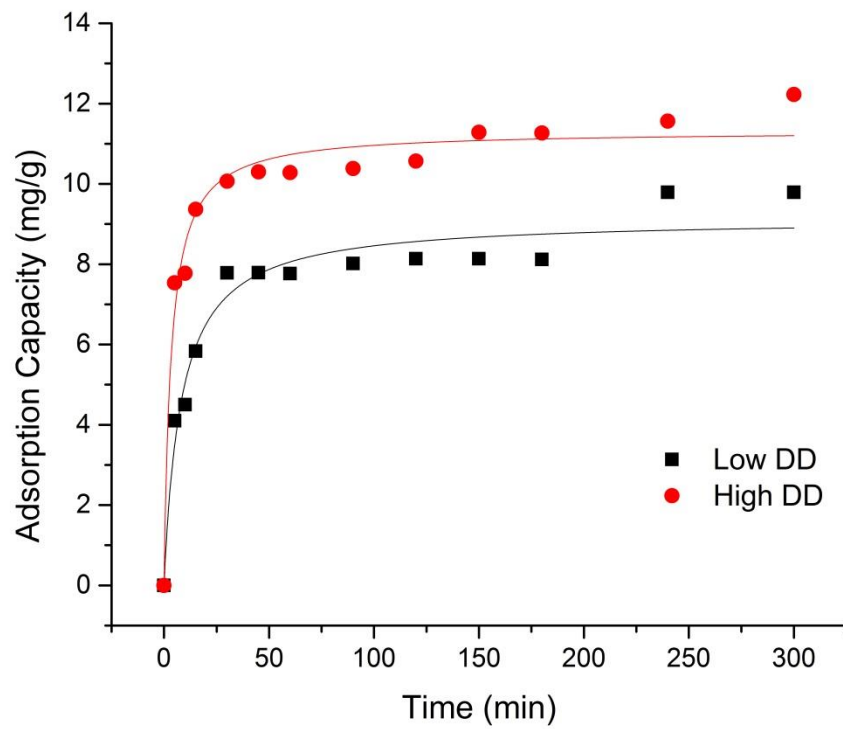


Figure 4.16 Non-linear pseudo first order model of Cadmium with effect of DD @ pH-5.5



University of Moratuwa, Sri Lanka.
 Electronic Theses & Dissertations
www.lib.mrt.ac.lk

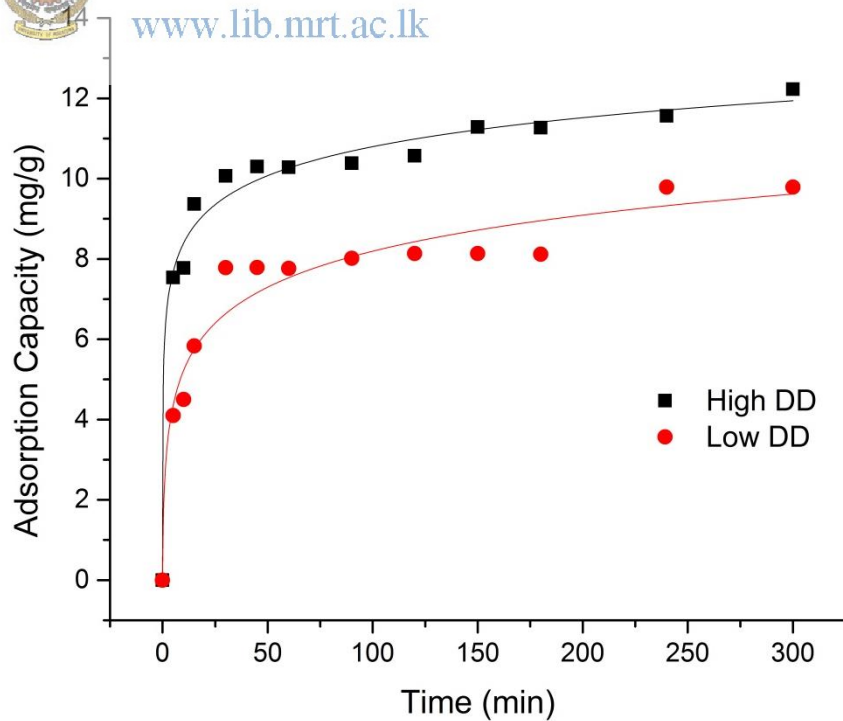


Figure 4.17 Non-linear Elovich model of Cadmium with effect of DD @ pH- 5.5

Table 4.2 Non-linear regression kinetic parameter estimates for cadmium with effect of DD

	Pseudo first order model		
	K₁ (min⁻¹)	q_e (mg g⁻¹)	R²
Low DD	0.086±0.014	8.46 ±0.268	0.9217
High DD	0.171±0.027	10.81±0.273	0.9306
	Pseudo second order model		
	K₂ (g mg⁻¹ min⁻¹)	q_e (mg g⁻¹)	R²
Low DD	0.0135±0.003	9.14 ±0.278	0.9524
High DD	0.0265±0.005	11.32±0.216	0.9713
	Elovich model		
	α	β	R²
Low DD	7.195±3.875	0.771±0.083	0.9532
High DD	331.88±240.26	0.966±0.078	0.9863

The nonlinear and linear regression data, and parameter estimations for cadmium for different DD values are given in Table 4.2 and Table 4.3. According to the R² value for non-linear regression, pseudo second order model provides better fit than pseudo first order model, and the best fit with the experimental data was provided by both pseudo second order model and Elovich model. However, it is difficult to find a best fitting model by only considering the R² value. Although Elovich model shows good fit with the experimental data, the standard errors of the parameter estimation are significant. Since the R² values for all three models were slightly varied, it was difficult to identify the best model for heavy metal adsorption. Therefore, linear regression models were considered. As given in the Table 4.3, linear pseudo second order model best fit with experimental data with R² value nearly 0.99 for both high DD and low DD samples. To find the best fit model, most of the researchers were used linear regression method. However, both linear and non-linear regression methods have their own disadvantages and advantages.

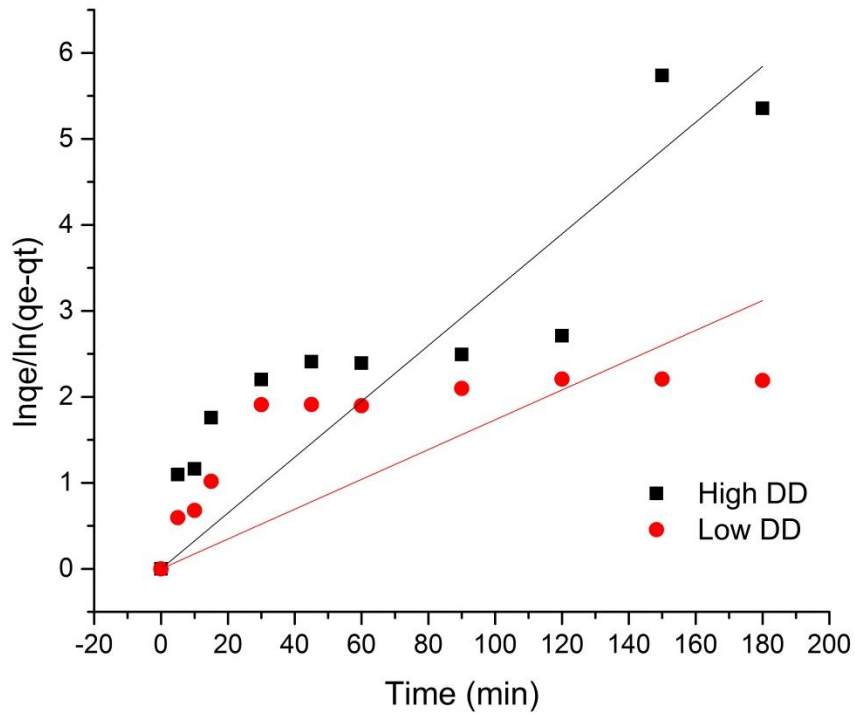


Figure 4.18 Linear Pseudo first order model of Cadmium with effect of DD @ pH- 5.5.

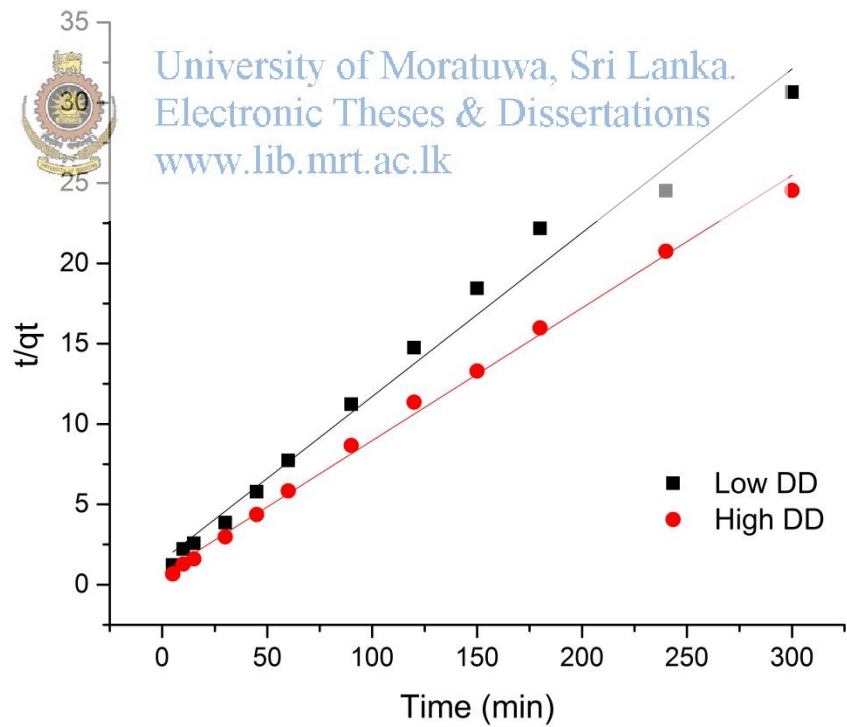


Figure 4.19 Linear pseudo second order model of cadmium with effect of DD @pH-5.5

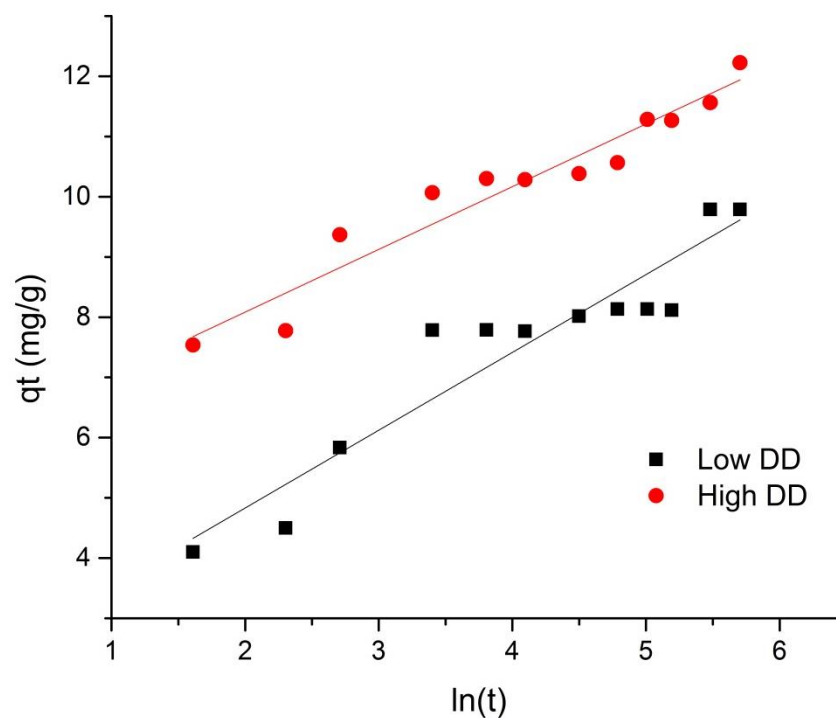


Figure 4.20 Linear Elovich model of Cadmium with effect of DD @ pH – 5.5

Table 4.3 Linear regression kinetic parameter estimates for cadmium with effect of DD



University of Moratuwa, Sri Lanka.
Electronic Theses & Dissertations
www.lib.mrt.ac.lk

Pseudo first order model			
	K_1 (min^{-1})	q_e (mg g^{-1})	R^2
Low DD	0.017	8.46	0.7794
High DD	0.032	10.81	0.9052
Pseudo second order model			
	K_2 ($\text{g mg}^{-1} \text{min}^{-1}$)	q_e (mg g^{-1})	R^2
Low DD	0.0068	9.812	0.9846
High DD	0.0096	12.108	0.9962
Elovich model			
	α	β	R^2
Low DD	7.36	0.774	0.8851
High DD	332.12	0.9605	0.9260

The obtained q_e (equilibrium adsorption capacity) value for both linear and non-linear pseudo second order model was not deviated much as expected (for Low DD; non-linear: 9.14 mg/g, linear: 9.81mg/g / for high DD; non-linear: 11.32mg/g, linear: 12.108mg/g). Normally, when linear model transform into non-linear model, error distribution and model parameters can be distorted (Lin & Wang, 2009). Same behavior was observed also for Elovich model as indicated in the Table 4.2 and 4.3. From above data, Pseudo second order model best fit with experimental data with higher R^2 values for both linear and non-linear model.

Linear pseudo first order model and linear pseudo second order model were widely used to determine the most fitted kinetic model in lot of studies. As stated on the literature, when non-linear model was converted into linear model, measurements of the model parameters were varied. However, very few studies were done to compare the linear and non-linear parameter estimations. According to Table 4.2 and 4.3, pseudo first order rate constant (K_1) and pseudo second order rate constant (K_2) were significantly changed with the linear and non-linear model. However, equilibrium adsorption capacity (q_e) was not significantly changed as expected. Interestingly, linear and non-linear parameter estimations for Elovich equation were not changed. This was further discussed in the end of this sub section.

The equilibrium adsorption capacity (q_e) should be known to fit the Equation 4.5 to experimental data. This pseudo first order model generally differs from true first order equation in two ways. In true first order system, the parameter q_e represents the number of available sites but, in this model it doesn't represent available sites. Secondly, $\ln(q_e)$ is an adjustable parameter, but in true first order equation $\ln(q_e)$ should equal to the intercept of a plot of $\ln(q_e - q_t)$ against t . Pseudo first order kinetic equation is only an approximate solution to the true first order equation (Y.S. Ho, Ng, & McKay, 2000). However, in this study more simplified equation was used and the above variations are also possible for this model which is given in Equation 4.5.

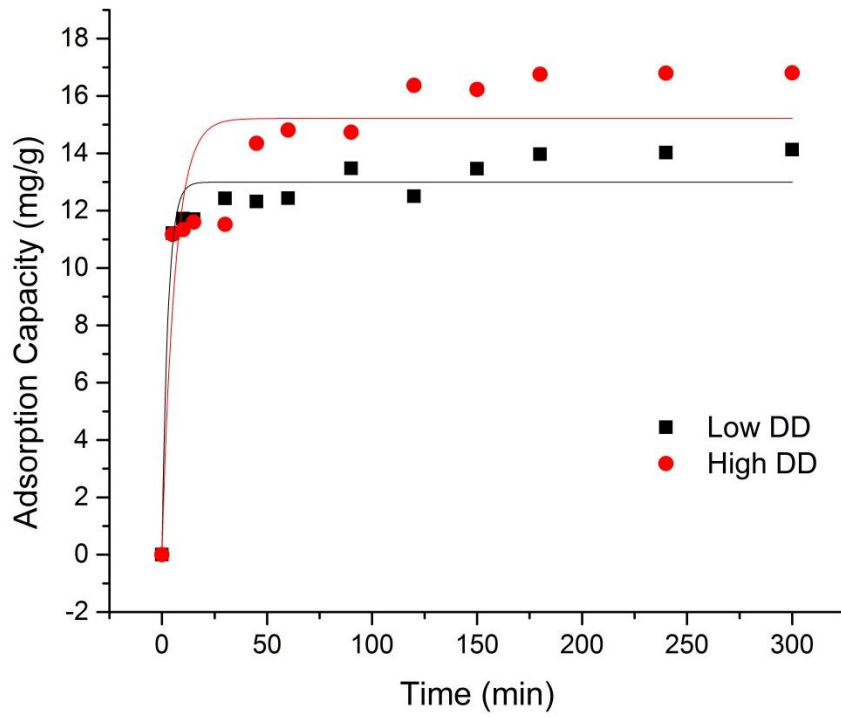


Figure 4.21 Non-linear pseudo first order model of Lead with effect of DD @ pH- 3

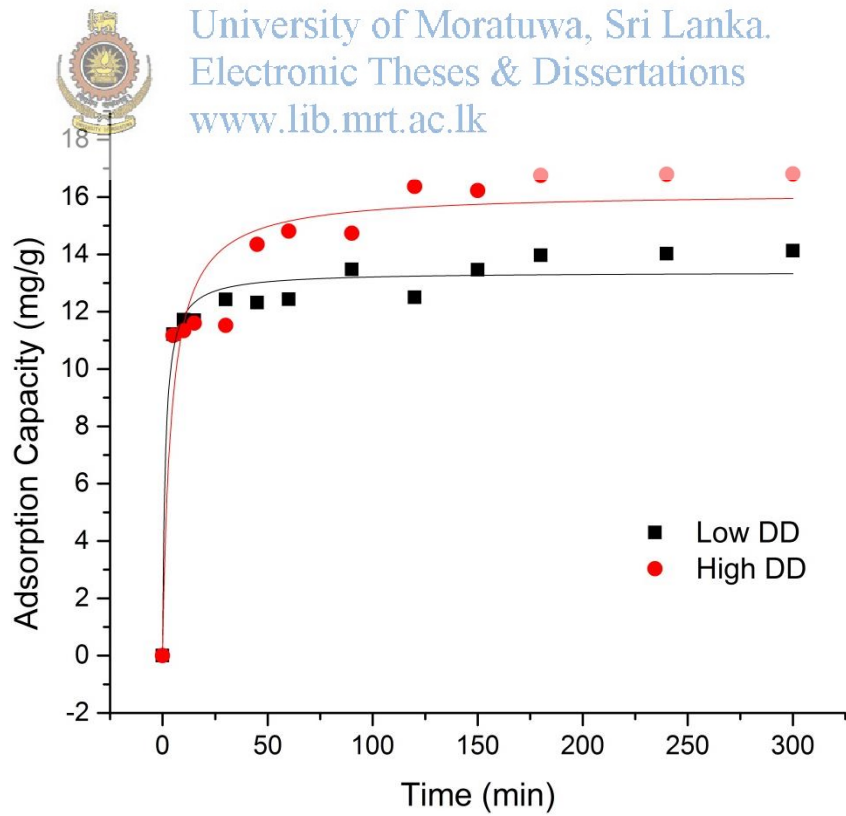


Figure 4.22 Non-linear pseudo second order model of Lead with effect of DD @ pH - 3

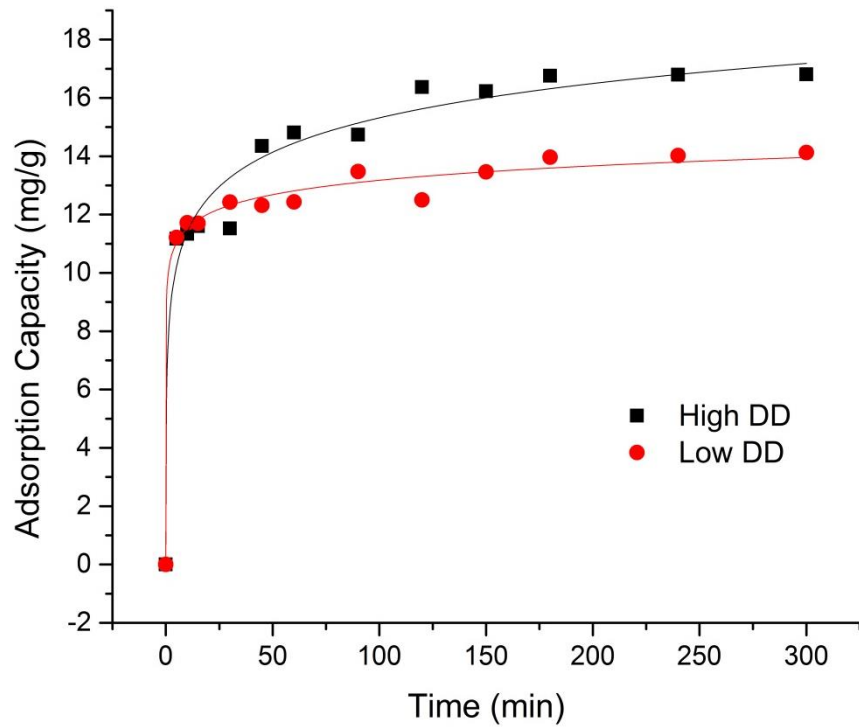


Figure 4.23 Non-linear Elovich model for lead with effect of DD @ pH-3

Table 4.4 Non-linear regression kinetic parameter estimates for lead with effect of DD



University of Moratuwa, Sri Lanka.
Electronic Theses & Dissertations
www.lib.mrt.ac.lk

	Pseudo first order model		
	K_1 (min^{-1})	q_e (mg g^{-1})	R^2
Low DD	0.356 ± 0.0688	12.996 ± 0.2724	0.8528
High DD	0.165 ± 0.036	15.269 ± 0.6383	0.95315
	Pseudo second order model		
	K_2 ($\text{g mg}^{-1} \text{min}^{-1}$)	q_e (mg g^{-1})	R^2
Low DD	0.0808 ± 0.0239	12.996 ± 0.2724	0.9682
High DD	0.02309 ± 0.0061	15.269 ± 0.6383	0.9117
	Elovich model		
	α	β	R^2
Low DD	139.35 ± 101.83	0.5884 ± 0.0569	0.9758
High DD	$767868.5 \pm 1.45E6$	1.4037 ± 0.1573	0.9911



University of Moratuwa, Sri Lanka.
Electronic Theses & Dissertations
www.lib.mrt.ac.lk

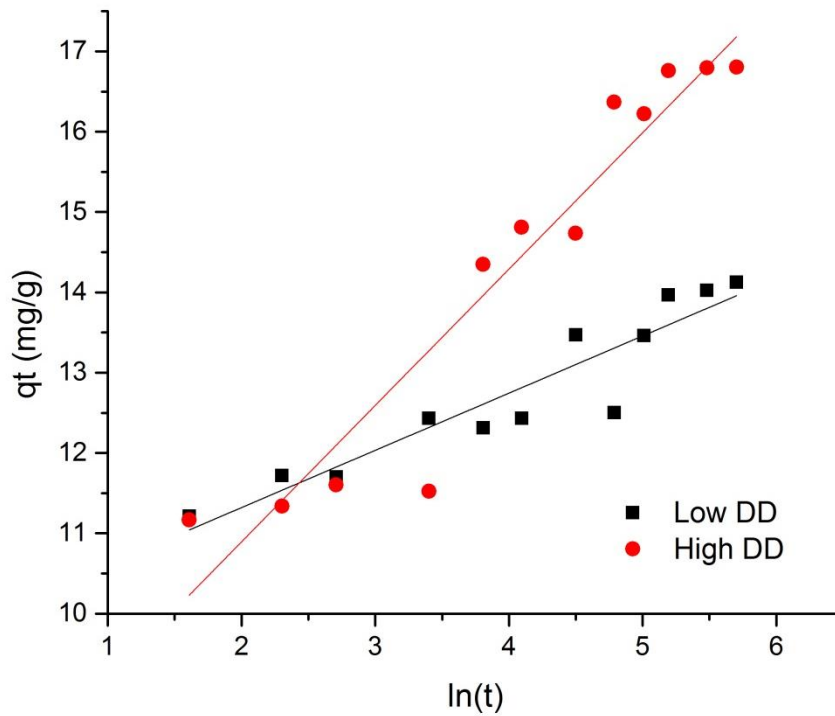


Figure 4.26 Linear Elovich model for lead with effect of DD @ pH-3



Table 4.5 Linear regression kinetic parameter estimates for lead with effect of DD

	Pseudo first order model		
	K_1 (min^{-1})	q_e (mg g^{-1})	R^2
Low DD	0.046	12.996	0.7745
High DD	0.034	15.269	0.9133
	Pseudo second order model		
	K_2 ($\text{g mg}^{-1} \text{min}^{-1}$)	q_e (mg g^{-1})	R^2
Low DD	0.0128	14.224	0.9978
High DD	0.0066	17.298	0.9983
	Elovich model		
	α	β	R^2
Low DD	767841.3	1.4037	0.8676
High DD	140.32	0.5888	0.8987

It was clearly observed that pseudo first order model does not fit well over the whole range of contact time under investigation. The poor R^2 value was due to that. This same phenomena was reported by the lot of researchers in the literature (Evans et al., 2002; Gupta & Babu, 2009; SenthilKumar et al., 2011). According to the literatures, pseudo first order model assumes mass transfer as rate limiting step. Since high agitation rates were used in this experiment, mass transfer step was eliminated. Therefore, linear form of pseudo first order model only valid at low agitation rate and according to the Ahmad et al, best correlation with experimental data were observed at initial time period (first 30minutes), where mass transfer is significant (Evans et al., 2002). Further studies are required to prove this.

4.3.2 Adsorption kinetics model for different pH

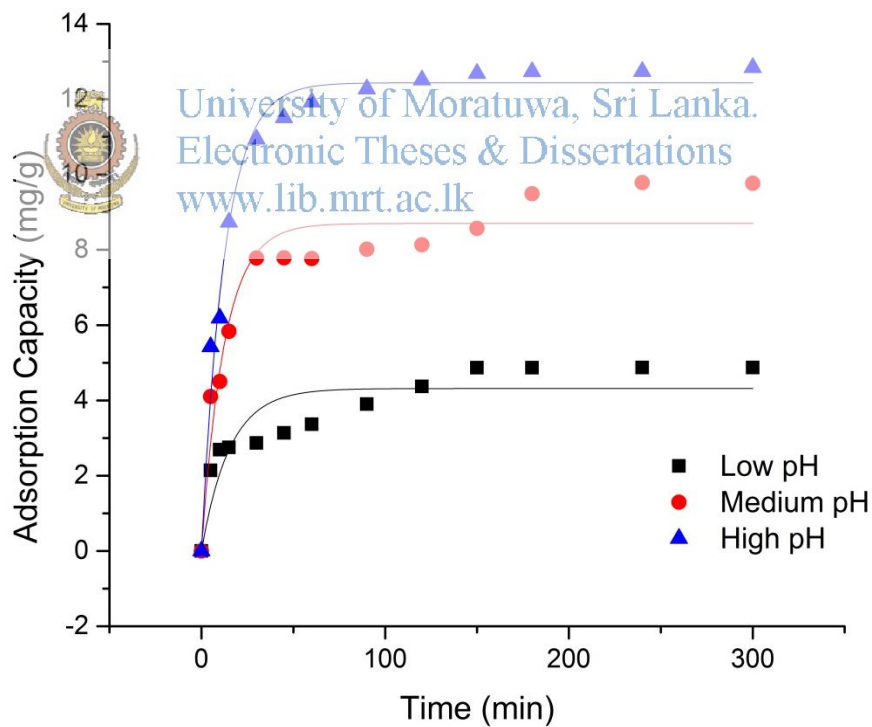


Figure 4.27 Non-linear pseudo first order model for Cadmium with effect of pH



University of Moratuwa, Sri Lanka.
Electronic Theses & Dissertations
www.lib.mrt.ac.lk



University of Moratuwa, Sri Lanka.
Electronic Theses & Dissertations
www.lib.mrt.ac.lk



University of Moratuwa, Sri Lanka.
Electronic Theses & Dissertations
www.lib.mrt.ac.lk



University of Moratuwa, Sri Lanka.
Electronic Theses & Dissertations
www.lib.mrt.ac.lk



University of Moratuwa, Sri Lanka.
Electronic Theses & Dissertations
www.lib.mrt.ac.lk



University of Moratuwa, Sri Lanka.
Electronic Theses & Dissertations
www.lib.mrt.ac.lk



University of Moratuwa, Sri Lanka.
Electronic Theses & Dissertations
www.lib.mrt.ac.lk

Table 4.9 Linear regression kinetic parameter estimates for lead with effect of pH of the initial metal ion solution

	Pseudo first order model		
	K₁ (min⁻¹)	q_e (mg g⁻¹)	R²
Low pH (2)	0.04869	12.0804	0.7834
Medium pH (3)	0.05106	13.9951	0.8653
High pH (4.5)	0.06985	16.1368	0.8562
	Pseudo second order model		
	K₂ (g mg⁻¹ min⁻¹)	q_e (mg g⁻¹)	R²
Low pH (2)	0.00541	14.4927	0.9924
Medium pH (3)	0.00619	16.4555	0.9953
High pH (4.5)	0.00515	19.0512	0.9924
	Elovich model		
	α	β	R²
Low pH (2)	18.2859	0.5742	0.8679
Medium pH (3)	144.7793	0.6423	0.8888
High pH (4.5)	144.3305	0.5467	0.8446

From Table 4.4 to 4.9, it was observed that parameter estimations were varied according to the linear and non-linear regression. As discussed previously, pseudo first order (PFO) model does not fit well with the experimental data for both cadmium and lead heavy metals. Since the equilibrium adsorption capacity (q_e) should be known for linear regression analysis of PFO model, the validity of the model depends on the determination of q_e . In some literatures the experimental equilibrium concentrations were used to calculate q_e . Ho et al., 2000, suggested the trial and error solution method to obtain equilibrium q_e . In this study, q_e was determined from the non-linear analysis. Therefore, to obtain the adsorption parameters, the non-linear kinetic equations of PFO model have the advantage of there being no need to know the value of q_e before fitting the experimental points (Lin & Wang, 2009).

From non-linear regression analysis, it was very difficult to find the best fit model, due to the small variations in the R^2 values in all three models. However, linear PSO model best fit with experimental data with R^2 value greater than 0.99 for all experimental states. Therefore, linear regression analysis was better suited to identify the best fit model for particular adsorption process. Parameter estimations for both PFO model and PSO model were varied according to the linear and non-linear regression method. However, the parameter estimations for linear and non-linear regression for Elovich model were very similar. So, it can be concluded that both linear and non-linear methods are suitable for parameter estimations of Elovich model.

By considering the R^2 value, it can be concluded that PSO model was the best fit model for adsorption of cadmium and lead onto chitosan biopolymer. However, it is difficult to find a rate limiting step by only considering the R^2 value. Relatively good fit to the Elovich model suggests that chemisorption was taken place during the process. Therefore, the determination of rate limiting step becomes ambiguous, as it shows multiple mechanisms, such as chemical adsorption, intra-particle diffusion. This suggests multiple rate limiting steps, which may be result in poor fit with the experimental data, when only one mechanism is considered as rate limiting.

4.3.3 Intra-particle diffusion model

Kinetic data were used to compare the Weber-Morris intra-particle diffusion model with the other kinetic models. Plot of q_t versus $t^{0.5}$ at different process conditions were used to analyze the data. According to the Cheung et al., 2007, three steps took place during the process. The first, boundary layer diffusion of solute atoms and the second portion attributed to the gradual adsorption stage where intra-particle diffusion was rate limiting. The final stage was the equilibrium stage where intra-particle diffusion slows down due to the decrease in adsorbate concentration. However, most of the literatures are considered only two steps as boundary layer diffusion and the intra-particle diffusion (Holfetz, 2012).



University of Moratuwa, Sri Lanka.
Electronic Theses & Dissertations
www.lib.mrt.ac.lk

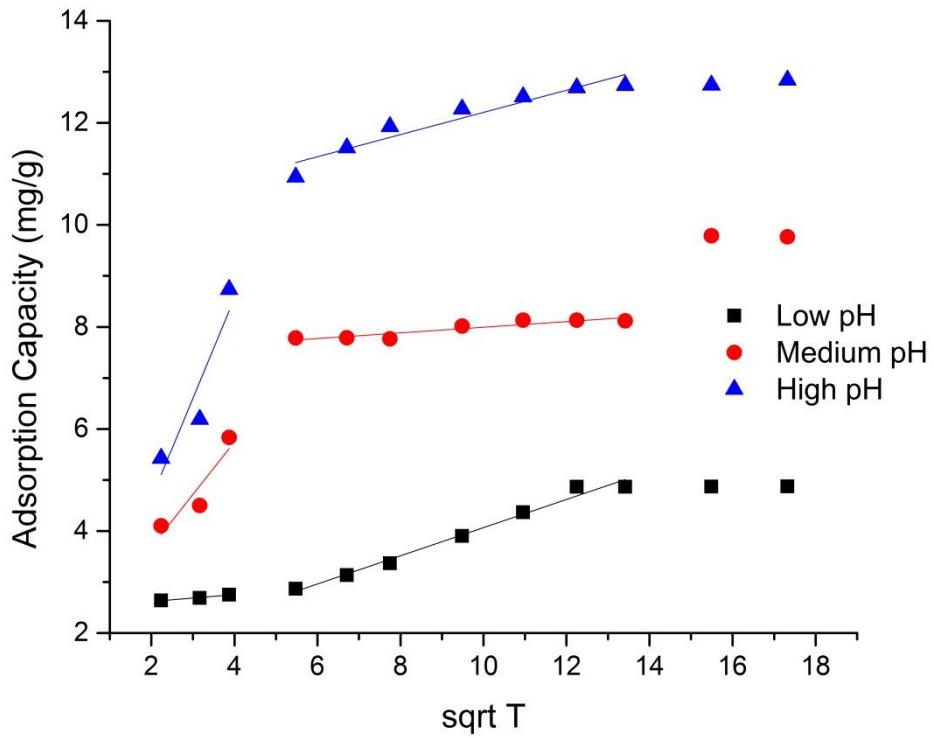


Figure 4.41 Intra-particle diffusion model of cadmium adsorption at different pH of metal ion solution

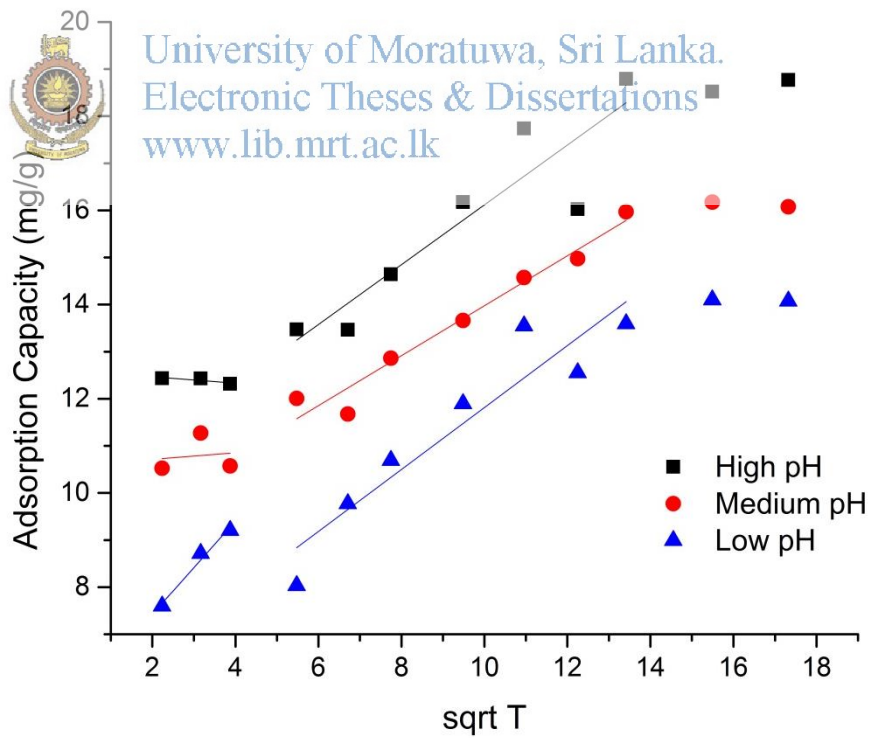


Figure 4.42 Intra-particle diffusion model of cadmium adsorption at different pH of metal ion solution

From Figure 4.39 to 4.42, it is clear that two linear portions are present. This suggests that there is more than one process which has influenced the adsorption process. The boundary layer diffusion is responsible for the first linear portion and second linear portion is due to the intra-particle diffusion (refers to section 2.6.1). Further, after 180 minutes, another linear portion is also visible in all figures but, due to lack of data after 180 minutes, that portion was not considered. According to the Cheung et al., 2007, that part was also due to the equilibrium state intra-particle diffusion. The transition point for the two linear sections was at approximately 30 minutes contact time for both cadmium and lead heavy metals. These different linear sections may be due to the different range of pore sizes in the chitosan, which gives different rate constants for different pore sizes (Abdelwahab & Amin, 2013). Therefore this facilitates the non-homogeneous nature of the adsorbent, chitosan.

The slope of the linear portion represents the rate of the adsorption process. The lower slope corresponds to the slower adsorption process. According to the Figure 4.39 and 4.41, boundary layer diffusion shows comparatively higher rate than that of intra-particle diffusion in cadmium adsorption process. However, according to the Figure 4.40 and 4.42, intra-particle diffusion is more significantly influenced the lead adsorption process. If the intra-particle diffusion was the only rate limiting step, the plot should pass through the origin (Cheung et al., 2007; Holfetz, 2012). But, according to the data, plots didn't pass through origin and therefore it can be concluded that the boundary layer diffusion was also responsible for the adsorption process to some degree. The thickness of the boundary layer can be determined from the intercept of the Webber-Morris plot.

If the adsorption kinetics greatly depend on the particle size that suggest the sorption process significantly governed by the intra-particle diffusion. But, percentage adsorption of metal ions was not significantly increased with decreasing particle size as discussed in section 4.2.4. According to Holfetz, 2012, the kinetic processes which require more than 24 hours reaching equilibrium are considered as diffusion controlled. Since cadmium and lead sorption becomes equilibrium state within 3 hours, it can be concluded that combine with particle size effect, cadmium

and lead sorption was not completely diffusion controlled and adsorption process was also play significant role.

Table 4.10 Intra-particle diffusion model parameter estimates for different DD values of chitosan

		Linear section	K_i (mg/g min ^{0.5})	C (mg/g)	R^2
Cd	High DD	One	1.0751	4.9039	0.5738
		Two	0.1533	9.1462	0.8239
	Low DD	One	1.0280	1.6341	0.7285
		Two	0.0553	7.4412	0.8231
Pb	High DD	One	0.2167	0.5604	0.9201
		Two	0.3694	11.8134	0.8498
	Low DD	One	0.3086	10.5913	0.5691
		two	0.1826	11.2171	0.5681

Table 4.11 Intra-particle diffusion model parameter estimates for different initial pH of the metal ion solution

		Linear section	K_i (mg/g min ^{0.5})	C (mg/g)	R^2
Cd	Low pH	One	0.0683	2.4808	0.9598
		Two	0.2760	1.3057	0.9811
	Medium pH	One	1.0280	1.6341	0.7285
		Two	0.0553	7.4412	0.8231
	High pH	One	1.9620	0.7185	0.7282
		Two	0.2174	10.0319	0.9046
Pb	Low pH	One	0.9917	5.4403	0.9571
		Two	0.6578	5.2358	0.8604
	Medium pH	One	0.0705	10.5722	0.9642
		Two	0.5303	8.6720	0.9542
	High pH	One	-0.0683	12.6037	0.3978
		Two	0.6351	9.7665	0.8035

4.4 Modeling of adsorption isotherms

Langmuir and Freundlich isotherm models were used to model the adsorption isotherm of cadmium and lead. Both linear and nonlinear regression method were used to determine the isotherm parameter and the best fit model. The isotherm parameters and R^2 value depend on the type of linear and nonlinear model which was used to estimation of those parameters.

Table 4.12 Linear and nonlinear forms of Langmuir and Freundlich isotherms

Isotherm	Nonlinear form	Linear form	plot
Langmuir	$q_e = \frac{q_m K C_e}{1 + K C_e}$	$\frac{C_e}{q_e} = \frac{C_e}{q_m} + \frac{1}{q_m K_L}$	$\frac{C_e}{q_e}$ Vs C_e (linear 1)
		$\frac{1}{q_e} = \frac{1}{q_m K_L C_e} + \frac{1}{q_m}$	$\frac{1}{q_e}$ Vs $\frac{1}{C_e}$ (linear 2)
		$\frac{q_e}{C_e} = q_m K - q_m q_e$	$\frac{q_e}{C_e}$ Vs q_e (linear 3)
Freundlich	$q_e = K_F C_e^{1/n}$	$\log q_e = \log K_F + \frac{1}{n} \log C_e$	$\log q_e$ Vs $\log C_e$

Table 4.8 shows the linear and nonlinear isotherm models used in this study (Febrianto et al., 2009). Three linear form of Langmuir isotherm were used in this analysis. According to the linearization method, parameter estimation and linear regression (R^2) were significantly varied as shown in the Table 4.13. Second linear model and the nonlinear model of Langmuir isotherm best fit with the both cadmium and lead experimental data and therefore the parameter estimations were statistically significant in those two models. However, as shown in Table 4.14, both linear and nonlinear form of Freundlich isotherm model shows better fit to the experimental data than Langmuir model. In other words, adsorption of cadmium and lead can be better described by using Freundlich model, as suggest that adsorption process is more likely to be heterogeneous multilayer process.

According to this analysis, Langmuir isotherm is dependent on the linearized model as second linear model best fit with experimental data. Further, first and third linearized model showed better correlation with experimental data,



University of Moratuwa, Sri Lanka.
Electronic Theses & Dissertations
www.lib.mrt.ac.lk



University of Moratuwa, Sri Lanka.
Electronic Theses & Dissertations
www.lib.mrt.ac.lk

Table 4.13 Langmuir isotherm model parameters for cadmium and lead adsorption

Metal	Model	q_m (mg/g)	K_L	R^2
Cd	Linear 1	234.74	0.0041	0.7870
	Linear 2	50.37	0.0388	0.9882
	Linear 3	223.21	0.0049	0.4458
	Nonlinear	97.45	0.0125	0.9765
Pb	Linear 1	421.94	0.0029	0.7656
	Linear 2	50.12	0.0327	0.9702
	Linear 3	393.7	0.00328	0.4163
	Nonlinear	101.27	0.0205	0.9654

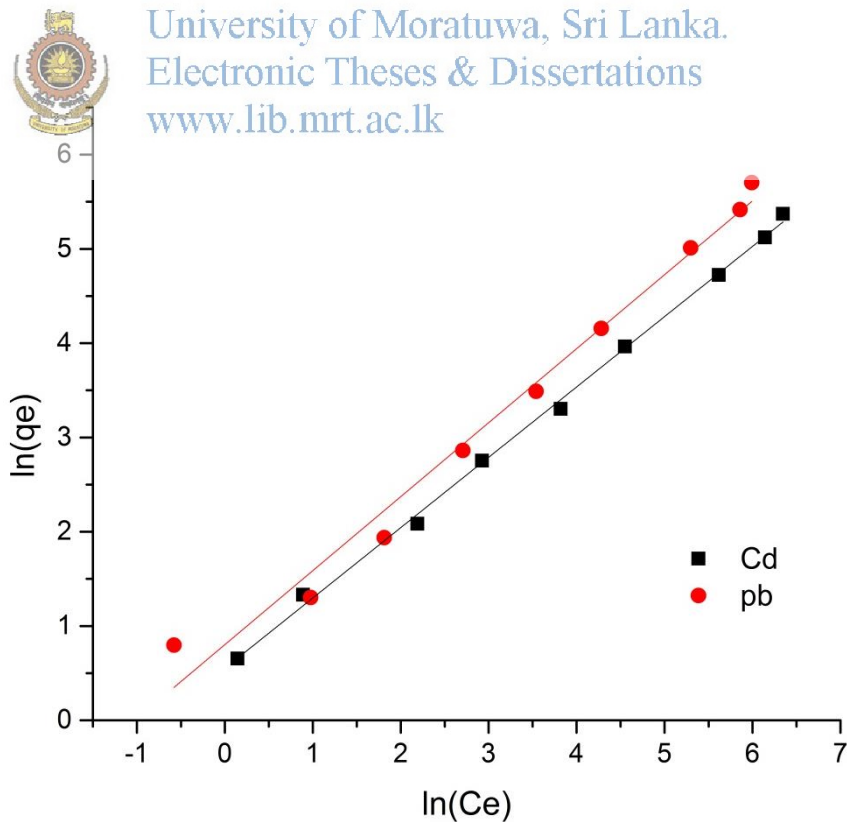


Figure 4.47 Linearized Freundlich isotherm model @ 28 ± 2 °C



University of Moratuwa, Sri Lanka.
Electronic Theses & Dissertations
www.lib.mrt.ac.lk

Where, C_0 is the initial concentration of heavy metal solution (mg/L), K_L is Langmuir constant.

Table 4.15 Effect of separation factor on shape of isotherm

R_L Value	Type of isotherm
$R_L > 1$	Unfavorable
$R_L = 0$	Linear
$0 < R_L < 1$	Favorable
$R_L = 0$	Irreversible

According to the Table 4.15, R_L values for both cadmium and lead for all initial metal ion concentrations (from 5 mg/L to 1000 mg/L) were between 0 and 1, as it suggest that favorable adsorption and further, it is reversible. This very important in designing actual adsorption system and chitosan can be recovered by removing adsorbed heavy metal ions by using suitable regeneration solution.

Table 4.16 Calculated values of separation factor, R_L , for different plot types

Metal	Type of graph	R_L	
		At 5 mg/L	At 1000 mg/L
Cd	Linear 1	0.9799	0.1960
	Linear 2	0.8375	0.0251
	Linear 3	0.9761	0.1694
	Non-linear	0.9412	0.0741
Pb	Linear 1	0.9857	0.2564
	Linear 2	0.8595	0.0296
	Linear 3	0.9838	0.2336
	Non-linear	0.9070	0.0465

In Freundlich model, the magnitude of heterogeneity factor $1/n$ gives an indication of the favorability of adsorption. When $n > 1$, that represent favorable physical adsorption; if value of $n = 0$, the adsorption is linear and if the value below

the unity, it represent unfavorable chemical adsorption (Ahmad et al., 2005; Senthil Kumar et al., 2010). As shown in Table 4.11, both linear and nonlinear model shows n values greater than one and therefore adsorption is favorable physical process.

In conclusion, R^2 values of Langmuir model depend on the type of the linear graph. Although non-linear plot fitted well with experimental data, standard error was comparatively high. Langmuir model best described the adsorption process in low concentrations and in high concentrations experimental data were deviated as indicated in the Figure 4.43 to Figure 4.45. So, the adsorption process of cadmium and lead onto chitosan biopolymer was a heterogeneous multilayer process and it was best described by the Freundlich isotherm model.

4.5 Thermodynamic Studies

4.5.1 Effect of Temperature

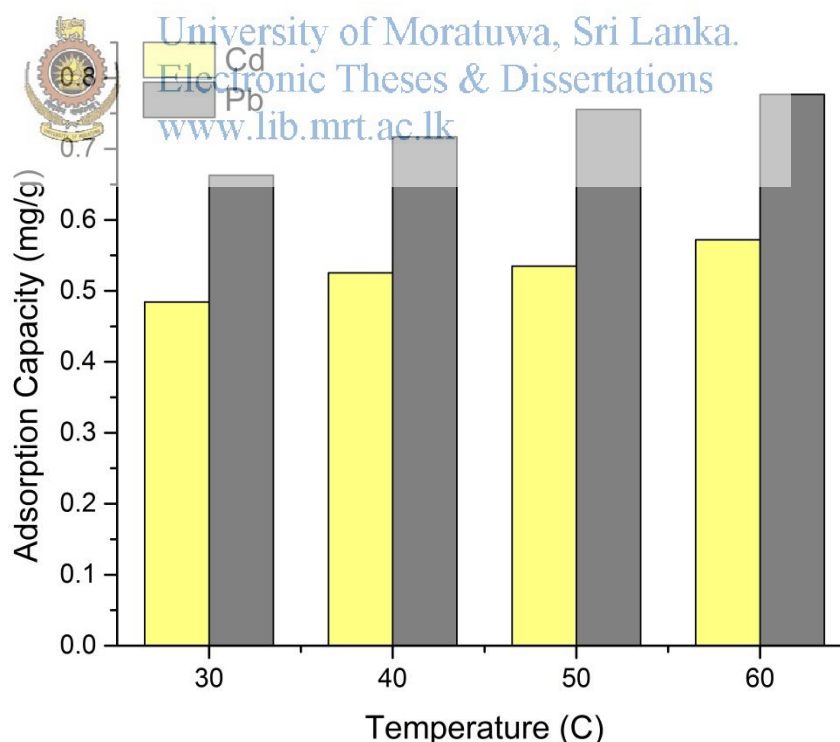


Figure 4.49 Effect of temperature on the adsorption capacity for Cadmium and Lead: C-50ppm, 0.1 g of chitosan dosage, contact time 3 hr



University of Moratuwa, Sri Lanka.
Electronic Theses & Dissertations
www.lib.mrt.ac.lk

Table 4.17 Thermodynamic parameter estimations of cadmium and lead adsorption

Metal ion	ΔH (J/mol)	ΔS (J/mol.K)	ΔG (J/mol)	
			30°C	60°C
Cd	7625.78	25.922	-228.586	-1006.246
Pb	6317.04	25.157	-1305.531	-2060.241

According to the results, adsorption capacity of chitosan for both cadmium and lead increased with increasing temperature, which indicates that the adsorption process was endothermic in nature. Thermodynamic parameters such as enthalpy change (ΔH^0), entropy change (ΔS^0), and free energy change (ΔG^0) for both cadmium and lead are shown in Table 4.17. Positive values of ΔH for both metals indicate the endothermic nature of the adsorption and also its magnitude indicates the type of adsorption, which can be either chemical or physical. If the enthalpy of adsorption between the 2.1 to 20.9 kJ/mol, it corresponds to the physical adsorption (Ahmed & Theydan, 2012). Therefore sorption of cadmium and lead into chitosan was an endothermic physical adsorption process.

The negative Gibbs free energy change indicates the thermodynamically spontaneous nature of the adsorption (Ahmed & Theydan, 2012; Doyurum & Çelik, 2006). The increase in free energy change at high temperature suggests that the adsorption feasibility is increased with increasing temperature.

4.6 Desorption Studies

Desorption studies were not deeply studied as adsorption studies. Distilled water and NaOH solutions were used as regeneration solution for metal adsorbed chitosan.

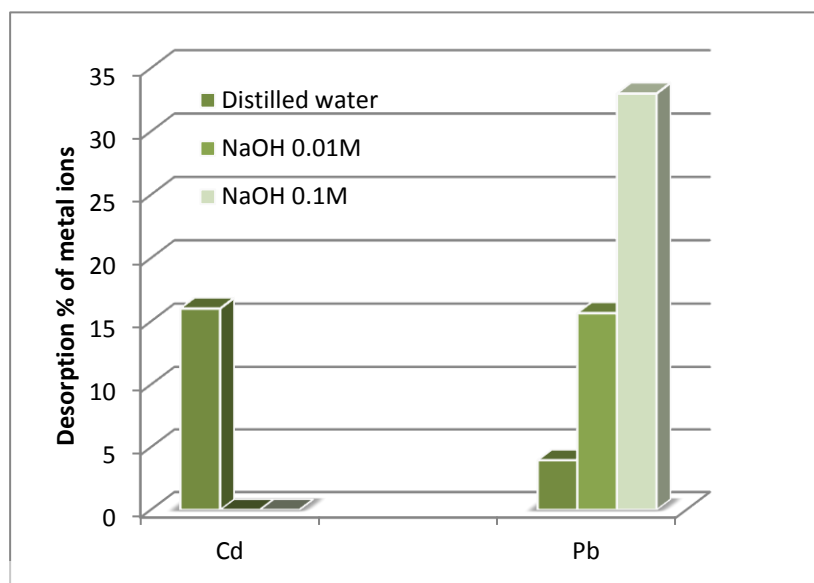


Figure 4.51 Desorption percentages of metal ions for three regeneration solution



As shown in Figure 4.51, desorption percentage was significantly varied with the type of regeneration solution. 16% of cadmium desorbed into distilled water and nearly 4% of lead desorbed into distilled water. When pH of solution increased, lead shows higher desorption. However, desorption of cadmium at higher pH was not feasible as shown in Figure 4.51. Therefore, Further studies should be carried out to check desorption of cadmium in lower pH.

5 Conclusions

- Chitosan was successfully synthesized from shrimp shells available in Sri Lanka. FTIR spectrum of chitosan showed all the characteristics bond energies of standard chitosan sample.
- Adsorption rate depends on the DD values. Significantly high rate of adsorption was observed in the chitosan which has higher DD value. So chemically modified chitosan is a good adsorbent.
- pH of the metallic ion solution was greatly affected to the adsorption rate of chitosan. According to the results, high pH values are preferred for good adsorption.
- Kinetic models were fitted to the experimental results and from that it should be concluded that the adsorption of cadmium and lead was controlled by the adsorption reaction as it best fitted with pseudo second order. The adsorption process was controlled by more than one method and therefore rate limiting step was difficult to analysis accurately.
- Particle size is not a significant factor for adsorption rate of lead into chitosan.
- According to the isotherms, adsorption of cadmium and lead ions into chitosan was best explained by the Freundlich model. Therefore adsorption of lead ion into chitosan is a heterogeneous process and it further facilitates multilayer adsorption.
- Thermodynamic studies showed that the adsorption of cadmium and lead into chitosan was a physical adsorption and it was a favorable.

According to the study chitosan can be a good candidate to remove heavy metals from wastewater. Chitosan may offer an alternative to traditional adsorbent materials in wastewater treatment. The unique properties of chitosan together with availability make chitosan an exciting and promising agent for the heavy metal adsorption from wastewater.

6 Suggestions for Future Works

In this study, flake chitosan was used to analyze the adsorption characteristics of cadmium and lead heavy metals. It was observed that chitosan plays a significant role in adsorption of cadmium and lead heavy metals and it can be implemented in heavy metal adsorption systems used in industry. Since the affinity for heavy metals in chitosan is not only restricted to cadmium and lead, other heavy metals such as zinc, mercury, copper, chromium, arsenic and nickel can also be tested for adsorption. The adsorption capacity of chitosan can be significantly increased by physical and chemical modifications. In this study, only modification was the change in DD; increased the $-NH_2$ group content by increasing the severity of deacetylation process.

Chitosan flakes and powder can be modified into gel form such as beads, membranes, fibers, sponges, hollow fibers etc. (Miretzky & Cirelli, 2009). These gel forms enhance the adsorption capacity by improving expansion of the polymer network as it improves access to internal adsorption sites and enhances diffusion mechanisms. Chemically and physically modified chitosan shows significantly high adsorption capacity as reported on the literature.



University of Moratuwa, Sri Lanka
Electronic Theses & Dissertations
www.lib.mrt.ac.lk

According to Jeon & Höll, 2003, aminated chitosan beads with ethylenediamine show higher adsorption capacity in mercury ion removal. Chemically modified, epichlorohydrin cross-linked xanthate chitosan (ECXCs) was also used to improve the adsorption capacity of chitosan beads (Kannamba et al., 2010). Therefore these types of chemical and physical modifications can be done for locally synthesized chitosan, and adsorption capacity can be further increased.

Chitosan can be added to improve existing adsorption capacity of traditional adsorbent materials like zeolite and activated carbon. The chitosan/zeolite conjugate film shows higher adsorption capacity compared to the individual adsorption capacity of both zeolite and chitosan (Batista, Villanueva, Amorim, Tavares, & Campos-Takaki, 2011). Chitosan impregnated polyurethane films (Prakash, n.d.) and chitosan coated polyvinylchloride (PVC) beads (Popuri, Vijaya, Boddu, & Abburi, 2009) show significantly high adsorption capacity. Furthermore,

chitosan coated oil palm shell charcoal shows high adsorption capacity (Nomanbhay & Palanisamy, 2005) and this method can be used in Sri Lanka by using coconut shell charcoal. Lots of practical methods were discussed by the previous researchers, and therefore by combining all the suitable techniques, heavy metal filter for domestic applications can be developed.

Chitosan is also used as a removal of organic dyes, and oil from waste water effluents. This research work can be further extended with regards to above mentioned areas. Desorption experiments were not done completely. Further studies should be continued until finding a good regeneration solution and kinetic and equilibrium studies for desorption should be further studied.



University of Moratuwa, Sri Lanka.
Electronic Theses & Dissertations
www.lib.mrt.ac.lk

7 References

- Abadin, H., Ashizawa, A., Stevens, Y.-W., Lladós, F., Diamond, G., Sage, G., ... Swarts, S. G. (2007). Toxicological Profile for Lead. *U.S Public Health Service, Agency for Toxic Substances and Disease Registry*, (August), 582. Retrieved from <http://www.atsdr.cdc.gov/toxprofiles/tp13.pdf>
- Abdelwahab, O., & Amin, N. K. (2013). Adsorption of phenol from aqueous solutions by *Luffa cylindrica* fibers: Kinetics, isotherm and thermodynamic studies. *The Egyptian Journal of Aquatic Research*, 39(4), 215–223. doi:10.1016/j.ejar.2013.12.011
- Aderonke, a. O., Abimbola, B. A., Ifeanyi, E., Omotayo, S. A., Oluwagbemiga, S. A., & Oladotun, W. M. (2014). Adsorption of heavy metal ions onto chitosan grafted cocoa husk char. *African Journal of Pure and Applied Chemistry*, 8(10), 147–161. doi:10.5897/AJPAC2014.0591
- Agrawal, A., & Sahu, K. K. (2006). Kinetic and isotherm studies of cadmium adsorption on manganese nodule residue. *Journal of Hazardous Materials*, 137(2), 915–924. doi:10.1016/j.jhazmat.2006.03.039
- Ahmad, A. L., Sumathi, S., & Hameed, B. H. (2005). Adsorption of residue oil from palm oil mill effluent using powder and flake chitosan: Equilibrium and kinetic studies. *Water, Air, and Soil Pollution*, 39(12), 2483–2494. doi:10.1016/j.watres.2005.03.035
- Ahmed, M. J., & Theydan, S. K. (2012). Equilibrium isotherms, kinetics and thermodynamics studies of phenolic compounds adsorption on palm-tree fruit stones. *Ecotoxicology and Environmental Safety*, 84, 39–45. doi:10.1016/j.ecoenv.2012.06.019
- Alvarenga, E. S. De. (2011). Characterization and Properties of Chitosan. *Biotechnology of Biopolymers*, 91–108. Retrieved from <http://www.intechopen.com/books/biotechnology-of-biopolymers/characterization-and-properties-of-chitosan>
- Aranaz, I., Mengibar, M., Harris, R., Paños, I., Miralles, B., Acosta, N., ... Heras, Á. (2009). Functional Characterization of Chitin and Chitosan. *Current Chemical Biology*, 3, 203–230. doi:10.2174/187231309788166415
- Ashori, A., Raverty, W. D., & Harun, J. (2005). Effect of chitosan addition on the surface properties of kenaf (*Hibiscus cannabinus*) paper. *Fibers and Polymers*, 6(2), 174–179. doi:10.1007/BF02875611

- Azizian, S. (2004). Kinetic models of sorption: a theoretical analysis. *Journal of Colloid and Interface Science*, 276(1), 47–52. doi:10.1016/j.jcis.2004.03.048
- Azouaou, N., Sadaoui, Z., Djaafri, a., & Mokaddem, H. (2010). Adsorption of cadmium from aqueous solution onto untreated coffee grounds: Equilibrium, kinetics and thermodynamics. *Journal of Hazardous Materials*, 184(1-3), 126–134. doi:10.1016/j.jhazmat.2010.08.014
- Batista, A. C. L., Villanueva, E. R., Amorim, R. V. S., Tavares, M. T., & Campos-Takaki, G. M. (2011). Chromium (VI) ion adsorption features of chitosan film and its chitosan/zeolite conjugate 13X film. *Molecules*, 16(5), 3569–3579. doi:10.3390/molecules16053569
- Benavente, M. (2008). *Adsorption of metallic ions onto chitosan: equilibrium and kinetic studies*. Royal Institute of Technology. Retrieved from <http://kth.diva-portal.org/smash/record.jsf?pid=diva2:13755>
- Blanchard, G., Maunaye, M., & Martin, G. (1984). Removal of heavy metals from waters by means of natural zeolites. *Water Research*, 18(12), 1501–1507. doi:10.1016/0043-1354(84)90124-6
- Cheung, W. H., Szeto, Y. S., & McKay, G. (2007). Intraparticle diffusion processes during acid dye adsorption onto chitosan. *Bioresource Technology*, 98(15), 2897–2904. doi:10.1016/j.biortech.2006.09.045
- Chu, K. H. (2002). Removal of copper from aqueous solution by chitosan in prawn shell: Adsorption equilibrium and kinetics. *Journal of Hazardous Materials*, 90(1), 77–95. doi:10.1016/S0304-3894(01)00332-6
- Crini, G. (2005). Recent developments in polysaccharide-based materials used as adsorbents in wastewater treatment. *Progress in Polymer Science*, 30(1), 38–70. doi:10.1016/j.progpolymsci.2004.11.002
- Dos Santos, Z. M., Caroni, A. L. P. F., Pereira, M. R., da Silva, D. R., & Fonseca, J. L. C. (2009). Determination of deacetylation degree of chitosan: a comparison between conductometric titration and CHN elemental analysis. *Carbohydrate Research*, 344(18), 2591–5. doi:10.1016/j.carres.2009.08.030
- Doyurum, S., & Çelik, A. (2006). Pb(II) and Cd(II) removal from aqueous solutions by olive cake. *Journal of Hazardous Materials*, 138(1), 22–28. doi:10.1016/j.jhazmat.2006.03.071
- Dzul Erosa, M. S., Saucedo Medina, T. I., Navarro Mendoza, R., Avila Rodriguez, M., & Guibal, E. (2001). Cadmium sorption on chitosan sorbents: kinetic and

equilibrium studies. *Hydrometallurgy*, 61(3), 157–167. doi:10.1016/S0304-386X(01)00166-9

El Hadrami, A., Adam, L. R., El Hadrami, I., & Daayf, F. (2010). Chitosan in plant protection. *Marine Drugs*, 8(4), 968–987. doi:10.3390/md8040968

Evans, J. R., Davids, W. G., MacRae, J. D., & Amirbahman, A. (2002). Kinetics of cadmium uptake by chitosan-based crab shells. *Water Research*, 36(13), 3219–3226. doi:10.1016/S0043-1354(02)00044-1

Febrianto, J., Kosasih, A. N., Sunarso, J., Ju, Y. H., Indraswati, N., & Ismadji, S. (2009). Equilibrium and kinetic studies in adsorption of heavy metals using biosorbent: A summary of recent studies. *Journal of Hazardous Materials*, 162(2-3), 616–645. doi:10.1016/j.jhazmat.2008.06.042

Gupta, S., & Babu, B. V. (2009). Removal of toxic metal Cr(VI) from aqueous solutions using sawdust as adsorbent: Equilibrium, kinetics and regeneration studies. *Chemical Engineering Journal*, 150(2-3), 352–365. doi:10.1016/j.cej.2009.01.013

Ho, Y. S. (1995). *Adsorption of heavy metals from waste water by peat*. University of Birmingham, Birmingham, UK.

Ho, Y. S. (2006). Review of second-order models for adsorption systems. *Journal of Hazardous Materials*, 136(3), 681–689. doi:10.1016/j.jhazmat.2005.12.043

Ho, Y. S., Ng, J. C. Y., & McKay, G. (2000). Kinetics of pollutant sorption by biosorbents: review. *Separation & Purification Methods*, 29(2), 189–232. doi:10.1081/SPM-100100009

Holfetz, V. E. (2012). *An Investigation of Chitosan for Sorption of Radionuclides*. Oregon State University. Retrieved from <https://ir.library.oregonstate.edu/xmlui/bitstream/handle/1957/31104/HolfetzVanessaE2012.pdf?sequence=3>

Jeon, C., & Höll, W. H. (2003). Chemical modification of chitosan and equilibrium study for mercury ion removal. *Water Research*, 37(19), 4770–4780. doi:10.1016/S0043-1354(03)00431-7

Kannamba, B., Reddy, K. L., & AppaRao, B. V. (2010). Removal of Cu(II) from aqueous solutions using chemically modified chitosan. *Journal of Hazardous Materials*, 175(1-3), 939–948. doi:10.1016/j.jhazmat.2009.10.098

- Kasaai, M. (2008). A review of several reported procedures to determine the degree of N-acetylation for chitin and chitosan using infrared spectroscopy. *Carbohydrate Polymers*, 71(4), 497–508. doi:10.1016/j.carbpol.2007.07.009
- Kelesglu, S. (2007). Comparative Adsorption Studie S of Heavy Metal Ions on Chitin and Chitosan Biopolymers. *A Thesis Submitted to MASTER OF SCIENCE in Chemistry*, (July).
- Khan, T. A., Peh, K. K., & Ch'ng, H. S. (2002). Reporting degree of deacetylation values of chitosan: The influence of analytical methods. *Journal of Pharmacy and Pharmaceutical Sciences*, 5(3), 205–212.
- Khanafari, a, & Marandi, R. (2008). Recovery of Chitin and Chitosan From Shrimp Waste By Chemical and Microbial Methods. *Iran. J. Environ. Health. Sci. Eng*, 5(1), 19–24.
- Lagergren, S. (1898). ur theorie der sogenannten adsorption geloster stoffe. *K. Sven. Vetenskapsakad. Handl*, 24, 1–39.
- Lavertu, M., Xia, Z., Serreqi, a. N., Berrada, M., Rodrigues, a., Wang, D., ... Gupta, A. (2003). A validated ¹H NMR method for the determination of the degree of deacetylation of chitosan. *Journal of Pharmaceutical and Biomedical Analysis*, 32(6), 1149–1158. doi:10.1016/S0731-7085(03)00155-9
- Lenntech BV (2014a). Cadmium (Cd) - Chemical properties, Health and Environmental effects. Retrieved February 20, 2015, from <http://www.lenntech.com/periodic/elements/cd.htm>
- Lenntech BV. (2014b). Lead (Pb) - Chemical properties, Health and Environmental effects. Retrieved February 20, 2015, from <http://www.lenntech.com/periodic/elements/pb.htm>
- Liang, S., Guo, X., Feng, N., & Tian, Q. (2010). Isotherms, kinetics and thermodynamic studies of adsorption of Cu²⁺ from aqueous solutions by Mg²⁺/K⁺ type orange peel adsorbents. *Journal of Hazardous Materials*, 174(1-3), 756–762. doi:10.1016/j.jhazmat.2009.09.116
- Lin, J., & Wang, L. (2009). Comparison between linear and non-linear forms of pseudo-first-order and pseudo-second-order adsorption kinetic models for the removal of methylene blue by activated carbon. *Frontiers of Environmental Science and Engineering in China*, 3(3), 320–324. doi:10.1007/s11783-009-0030-7
- Mahmoud Abbas, A. O. (2010). *Chitosan for biomedical applications*. The University of Iowa.

- Miretzky, P., & Cirelli, a. F. (2009). Hg(II) removal from water by chitosan and chitosan derivatives: A review. *Journal of Hazardous Materials*, 167(1-3), 10–23. doi:10.1016/j.jhazmat.2009.01.060
- Mizera, J., Mizerová, G., Machovic, V., & Borecká, L. (2007). Sorption of cesium, cobalt and europium on low-rank coal and chitosan. *Water Research*, 41(3), 620–6. doi:10.1016/j.watres.2006.11.008
- Ng, J. C. Y., Cheung, W. H., & McKay, G. (2003). Equilibrium studies for the sorption of lead from effluents using chitosan. *Chemosphere*, 52(6), 1021–1030. doi:10.1016/S0045-6535(03)00223-6
- Ngah, W. S. W., & Fatinathan, S. (2008). Adsorption of Cu(II) ions in aqueous solution using chitosan beads, chitosan-GLA beads and chitosan-alginate beads. *Chemical Engineering Journal*, 143(1-3), 62–72. doi:10.1016/j.cej.2007.12.006
- Noble, A., & Amerasinghe, P. (2014). *Review of Literature on Chronic Kidney Disease of Unknown Etiology (CKDu) in Sri Lanka*. Sa.Indiaenvironmentportal.Org.in. doi:10.5337/2014.206
- Nomanbhay, S. M., & Palanisamy, K. (2005). Removal of heavy metal from industrial wastewater using chitosan coated oil palm shell charcoal. *Electronic Journal of Biotechnology*, 8(1), 43–53. doi:10.2225/vol8-issue1-fulltext-7
- Ogawa, K., & Oka, K. (1993). X-ray Study of Chitosan-Transition Metal Complexes. *Chemistry of Materials*, 5(5), 726–728. doi:10.1021/cm00029a026
- Paulino, A. T., Guilherme, M. R., Reis, A. V., Tambourgi, E. B., Nozaki, J., & Muniz, E. C. (2007). Capacity of adsorption of Pb²⁺ and Ni²⁺ from aqueous solutions by chitosan produced from silkworm chrysalides in different degrees of deacetylation. *Journal of Hazardous Materials*, 147(1-2), 139–147. doi:10.1016/j.jhazmat.2006.12.059
- Pérez-Marín, a. B., Zapata, V. M., Ortuño, J. F., Aguilar, M., Sáez, J., & Lloréns, M. (2007). Removal of cadmium from aqueous solutions by adsorption onto orange waste. *Journal of Hazardous Materials*, 139(1), 122–131. doi:10.1016/j.jhazmat.2006.06.008
- Piron, E., & Domard, A. (1997). Interaction between chitosan and uranyl ions. *International Journal of Biological Macromolecules*, 21(4), 327–335. doi:10.1016/S0141-8130(97)00081-0
- Pitakpoolsil, W., & Hunsom, M. (2014). Treatment of biodiesel wastewater by adsorption with commercial chitosan flakes: Parameter optimization and

- process kinetics. *Journal of Environmental Management*, 133, 284–292. doi:10.1016/j.jenvman.2013.12.019
- Popuri, S. R., Vijaya, Y., Boddu, V. M., & Abburi, K. (2009). Adsorptive removal of copper and nickel ions from water using chitosan coated PVC beads. *Bioresource Technology*, 100(1), 194–199. doi:10.1016/j.biortech.2008.05.041
- Prakash, N. (n.d.). Kinetics of Copper and Nickel Removal From Industrial Waste, 01(4), 1–11.
- Rinaudo, M. (2006). Chitin and chitosan: Properties and applications. *Progress in Polymer Science*, 31(7), 603–632. doi:10.1016/j.progpolymsci.2006.06.001
- Schlick, S. (1986). Binding sites of copper²⁺ in chitin and chitosan. An electron spin resonance study. *Macromolecules*, 19(1), 192–195. doi:10.1021/ma00155a030
- Semerjian, L. (2010). Equilibrium and kinetics of cadmium adsorption from aqueous solutions using untreated *Pinus halepensis* sawdust. *Journal of Hazardous Materials*, 173(1-3), 236–242. doi:10.1016/j.jhazmat.2009.08.074
- Senarathne, P., & Pathiratne, K. a S. (2007). Accumulation of heavy metals in a food fish, *Mystus gulio* inhabiting Bolgoda Lake, Sri Lanka. *Sri Lanka Journal of Aquatic Sciences*, 12, 61–75.
- Senthil Kumar, P., Ramalingam, S., Senthamarai, C., Niranjanaa, M., Vijayalakshmi, P., & Sivanesan, S. (2010). Adsorption of dye from aqueous solution by cashew nut shell: Studies on equilibrium isotherm, kinetics and thermodynamics of interactions. *Desalination*, 261(1-2), 52–60. doi:10.1016/j.desal.2010.05.032
- SenthilKumar, P., Ramalingam, S., Sathyaselvabala, V., Kirupha, S. D., & Sivanesan, S. (2011). Removal of copper(II) ions from aqueous solution by adsorption using cashew nut shell. *Desalination*, 266(1-3), 63–71. doi:10.1016/j.desal.2010.08.003
- Solier, P., Denuziere, A., Viton, C., & Dormard, A. (2001). Relation between the Degree of Acetylation and the Electrostatic Properties of Chitin and Chitosan. *Biomacromolecules*, 2(3), 765–772. doi:10.1021/bm015531+
- Struszczyk, M. H. (2002). Chitin and Chitosan. *Polimery*, 47(6), 396–403.
- Synowiecki, J., & Al-Khateeb, N. A. (2003). Production, properties, and some new applications of chitin and its derivatives. *Critical Reviews in Food Science and Nutrition*, 43(2), 145–171. doi:10.1080/10408690390826473

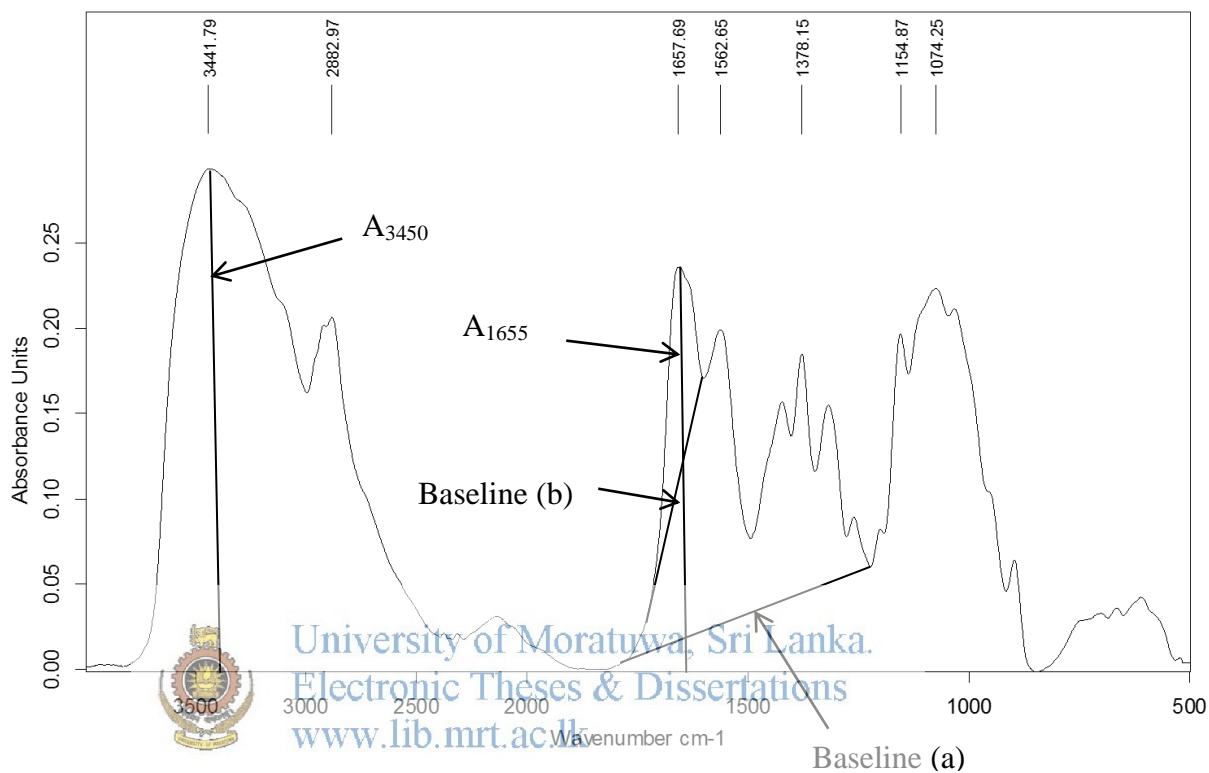
- Syuhadah, S. N., Muslim, N. Z., & Rohasliney, H. (2015). Determination of Heavy Metal Contamination from Batik Factory Effluents to the Surrounding Area. *International Journal of Chemical, Environmental & Biological Sciences*, 3(1), 3–5.
- Tanhaei, B., Ayati, A., Lahtinen, M., & Sillanpää, M. (2015). Preparation and characterization of a novel chitosan/Al₂O₃/magnetite nanoparticles composite adsorbent for kinetic, thermodynamic and isotherm studies of Methyl Orange adsorption. *Chemical Engineering Journal*, 259, 1–10. doi:10.1016/j.cej.2014.07.109
- Trung, T. S., Thein-Han, W. W., Qui, N. T., Ng, C.-H., & Stevens, W. F. (2006). Functional characteristics of shrimp chitosan and its membranes as affected by the degree of deacetylation. *Bioresource Technology*, 97(4), 659–63. doi:10.1016/j.biortech.2005.03.023
- Tseng, R. L., & Wu, F. C. (2009). Analyzing a liquid-solid phase countercurrent two- and three-stage adsorption process with the Freundlich equation. *Journal of Hazardous Materials*, 162(1), 237–248. doi:10.1016/j.jhazmat.2008.05.031
- Unlü, N., & Ersoz, M. (2006). Adsorption characteristics of heavy metal ions onto a low cost biopolymeric sorbent from aqueous solutions. *Journal of Hazardous Materials*, 136(2), 272–280. doi:10.1016/j.jhazmat.2005.12.013
- Vadivelan, V., & Kumar, K. V. (2005). Equilibrium, kinetics, mechanism, and process design for the sorption of methylene blue onto rice husk. *Journal of Colloid and Interface Science*, 286(1), 90–100. doi:10.1016/j.jcis.2005.01.007
- Van de Velde, K., & Kiekens, P. (2004). Structure analysis and degree of substitution of chitin, chitosan and dibutylchitin by FT-IR spectroscopy and solid state C NMR. *Carbohydrate Polymers*, 58(4), 409–416. doi:10.1016/j.carbpol.2004.08.004
- Van Toan, N., Ng, C. H., Aye, K. N., Trang, T. S., & Stevens, W. F. (2006). Production of high-quality chitin and chitosan from preconditioned shrimp shells. *Journal of Chemical Technology and Biotechnology*, 81(7), 1113–1118. doi:10.1002/jctb.1437
- Wanigasuriya, K. (2012). Aetiological factors of Chronic Kidney Disease in the North Central Province of Sri Lanka: A review of evidence to-date. *Journal of the College of Community Physicians of Sri Lanka*, 17(1), 21–42. doi:10.4038/jccpsl.v17i1.4931

- WHO. (2010). Exposure to cadmium: a major public health concern. *World Health Organization*, 3–6. Retrieved from <http://www.who.int/ipcs/features/cadmium.pdf>
- Wu, F. C., Tseng, R. L., & Juang, R. S. (2009). Initial behavior of intraparticle diffusion model used in the description of adsorption kinetics. *Chemical Engineering Journal*, 153(1-3), 1–8. doi:10.1016/j.cej.2009.04.042
- Yu, F., Wu, Y., Ma, J., & Zhang, C. (2013). Adsorption of lead on multi-walled carbon nanotubes with different outer diameters and oxygen contents: Kinetics, isotherms and thermodynamics. *Journal of Environmental Sciences*, 25(1), 195–203. doi:10.1016/S1001-0742(12)60023-0
- Zeldowitsch, J. (1934). Uber den mechanismus der katalytischen oxydation von CO an MnO₂. *Acta Physicochim, URSS 1*, 364–449.



University of Moratuwa, Sri Lanka.
Electronic Theses & Dissertations
www.lib.mrt.ac.lk

[Appendix - I: Determination of Degree of deacetylation]



Baseline (a) equation

$$DD = 100 - \left[\left(\frac{A_{1655}}{A_{3450}} \right) \times \frac{100}{1.33} \right]$$

Baseline (b) equation

$$DD = 100 - \left[\left(\frac{A_{1655}}{A_{3450}} \right) \times 115 \right]$$

The acid base titration method was used to determine the DD from the amino group content in chitosan. Dry chitosan (0.3g) was dissolved in 30ml of HCL standard solution (0.1M). Methyl orange and aniline blue mixing indicators were added. A standard solution of NaOH (0.1M) was used for titration until the solution became blue green. The following formulas were used to calculate the DD of the product.

$$(-\text{NH}_2)\% = \frac{0.016(C_1V_1 - C_2V_2)}{W} \times 100$$

$$\text{DD}\% = \frac{203(-\text{NH}_2\%)}{16 + 42(-\text{NH}_2\%)} \times 100$$

Where C_1 , V_1 , C_2 , and V_2 are the concentrations and volumes for the HCl standard solution and NaOH standard solution, respectively, and W is the weight of the sample.



University of Moratuwa, Sri Lanka.
Electronic Theses & Dissertations
www.lib.mrt.ac.lk

Sample	FTIR base line a method	FTIR base line b method	Titration method
Low DD	72	88.6	94.2
High DD	85.6	93.6	98.5

[Appendix - II: FTIR Characterization of heavy metal adsorbed chitosan]

Characteristic peaks which affect the adsorption of heavy metals are as follows,

- N-H stretching band of amine group – 3270- 3300 cm^{-1}
- C=O stretching of amide I – 1655 cm^{-1}
- C-N stretching of amide I – 1625 cm^{-1}
- N-H bending band due to the presence of NH_2 band – 1590 cm^{-1}

Due to the presence of number of peaks in the near wave number values, it is very difficult to find the actual intensity of the particular peak. For that, FTIR graphs were normalized relative to the O-H Stretching peak (Because OH doesn't involve with the adsorption process) and then the graph was deconvoluted to find the correct intensity.

When heavy metal adsorbed in to NH_2 , shift and broadening of the peak can be observed. That can be analyzed by calculating the full width at half maximum of NH_2 absorption band as represent in Figure 1.



University of Moratuwa, Sri Lanka.
E-theses, Theses & Dissertations
www.lib.mrt.ac.lk

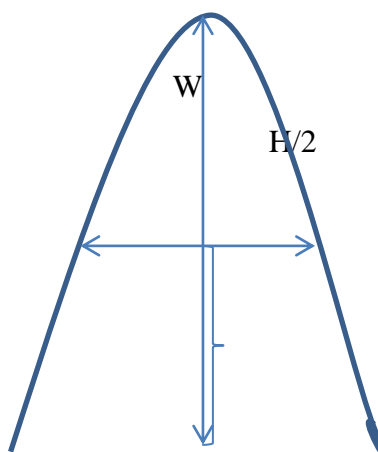


Figure 1. Representation of full width at half

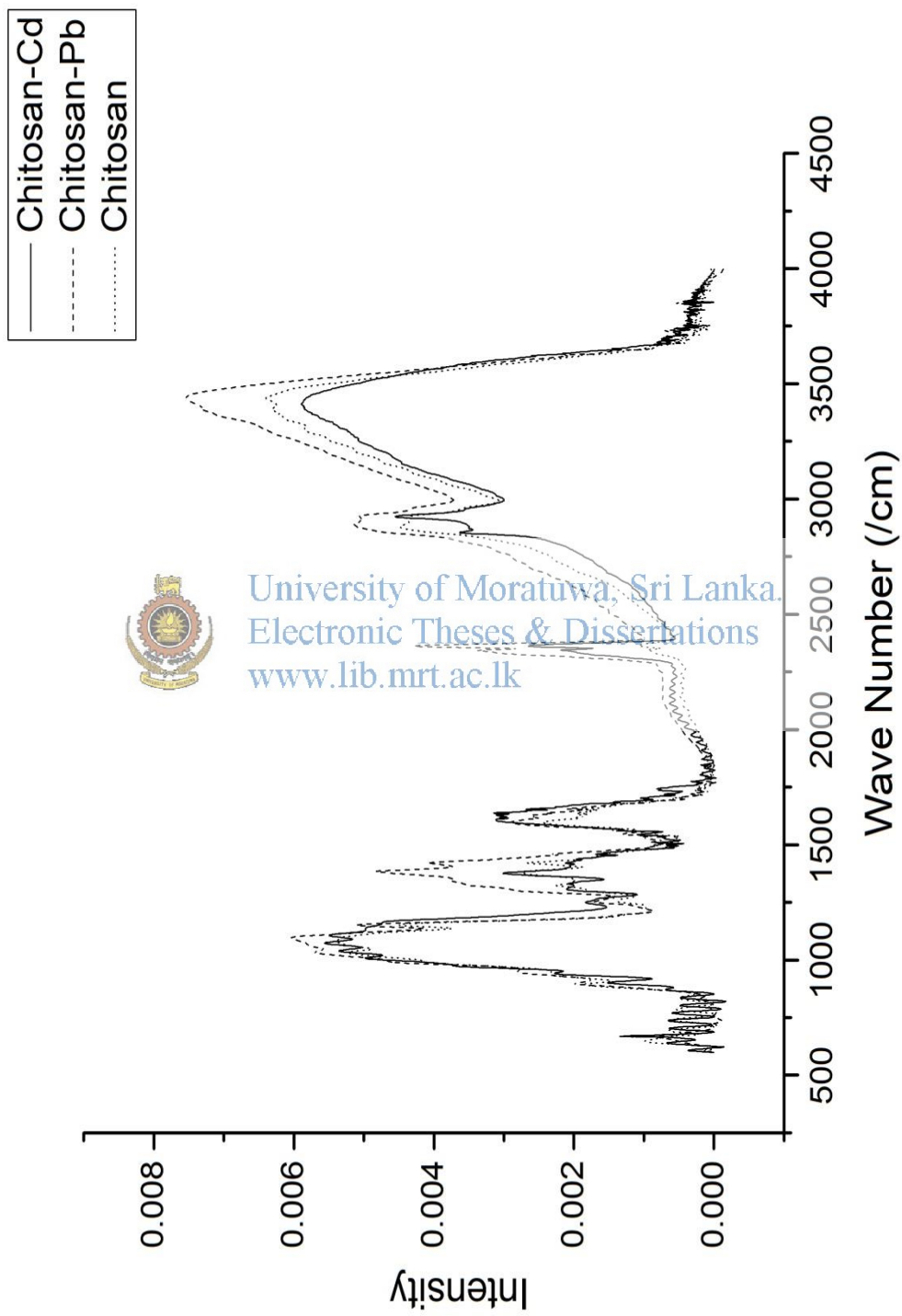


Figure 2. FTIR spectrum comparison of different chitosan samples

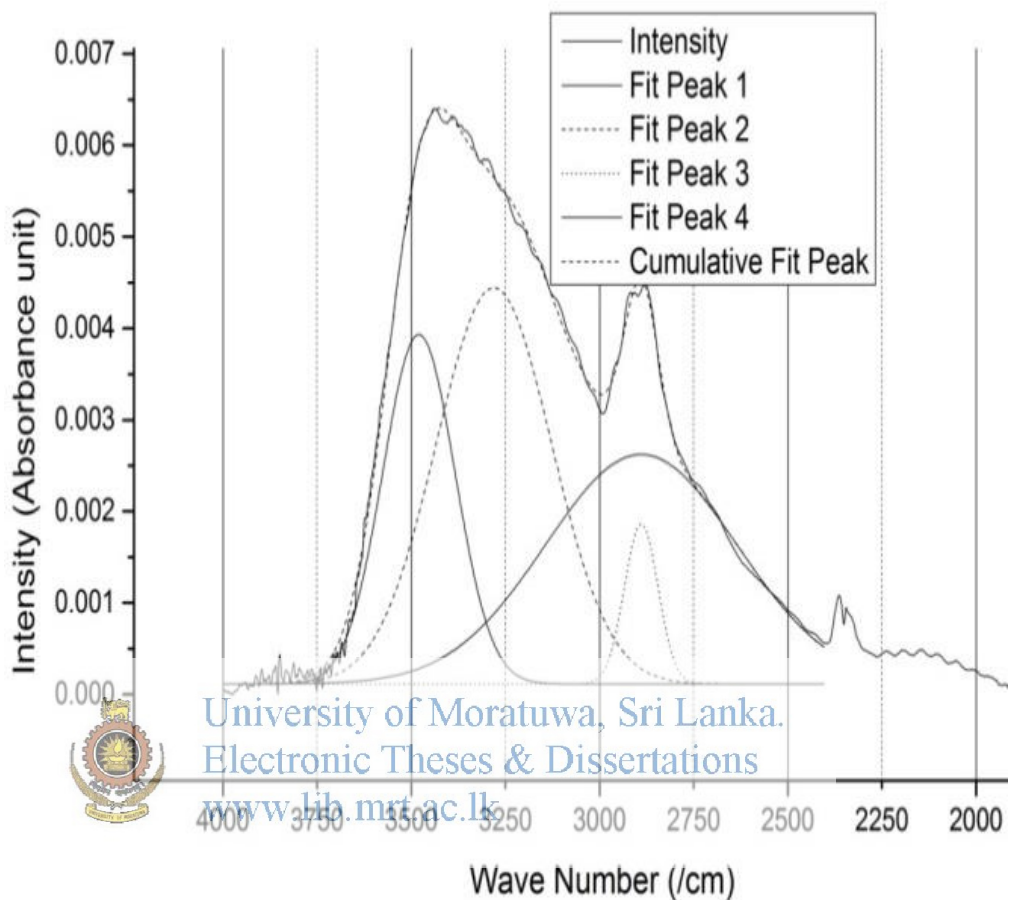


Figure 3. Deconvolute graph of chitosan

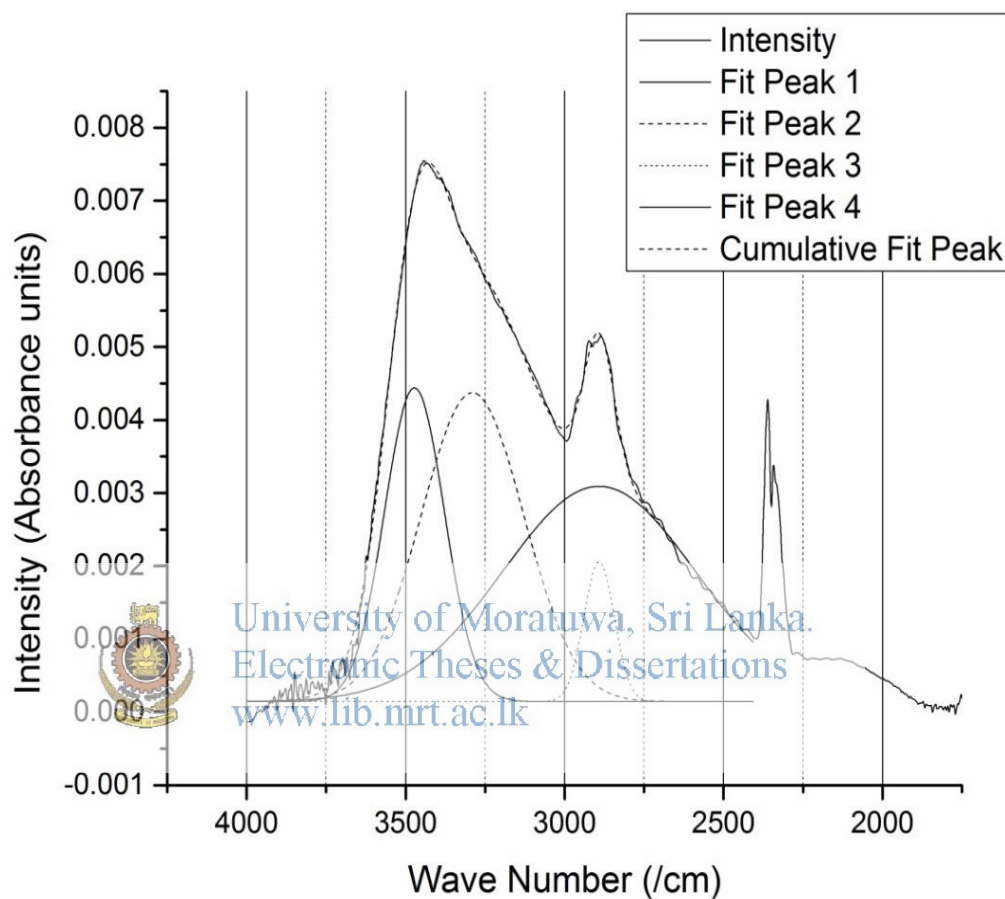


Figure 4. Deconvolute graph of Cd-chitosan

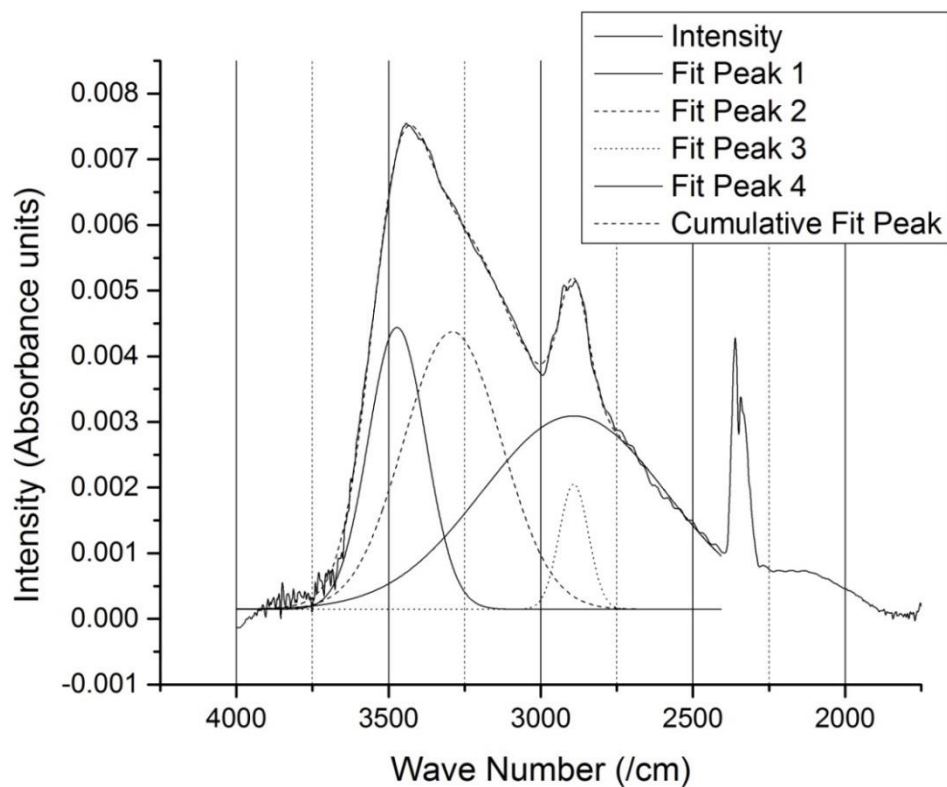


Figure 5. Deconvolute graph of Pb-chitosan

In all above three graphs, peak 2 is responsible for stretching of N-H bonds. So, if the Cd and Pb were connected to the NH₂ groups by forming complex structure, broadening of the peak can be observed. In the following Table 1, full widths at half maximum (W) data are given.

Table 1. Full width at half maximum values for chitosan samples

	W (nm)
Pure Chitosan	360.78
Cd Adsorbed Chitosan	377.97
Pb Adsorbed Chitosan	378.97

Finally, it can be concluded that the cadmium and lead were adsorbed by the NH₂ groups in chitosan.

[Appendix - III: Adsorption test results]

Cd

	Time (min)	Final concentration of solution (ppm)	Adsorbed amount into chitosan (ppm)	Adsorption capacity (mg/g)
Low DD pH- 5.5 28±2 ⁰ C 0.1 g dose 50ppm	5	41.8	8.2	4.1
	10	41	9	4.5
	15	38.333	11.667	5.8335
	30	34.433	15.567	7.7835
	45	34.425	15.575	7.7875
	60	34.467	15.533	7.7665
	90	33.966	16.034	8.017
	120	33.733	16.267	8.1335
	150	33.733	16.267	8.1335
	180	33.766	16.234	8.117
	240	30.425	19.575	9.7875
300	30.426	19.574	9.787	
High DD pH- 5.5 28±2 ⁰ C 0.1 g dose 50ppm	5	34.925	15.075	7.5375
	10	34.45	15.55	7.775
	15	31.266	18.734	9.367
	30	29.867	20.133	10.0665
	45	29.4	20.6	10.3
	60	29.433	20.567	10.2835
	90	29.233	20.767	10.3835
	120	28.867	21.133	10.5665
	150	27.433	22.567	11.2835
	180	27.467	22.533	11.2665
	240	26.874	23.126	11.563
300	26.548	23.452	12.226	
High pH-6.5 28±2 ⁰ C 0.1 g dose 50ppm	5	39.15	10.85	5.425
	10	37.625	12.375	6.1875
	15	32.533	17.467	8.7335
	30	28.123	21.877	10.9385
	45	26.98	23.02	11.51
	60	26.15	23.85	11.925
	90	25.456	24.544	12.272
	120	24.98	25.02	12.51
	150	24.625	25.375	12.6875
	180	24.533	25.467	12.7335
	240	24.523	25.477	12.7385
300	24.321	25.679	12.8395	

Low pH-3.5 28±2⁰C 0.1 g dose 50ppm	5	45.725	4.275	2.1375
	10	44.625	5.375	2.6875
	15	44.499	5.501	2.7505
	30	44.267	5.733	2.8665
	45	43.733	6.267	3.1335
	60	43.267	6.733	3.3665
	90	42.2	7.8	3.9
	120	41.266	8.734	4.367
	150	40.267	9.733	4.8665
	180	40.266	9.734	4.867
	240	40.261	9.739	4.8695
300	40.256	9.744	4.872	
106 microns pH- 6.5 28±2⁰C 0.1 g dose of chitosan 50ppm	5	38	12	6
	10	35.64	14.36	7.18
	15	35.36	14.64	7.32
	30	32.64	17.36	8.68
	45	31.42	18.58	9.29
	60	29.26	20.74	10.37
	90	28.4	21.6	10.8
	120	26.06	23.94	11.97
	150	24.86	25.14	12.57
	180	22.36	27.64	13.82
	240	22.3	27.7	13.85
300	22.06	27.94	13.97	
75 microns pH- 6.5 28±2⁰C 0.1 g dose of chitosan 50ppm	5	35.8	14.2	7.1
	10	35.32	14.68	7.34
	15	34.12	15.88	7.94
	30	32.02	17.98	8.99
	45	31.58	18.42	9.21
	60	28.16	21.84	10.92
	90	27.36	22.64	11.32
	120	25.02	24.98	12.49
	150	23.06	26.94	13.47
	180	21.06	28.94	14.47
	240	21.16	28.84	14.42
300	20.8	29.2	14.6	

25 ppm pH- 6.5 28±2 ⁰ C 0.1 g dose of chitosan	5	19.19	5.81	2.905
	10	19.4	5.6	2.8
	15	17.18	7.82	3.91
	30	11.41	13.59	6.795
	45	10.35	14.65	7.325
	60	10.81	14.19	7.095
	90	10.32	14.68	7.34
	120	9.3	15.7	7.85
	150	8.5	16.5	8.25
	180	7.85	17.15	8.575
	240	7.64	17.36	8.68
	300	6.5	18.5	9.25
5 ppm pH- 6.5 28±2 ⁰ C 0.1 g dose of chitosan	5	0.806	4.194	2.097
	10	0.798	4.202	2.101
	15	0.66	4.34	2.17
	30	0.798	4.202	2.101
	45	0.706	4.294	2.147
	60	0.652	4.348	2.174
	90	0.672	4.328	2.164
	120	0.602	4.398	2.199
	150	0.638	4.362	2.181
	180	0.592	4.408	2.204
	240	0.576	4.424	2.212
	300	0.562	4.438	2.219
0.05 g pH- 6.5 28±2 ⁰ C 50ppm	5	42.65	7.35	7.35
	10	40.875	9.125	9.125
	15	41.725	8.275	8.275
	30	41.4	8.6	8.6
	45	37.95	12.05	12.05
	60	39.375	10.625	10.625
	90	38.7	11.3	11.3
	120	37.625	12.375	12.375
	150	36.25	13.75	13.75
	180	35.85	14.15	14.15
	240	33.94	16.06	16.06
	300	33.175	16.825	16.825

0.025g pH- 6.5 28±2 ⁰ C 50ppm	5	43.9	6.1	12.2
	10	43.725	6.275	12.55
	15	42.725	7.275	14.55
	30	42.6	7.4	14.8
	45	42.625	7.375	14.75
	60	42.075	7.925	15.85
	90	40.98	9.02	18.04
	120	40.175	9.825	19.65
	150	40.7	9.3	18.6
	180	39.35	10.65	21.3
	240	39.15	10.85	21.7
	300	38.95	11.05	22.1



University of Moratuwa, Sri Lanka.
Electronic Theses & Dissertations
www.lib.mrt.ac.lk

Pb

	Time (min)	Final concentration of solution (ppm)	Adsorbed amount into chitosan(ppm)	Adsorption capacity(mg/g)
Low DD pH- 3.5 28±2 ⁰ C 0.1 g dose of chitosan 50 ppm	5	27.665	22.335	11.1675
	10	26.795	23.205	11.6025
	15	27.325	22.675	11.3375
	30	26.955	23.045	11.5225
	45	24.605	25.395	12.6975
	60	22.65	27.35	13.675
	90	21.38	28.62	14.31
	120	17.265	32.735	16.3675
	150	20.525	29.475	14.7375
	180	16.48	33.52	16.76
	240	17.55	32.45	16.225
300	17.45	32.55	16.275	
High DD pH- 3.5 28±2 ⁰ C 0.1 g dose of chitosan 50 ppm	5	25.135	24.865	12.4325
	10	25.14	24.86	12.43
	15	25.37	24.63	12.315
	30	23.055	26.945	13.4725
	45	23.075	26.925	13.4625
	60	20.715	29.285	14.6425
	90	17.65	32.35	16.175
	120	14.526	35.474	17.737
	150	17.95	32.05	16.025
	180	12.42	37.58	18.79
	240	12.96	37.04	18.52
300	12.76	37.24	18.52	
High pH-4.5 28±2 ⁰ C 0.1 g dose of chitosan 50 ppm	5	25.135	24.865	12.4325
	10	25.14	24.86	12.43
	15	25.37	24.63	12.315
	30	23.055	26.945	13.4725
	45	23.075	26.925	13.4625
	60	20.715	29.285	14.6425
	90	17.65	32.35	16.175
	120	14.526	35.474	17.737
	150	17.95	32.05	16.025
	180	12.42	37.58	18.79
	240	12.96	37.04	18.52
300	12.76	37.24	18.52	

Low pH-2.0 28±2 ⁰ C 0.1 g dose of chitosan 50 ppm	5	34.805	15.195	7.5975
	10	32.57	17.43	8.715
	15	31.595	18.405	9.2025
	30	33.935	16.065	8.0325
	45	30.455	19.545	9.7725
	60	28.615	21.385	10.6925
	90	26.205	23.795	11.8975
	120	22.905	27.095	13.5475
	150	24.895	25.105	12.5525
	180	22.815	27.185	13.5925
	240	21.8	28.2	14.1
	300	21.68	28.32	14.16
106 microns pH- 4.5 28±2 ⁰ C 0.1 g dose of chitosan 50 ppm	5	24.5	25.5	12.75
	10	23.676	26.324	13.162
	15	23.652	26.348	13.174
	30	22.724	27.276	13.638
	45	22.752	27.248	13.624
	60	21.608	28.392	14.196
	90	19.0925	30.9075	15.45375
	120	18.9142	31.0858	15.5429
	150	17.6168	32.3832	16.1916
	180	16.593	33.407	16.7035
	240	16.9824	33.0176	16.5088
	300	15.732	34.268	17.134
75 microns pH- 4.5 28±2 ⁰ C 0.1 g dose of chitosan 50 ppm	5	24.98	25.02	12.51
	10	24.4	25.6	12.8
	15	23.2167	26.7833	13.39165
	30	22.4466	27.5534	13.7767
	45	21.349	28.651	14.3255
	60	19.621	30.379	15.1895
	90	18.315	31.685	15.8425
	120	17.7111	32.2889	16.14445
	150	17.5329	32.4671	16.23355
	180	16.869	33.131	16.5655
	240	15.732	34.268	17.134
	300	15.032	34.968	17.484



25 ppm pH- 4.5 28±2 ⁰ C 0.1 g dose of chitosan	5	6.04	18.96	9.48
	10	5.326	19.674	9.837
	15	5.136	19.864	9.932
	30	4.864	20.136	10.068
	45	4.624	20.376	10.188
	60	4.806	20.194	10.097
	90	4.214	20.786	10.393
	120	3.56	21.44	10.72
	150	3.97	21.03	10.515
	180	3.19	21.81	10.905
	240	2.282	22.718	11.359
	300	2.012	22.988	11.494
5 ppm pH- 4.5 28±2 ⁰ C 0.1 g dose of chitosan	5	0.775	4.225	2.1125
	10	0.551	4.449	2.2245
	15	0.513	4.487	2.2435
	30	0.54	4.46	2.23
	45	0.346	4.654	2.327
	60	0.318	4.682	2.341
	90	0.271	4.729	2.3645
	120	0.119	4.881	2.4405
	150	0.062	4.938	2.469
	180	0.008	4.992	2.496
	240	0.008	4.992	2.496
	300	0.007	4.993	2.4965



University of Moratuwa, Sri Lanka
Electronic Theses & Dissertations
www.lib.mrt.ac.lk

[Appendix – IV: Publications]


1. IEEE Conference Publications

Unagolla, J. M., Adikary, S. U., “Adsorption of cadmium and lead heavy metals by chitosan biopolymer: A study on equilibrium isotherms and kinetics”, *Moratuwa Engineering Research Conference (MERCon), 2015*, pp 234-239, 2015, DOI: 10.1109/MERCon.2015.7112351

2. Unagolla J. M., Adikary S. U.; “Adsorption Characteristics of Cadmium and Lead heavy metal into Locally Synthesized Chitosan Biopolymer” *Tropical Agricultural Research Journal*, Vol 26(2), pp395-401,2014; ISSN: 1016.1422.

Available online at, http://www.pgia.ac.lk/files/Annual_congress/ journal/v26

3. Unagolla J.M., Adikary S. U.;“Adsorption of Lead heavy metal ions by Chitosan Biopolymer: Kinetics and Equilibrium” *108th Annual transactions of Institute of Engineers Sri Lanka*, Vol 1 – Part B, pp 155-162, 2014.

 4. Unagolla, J. M., Adikary, S. U.; “Study of Adsorption Characteristics of Cadmium into Chitosan Biopolymer to be used for Waste Water Treatments” *107th Annual transactions of Institute of Engineers Sri Lanka*, Vol 1- Part B, pp 313-319, 2013.

Available online at, <http://www.scribd.com/doc/202126465/IESL-Technical-Papers-Oct-2013#scribd>